NF-κB/RELISH AND THE CONTROL OF CELLULAR TRIGLYCERIDE METABOLISM IN *DROSOPHILA MELANOGASTER*

A Dissertation

by

MARAL MOLAEI

Submitted to the Office of Graduate and Professional Studies of
Texas A&M University
in partial fulfillment of the requirements for the degree of

DOCTOR OF PHILOSOPHY

Chair of Committee,	Jason Karpac
Committee Members,	Robert Alaniz
	Vytas Bankaitis
	Michael Criscitiello
Head of Department,	Ramesh Vemulapalli

December 2019

Major Subject: Biomedical Sciences

ABSTRACT[1]

Metabolic and innate immune signaling pathways have co-evolved to elicit coordinated responses. However, dissecting the integration of these ancient signaling mechanisms remains a challenge. Using *Drosophila*, we uncovered a role for the innate immune transcription factor NF-κB/Relish in governing lipid metabolism during metabolic adaptation to fasting. We found that Relish is required to restrain fasting-induced lipolysis, and thus conserve cellular triglyceride levels during metabolic adaptation, through specific repression of ATGL/Brummer lipase gene expression in adipose (fat body). Fasting-induced changes in Brummer expression and, consequently, triglyceride metabolism are adjusted by Relish-dependent attenuation of FoxO transcriptional activation function, a critical metabolic transcription factor. Relish limits FoxO function by influencing fasting-dependent histone deacetylation and subsequent chromatin modifications within the Bmm locus. These results highlight that the antagonism of Relish and FoxO functions are crucial in the regulation of lipid metabolism during metabolic adaptation, which may further influence the coordination of innate immune-metabolic responses.

DEDICATION

I would like to dedicate this dissertation to my beloved husband, Dr. Jose Florez, for his patience, support, and help.

ACKNOWLEDGEMENTS

I would like to thank my committee chair, Dr. Jason Karpac, who has provided me the opportunity and resources to pursue my Ph.D. His training, guidance, and support were essential in completion of this study. He has been always willing to answer my questions and his brilliant ideas and long, meaningful discussions have helped me to obtain a deeper understanding of science.

I would like to thank my committee members, Dr. Vytas Bankaitis, Dr. Mike Criscitiello, and Dr. Robert Alaniz for their continuous support, guidance, and encouragement not only throughout the course of this research but also in my life. I am grateful for having them in my committee.

My sincere thanks go Dr. Patricia Holman (former graduate advisor) for her kindness, support, and sympathy during some of the hard days of my life.

I would like to thank Dr. Karpac's team, my friends and colleagues, faculty and staff of Health Science Center and College of Veterinary Medicine and Biomedical Sciences, especially Carol Vargas, Kathie Smith, Dee Cooper, Janis Chmiel, Amy Griffin and Lisa Eubanks, for trying to help whenever possible or just being an ear to listen.

Finally, my very special thanks go to my parents, my husband and my daughter, the ones who suffered the most, yet, motivated me the most when I was desperate and disappointed.

CONTRIBUTORS AND FUNDING SOURCES

Contributors

This research was supervised by a dissertation committee consisting of Dr. Jason Karpac (Advisor), Dr. Vytas Bankaitis, Dr. Michael Criscitiello and Dr. Robert Alaniz (committee members).

Dr. Criscitiello has also kindly provided the Linux server to run the Clover software.

Dr. Karpac has performed the experiments related to AMPK, Sirt2 and FoxO-dependent expression of Bmm (Figure 3.18).

Crissie Vandehoef (graduate student) has conducted the experiment related to Rpd3-dependent regulation of Bmm expression (Figure 3.16B).

Funding Sources

This work was supported in part by the National Institute of Diabetes and Digestive and Kidney Diseases (grant R01 DK108930 to Jason Karpac) and by the American Heart Association (pre-doctoral fellowship to Maral Molaei).

TABLE OF CONTENTS

Page

LIST OF FIGURES

Page

LIST OF TABLES

Page

1. INTRODUCTION AND LITERATURE REVIEW

1.1 Immunometabolism

1.1.1 Integration of innate immune and metabolic systems

Starvation and infection are two ancient stressors in multicellular organisms. In a natural environment, organisms are inevitably exposed to various pathogens and stressors while they strive to obtain nutrients from their environment. Therefore, while the metabolic system is trying to maintain energy homeostasis through gaining nutrients from the environment and turning them into building blocks, or energy, the immune system works to fight against microorganisms and other stressors (Wang et al., 2019).

Metabolism can be divided into catabolism and anabolism. Catabolism generates energy by breaking down energy storage and metabolites, while anabolism is the energy-consuming biosynthetic process. Biological functions depend on primarily anabolic or catabolic metabolism that are integrated and overlapped. Immune responses are energy-costing (highly energy-consuming) processes. Therefore, immune inputs (pathogens) lead to a shift in metabolism toward immune response and away from reproduction and growth. It is known that immune responses require anabolism that is activated by inflammation. Metabolism can be reprogrammed in immune cells based on the required response (Loftus and Finlay, 2016; Wang et al., 2019). For example memory and naïve T-cells mainly rely on catabolism, however after immune stimulation effector T-cells and macrophages rely on anabolism to provide proper immune responses (Dominguez-Andres et al., 2018). Therefore, metabolism needs to be under precise control in immune cells in

order to maintain a proper immune response. On the other hand, metabolic organs need to maintain energy homeostasis and storage in order to provide energy resources for immune cells while still maintaining the function of other tissues through proper allocation of energy. Therefore, immune and metabolic system have coevolved in order to maintain the whole body homeostasis and promote growth and reproduction (Hotamisligil, 2017a; Loftus and Finlay, 2016; Wang et al., 2019).

Indeed, during the course of evolution, multicellular organisms have developed a crosstalk/cross-regulation of immune and metabolic systems to be able to coordinate responses to both infections (immune input) and nutrition availability (metabolic input). A complex interaction between immune and metabolic systems in cellular, tissue and whole-body levels is critical to maintaining body homeostasis and proper biological function (Wang et al., 2019) (Figure 1.1).

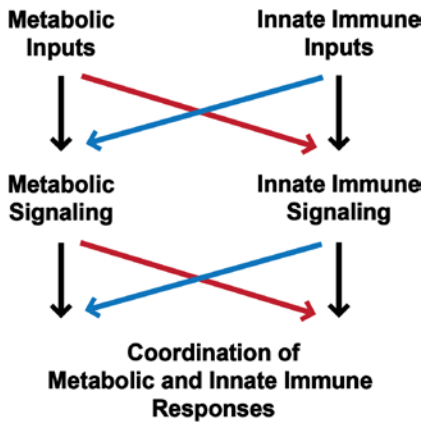

Figure 1.1 Integration of innate immune and metabolic pathways

Immunometabolism is the study of the interaction of immune and metabolic systems and can be broken down into two main subcategories: systemic (whole-body) metabolism and cellular

bioenergetics. Previously, immunometabolism was mainly focused on how inflammation can cause metabolic disease. However, recently this growing field includes a variety of topics such as M1-M2 macrophages switch and their role in inflammation, metabolism in immune cells, the role of immune cells and signaling in dictating systemic and cellular metabolism, allocation of energy and metabolites during immune responses, cellular and molecular mechanism of immune and metabolic crosstalk, and eventually the role of epigenetics in the regulation of both immune and metabolic systems (Guzik and Cosentino, 2018; Hotamisligil, 2017a; Loftus and Finlay, 2016; Shakespear et al., 2011; Sohrabi et al., 2018; Wang et al., 2019).

The crosstalk between innate immune and metabolic pathways is an intriguing section of immunometabolism studies. Researchers have uncovered that these pathways share some regulatory points and axes that allow the bi-directional regulation of these pathways and play role in the integration of innate immune and metabolic systems (Murray et al., 2015; Odegaard and Chawla, 2013; Osborn and Olefsky, 2012). In addition, some molecules have reported to act as "immunometabolic factors", directly linking metabolism and immunity, such as MEF2 and Lime in *Drosophila*.

MEF2 is reported as an immune-metabolic switch in *Drosophila*. It is required for anabolic function and immune response. Under normal conditions, it is phosphorylated and involved in the expression of lipogenic and glycogenic genes. However, upon infection, dephosphorylated MEF2 enhances the expression of antimicrobial peptides (Clark et al., 2013).

Recently, Mihajlovic *et al.* have identified a *Drosophila* gene named Lime (Linking Immunity and Metabolism, CG18446) as a new immunometabolic factor. This protein is expressed

in larval plasmatocyte and the fat body and links hemocyte development with systemic metabolism in *Drosophila* (Mihajlovic et al., 2019).

While innate immune and metabolic pathways are under precise regulation, some factors such as gene mutation, over nutrition, high fat or high sugar diet may lead to misregulation of these pathways and eventually, promote the development of disorders such as inflammation, obesity, insulin resistance, Type 2 diabetes, and fatty liver (Baker et al., 2011; Cai et al., 2005; Chen et al., 2015; Glass and Olefsky, 2012; Guzik and Cosentino, 2018; Hotamisligil, 2017a, b; Norata et al., 2015; Odegaard and Chawla, 2013). Therefore, uncovering the molecular mechanism of immunometabolism crosstalk and particularly the molecular nodes that play major roles in the regulation of both pathways is critical for understanding the origin of the disease. Indeed, uncovering the molecular mechanism of bi-directional regulation of innate immune and metabolic systems, will help us to better understand the underlying mechanisms of immune and metabolic disorders and eventually may provide new ideas for designing therapeutic intervention in order to treat metabolic disorders such as obesity, and insulin resistance (Figure 1.2).

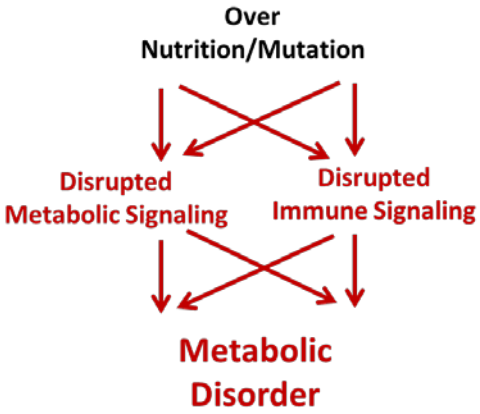

Figure 1.2 Mis-regulation of innate immune and metabolic pathways

NF-κB transcription factors/pathway appear to serve as one of immunometabolic factors involved in the coordination of metabolism and immunity. In both mammals and flies, the NF-κB signaling pathway, main regulators of innate immunity, are also known as an indirect regulator of metabolism through their effect on inflammation which may lead to insulin resistance and type 2 diabetes (Chen et al., 2015; Galenza and Foley, 2019). Furthermore, some direct regulation of metabolic genes (such as GLUT3 and SCO2) by NF-κB (Mauro et al., 2011) as well as interaction of NF-κB with other metabolic transcription factors are reported (Oeckinghaus et al., 2011) (explained more in section 1.4). However, more studies are required to uncover the role of NF-κB signaling pathway in the regulation of metabolism.

1.1.2 Inflammation and obesity: The role of macrophages

Macrophages are the major immune cells residing in adipose tissue. The adipose tissue macrophages (ATMs) play role in adipose tissue health and disease. These cells have been implicated to obesity-induced inflammation and subsequently, insulin resistance. Obesity is considered as an imbalance in the ratios of M1/M2 macrophages. M1 macrophages are pro-inflammatory, classically activated, with higher abundance in obesity and are stimulated by TLR agonist, IFN-γ, and TNF-α. These macrophages secrete pro-inflammatory cytokines such as IL-1 β, TNF-α, IL-6, IL-12 and IL-23 and, therefore are responsible for the promotion of inflammation (Boutens and Stienstra, 2016).

M2 macrophages are anti-inflammatory, alternatively activated and are stimulated by PPAR-γ[2] agonists, IL-4, IL-10, and IL-13. These macrophages help with the resolution of inflammation by secreting anti-inflammatory cytokines such as IL-10. They are also involved in wound healing and tissue remodeling. In the lean state, M2 anti-inflammatory macrophages are dominant in adipose tissue. The M2 phenotype is maintained by secretion of IL-10 and IL-4 from eosinophils and Tregs, which also are located in lean adipose tissue (Kraakman et al., 2014; Lumeng et al., 2007).

Obesity acts as cellular stress for adipose tissue and results in the recruitment of monocytes to the adipose tissue and differentiation into M1 pro-inflammatory macrophages through secretion of pro-inflammatory cytokines and chemokines. M1 macrophages contribute to the onset of inflammation by producing cytokines, cytokine receptors and activation of signal transducers and activators of transcription 1 (STAT1) and interferon regulatory factor (IRF). The cytokines secreted by macrophages may be released into circulation and therefore, work in an endocrine manner. This may lead to the development of systemic inflammation and eventually insulin resistance. Obesity is also associated with a shift in other immune cells, characterized by a decrease in the number of eosinophils and regulatory T cells (Tregs) and increase in effector T cells and B cells. B cells, in turn, facilitate M1 polarization by activating T cells (Eguchi et al., 2013; Kraakman et al., 2014; Lumeng et al., 2007).

[2] PPARs (peroxisome proliferator activated receptor) are ligand regulated transcription factors and involved in the expression of metabolic genes. These nuclear receptor family play role in the regulation of lipid metabolism by controlling beat-oxidation, fatty acid synthesis and ketogenesis. PPAR-γ is linked to adipocyte differentiation and hypertrophy as well as glucose and lipid metabolic disorders in cancer and inflammation conditions.

Additionally, macrophages in adipose tissue are involved in lipid buffering during lipolysis. During fasting-induced lipolysis, macrophages infiltrate adipose tissue and adopt an anti-inflammatory phenotype. These macrophages uptake excessive adipocyte-released lipids and release them gradually into the bloodstream (Kosteli et al., 2010).

Also, there is evidence of the regulatory role of macrophages in lipolysis and thermogenesis during cold exposure. Therefore, macrophages are involved in adjusting to environmental challenges such as fasting and cold exposure (Nguyen et al., 2011; Rao et al., 2014)

Similar to mammals, starvation leads to enhanced differentiation of hematopoietic cells (immune cell progenitors) and infiltration of hemocytes (macrophages) to the fat body (adipose tissue) in *Drosophila* (Shim et al., 2012).

Interestingly, recently, it is shown that metabolic intermediate metabolites of TCA cycle and cholesterol synthesis pathway (altered cellular metabolism), induced by a stimulus such as B-glucan (allergen from *Candida albicans*) results in metabolic and epigenetic reprogramming of immune cells/macrophages and therefore, establishing trained innate immunity (TI) (Dominguez-Andres et al., 2018; Sohrabi et al., 2018).

1.1.3 Insulin resistance

Obesity-induced inflammation is a major cause of insulin resistance. Adipose tissue macrophages (ATMs) play an important role in the onset of insulin resistance through the

induction of JNK[3] and IKK/NF-κB pathway and production of pro-inflammatory cytokines (McNelis and Olefsky, 2014). Chronic overnutrition, saturated fatty acids, and high sugar diet act as metabolic inputs that can activate NF-κB signaling pathway through TLR2 and TLR4 receptors. NF-κB then induces the expression of inflammatory cytokines such as IL-6 and TNF-β. These cytokines promote systemic inflammation and eventually insulin resistance. For example, TNF-α can promote phosphorylation of insulin receptor substrate (IRS-1 and 2) through activation of JNK as well as the IKK complex (an upstream component of NF-κB pathway which is required for the activation of NF-κB molecule). IRS-1 phosphorylation (at Ser 307) in turn blocks insulin signaling and causes insulin resistance. JNK can also activate activator protein 1 (AP1) transcription factor and lead to impaired insulin pathway, but the mechanism is not fully understood (Cai et al., 2005; Henstridge et al., 2012; Rui et al., 2001; Tarantino and Caputi, 2011).

IL-6 can decrease the expression of glucose transporter- 4 (GLUT-4) and IRS-1 through activation of JAK-STAT signaling pathway (a cytokine-activated pathway involved in cell proliferation, differentiation, and apoptosis). This decrease leads to less sensitivity to insulin. In addition, muscle IL-6 can induce the expression of TLR-4 which is the receptor involved in the NF-κB pathway. (Kim et al., 2013; Lukic et al., 2014).

Furthermore, insulin resistance is accompanied by increased release of FFAs which in turn may promote the accumulation of lipids in cardiac and liver and development of heart and liver

[3] JNK (c-Jun N-terminal kinase) is a serine/threonine protein kinase, which belongs to MAPK family. This pathway play role in inflammation, cell proliferation and differentiation, migration, apoptosis and glucose metabolism. TNF-alpha, UV, IL-1 beta, and endoplasmic reticulum stress are activators/inducers of JNK.

disease (Gao et al., 2004; Guzik and Cosentino, 2018; Norata et al., 2015; Osborn and Olefsky, 2012).

Similar to mammals, *Drosophila* can develop both systemic and tissue-specific insulin resistance in response to a high sugar diet (HSD). In both mammals and flies, obesity-induced insulin resistance leads to more infection susceptibility. This effect in *Drosophila* is associated with regulation of insulin receptor (InR) in the fat body. Activation of insulin signaling can reduce immune response (expression of AMP genes), while the host resistance and expression of immune genes are increased upon insulin signaling inactivation (Musselman et al., 2018). Studies in *Drosophila* have linked insulin resistance to Imd/Relish (NF-κB) pathway. Fat boy PGRP-SB2 (a negative regulator of Imd/Relish pathway) downregulation can protect flies against obesity-induced insulin resistance (Musselman et al., 2017, 2018).

1.2 Adipose tissue and lipolysis in mammals: The role of ATGL and FoxO

Adipose tissue consists of lipid-laden adipocytes, also other cell types such as fibroblasts, and a variety of immune cells particularly macrophages. This dynamic tissue undergoes major changes according to nutritional and immune inputs, and play a major role in both immune response and metabolic homeostasis (Rosen and Spiegelman, 2014).

In general, multicellular organisms can be in two different stages: growth/reproduction or maintenance. When nutrients are abundant, organisms are in growth/reproduction stage and anabolic metabolism is dominant. Maintenance has two different types. Under food scarcity, organisms undergo dormancy, which relays on energy-preserving catabolic metabolism. The

second type of maintenance is defense, which happens in response to infection or injury and requires anabolic metabolism (Wang et al., 2019).

Under food scarcity, adipose tissue plays a critical role in energy homeostasis and catabolic metabolism required for dormancy. Adipocytes contain lipid droplets (LDs) which are the major storage of triglycerides (TAGs). Hydrolysis of these lipids during catabolic state provides fatty acids and glycerol, which will be taken up by energy-consuming organs. Fatty acids which are the products of lipolysis are not only essential energy substrates but also, are required for synthesis of membrane lipids and serve as ligands in signaling pathways such as immune (NF-κB) pathway (Rosen and Spiegelman, 2014). Therefore, lipolysis is crucial for maintaining whole-body homeostasis and requires precise regulation in various levels such as transcriptional and posttranslational regulation of enzymes, interaction of pathways and transcription factors, and the regulation of TFs expression and activity. Indeed, misregulation of the lipolysis due to misregulation of genes, factors, enzymes or other proteins involved in this process may lead to several pathologies including fatty liver, obesity diabetes, and heart disease (Arner et al., 2011).

Adipose triglyceride lipase (ATGL or PNPLA2) and hormone-sensitive lipase (HSL, encoded by Lipe gene) are two major lipases involved in the hydrolysis of triglycerides (TAGs) and diglycerides (DAGs) (Schweiger et al., 2006). In the linear classical lipolysis pathway, TAGs are first broken down to DAGs and fatty acids by ATGL (and to a lower degree by HSL) on lipid droplet's surface. Next, the activated HSL (phosphorylated) cleaves DAGs to MAGs and fatty acids. The last step is the hydrolysis of monoacylglycerol (MAGs) by monoglyceride lipase (MGL) (Figure 1.3). Recently, it has been shown that under HSL-deficiency, an alternative pathway promotes lipolysis. In this non-linear (cyclic) pathway, ATGL transfers one fatty acid of

DAG to another DAG by its trans-acylation activity that is enhanced by high concentration of DAGs. This results to generation of one TAG and one DAG, thus, allows the lipolysis to continue (Zhang et al., 2019).

ATGL (also called desnutrin or PNPLA2) was discovered in 2004 as the major lipase initiating hydrolysis of TAGs, and the rate-limiting enzyme in the lipolysis process. It is reported that ATGL possesses phospholipase 2 activity and acylglycerol transacylase activities, in addition to its TAG hydrolyze activity. Nevertheless, these enzymatic activitie are not significant compared to the TAG hydrolysis activity, and their physiological effects are not well understood (Notari et al., 2006; Taschler et al., 2015; Zhang et al., 2019).

This enzyme is expressed in several tissues such as skeletal muscle, liver, heart, lung, retina, testes, pancreas, small intestine and immune cells at low levels. The higher protein levels are reported in brown and white adipose tissue. Association of ATGL with several physiological function and pathologies including obesity, thermogenesis, liver disease, heart disease, and cancer-associated cachexia, and type 2 diabetes, have been reported, which highlights the importance of the precise regulation of this lipase (Ahmadian et al., 2011; Schoenborn et al., 2006; Taschler et al., 2015; Zhang et al., 2016).

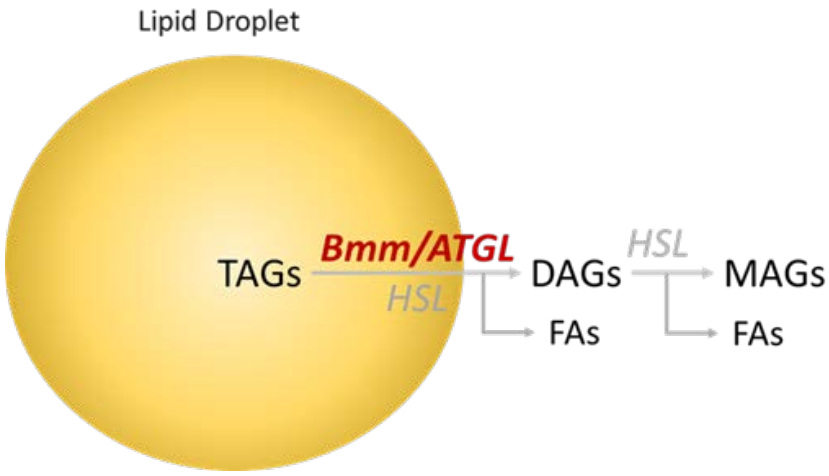

Figure 1.3 Triglyceride hydrolysis in lipid droplets.

In fact, the regulation of ATGL is at both transcriptional and post-transcriptional levels. Protein kinase A (PKA) and adenosine monophosphate (cAMP)-activated protein kinase (AMPK, a metabolic enzyme, which enhances O_2 consumption, glucose metabolism and fatty acid oxidation) are two major enzymes involved in the post-translational regulation of ATGL protein. PKA and AMPK both can enhance ATGL hydrolysis activity in mice by phosphorylation of its Ser406 residue (Ahmadian et al., 2011; Kim et al., 2016; Pagnon et al., 2012). Notably, AMPK and PKA are also involved in the regulation of HSL (Kim et al., 2016).

Perilipins (lipid droplet associated proteins) are other factors linked to ATGL post-transcriptional regulation. In adipose tissue, PLIN1 withholds ATGL co-activator (CGI-58, also known as alpha/beta-hydroxylase domain containing 5 (ABHD5)), and therefore, limits ATGL-mediated lipolysis under basal condition (by restricting the access of lipases to LDs). Phosphorylation of PLIN 1 by PKA result to release of CGI-58 as well as recruitment of HSL to lipid droplet surface, hence promotes lipolysis (Miyoshi et al., 2007).

Fat-specific protein 27 (FSP27) (co-localized with perilipins in LDs) is implicated in abiogenesis and formation of LDs in adipose tissue and negatively regulates lipolysis (Puri et al., 2007). In vivo analysis using human adipocytes has shown that FSP 27 can decrease ATGL-mediated lipolysis through physical interaction with ATGL protein (Grahn et al., 2014).

Several factors are involved in the transcriptional regulation of ATGL gene depending on different inputs/stimulus, such as starvation or growth hormones.

PPAR-γ positively regulates ATGL gene expression during adipogenesis via abolishing the inhibitory effect of SP1 (Kim et al., 2006; Roy et al., 2017). STAT5 is another positive transcriptional regulator of ATGL in adipose tissue in basal condition (Kaltenecker et al., 2017).

It is shown that leptin[4]-induced lipolysis is accompanied by increased number of ATGL protein, as well as, increased lipid droplet-localization of ATGL, suggesting that leptin is a positive regulator of ATGL lipase activity (Koltes et al., 2017).

However, starvation/fasting is a major factor that induces the upregulation of ATGL gene in adipose tissue, in order to promote lipolysis and provide energy for energy usage organs. It is well established that during fasting transcription of ATGL gene is induced by Forkhead O1 (FoxO1) transcription factor (Chakrabarti and Kandror, 2009; Zhang et al., 2016).

Forkhead subclass O transcription factor family are major regulators of body homeostasis and are involved in several biological processes such as apoptosis, autophagy, oxidative stress response, cell cycle, metabolism and immunity (Xing et al., 2018). In mammals, this family consists of 4 members: FoxO1 (FKHR), FoxO3a (FKHRL1), FoxO4 and FoxO6. FoxO1 and

[4] Leptin is an adiponectin secreted by adipose tissue. It works as an inhibitor of food intake and inducer of lipolysis.

FoxO3a are expressed in almost all tissues. FoxO4 has high expression in muscle, kidney and colorectal tissues. FoxO6 is primarily expressed in brain and liver. FoxO1 is considered as a representative member of the family, with essential transcriptional regulatory function. FOXO2 is identified as a homolog of FOXO3, and FOXO5 is only expressed in *Danio rerio* (FoxO3b). *Drosophila* carries only one FoxO gene, called dFoxO (Vihervaara and Puig, 2008). All FoxO molecules contain a forkhead domain (conserved DNA binding domain), nuclear localization signal (NLS), transactivation domain and nuclear export signal (NES) (Wang et al., 2014).

Several molecules, factors, and pathways are involved in the regulation of FoxO transcription factor activities in response to a various stimulus or environmental changes, including PI3K/Akt, JNK, p300-CBP (HAT complex), sirtuins, ubiquitin E3 ligase, and micro-RNAs. These pathways and molecules can affect FoxO activity through regulation of its abundance, post-translational modifications, nuclear-cytoplasmic shuttling, and subcellular localization. Variety of post-transcriptional modifications can occur on FoxO molecules, which lead to inhibition or induction of FoxO activity. Altogether, these post-modifications are called “FoxO code” and include phosphorylation, ubiquitination, acetylation/deacetylation, arginine methylation, and O-GlcNAcylation (Brown and Webb, 2018; Xing et al., 2018).

Akt is one of the major regulators of FoxO1 activity. In response to insulin signaling (nutrient abundance), Akt can phosphorylate FoxO1 molecule. This phosphorylation inhibits FoxO1 function by exporting and retaining it in the cytosol. Indeed, NES signal promotes cytosolic export of phosphorylated FoxO1. Afterward, phosphorylated FoxO1 is anchored in the cytosol by 14-3-3 protein and ultimately will be degraded due to interaction with ubiquitin E3 ligase. Akt-mediated phosphorylation of FoxO can be induced by insulin and insulin-like growth factor (IGF)

receptor/PI3K pathways. Conversely, PTEN mediates inhibition of Akt and results in subsequent activation of FoxO1 (Brown and Webb, 2018; Chakrabarti and Kandror, 2009).

Regulation of FoxO1 through acetylation/deacetylation is more controversial. Interestingly, it is shown that both acetylation and deacetylation can activate FoxO function depending on the target gene, tissue, and environmental stimulus. In response to oxidative stress, CBP/p300 acetylates FoxO. Acetylation can be reversed by sirtuin, which is a NAD-dependent histone deacetylase (class III HDAC). SIRT1 is one of the regulators of longevity and homeostasis in response to caloric restriction. It is shown that deceased SIRT1 activity is associated with enhanced expression of PEPCK and IGFB1 (insulin-like growth factor binding protein 1) by FoxO. However, other studies have demonstrated that CBP-dependent acetylation of FoxO can inhibit its transcriptional activity in response to oxidative stress. Also, this repression can be alleviated by SIRT1 (Chakrabarti et al., 2011; Mihaylova et al., 2011). In addition, recently Lo et al. have discovered that SIRT1 activation results in activation of FoxO and subsequent induction of ATGL expression (lipolysis) through SIRT1/AMPK/FoxO1/ATGL pathway (Lo et al., 2019).

Another study has shown that acetylation of FoxO3a decreases its transcriptional activity and nuclear localization in skeletal muscle. Indeed, skeletal muscles have basal FoxO activity. This activity is enhanced upon nutrient deprivation via HDAC1 and HDAC2 activity (Beharry et al., 2014).

Although some researchers have suggested that AMPK can positively regulate FoxO and therefore promotes lipolysis through PPAR-α/AMPK/FoxO1/ATGL pathway (Chen et al., 2012a) and SIRT1/AMPK/FoxO1/ATGL pathways (Lo et al., 2019), there are still some debates on how

AMPK affects FoxO function (Ahmadian et al., 2011; Chakrabarti et al., 2011; Daval et al., 2005; Gaidhu et al., 2009; Lo et al., 2019).

1.3 *Drosophila* as a model organism

1.3.1 Fat body

In the past decades, *Drosophila* has emerged as an important animal model to study immunometabolism. In addition to some advantages that this model organism provides such as high fecundity, remarkable genetic toolboxes, and ease of culture, it is well known that fundamental components and protein domains, as well as the foundation of immune and metabolic pathway, are conserved between mammals and flies. For example, insulin and insulin-like peptide (IIS), and target of rapamycin (TOR) pathways are similar between flies and mammals (Galenza and Foley, 2019; Musselman and Kuhnlein, 2018). Also, *Drosophila*'s Toll and Imd immune pathways share striking similarities with mammalian innate immune signaling pathways (Buchon et al., 2014; Hultmark, 2003).

Furthermore, insects possess a special tissue named fat body. Fat body in flies is equivalent to mammalian adipose tissue. Interestingly, this tissue also carries out some of the functions of vertebrate liver and immune system, and therefore, is involved in nutrient sensing, fat and glycogen storage, lipid metabolism and immune response. It is the main energy storage organ and provides a systemic immune response to pathogens by secreting antimicrobial peptides (AMPs). It can also sense different nutritional inputs (amino acids, lipids, glucose) and remotely control brain (Insulin-producing cells, IPCs) by secreting fat body signals (FBSs) such as unpaired 2 (Upd2) and CCHamid-2 (CCHa2) and is considered as the major endocrine organ in flies. According to

changes in energy demands, this tissue can produce various proteins, lipids, and carbohydrates, synthesize or hydrolyze TAGs, trehalose, and glycogen. In other words, this tissue has an integrated function of liver, adipose tissue and immune system before these systems have evolved into more complicated systems, and are assigned to more specified, complex organs in mammals (Arrese and Soulages, 2010; Li et al., 2019).

Combining the features of the liver, immune system and adipose tissue, the fat body plays a crucial role in the coordination of metabolic and immune pathways in response to nutritional and immune inputs. Therefore, this tissue provides a unique model to study the integration and coordination of immune and metabolic pathways/systems in one relatively simple tissue compared to extremely complicated, multi-tissue system in mammals (Dionne, 2014; Musselman et al., 2018).

In adult flies, the fat body is located in the abdomen and head (Figure 1.4). Similar to mammalian adipocytes, the fat cells within the flies' fat body are full of lipid droplets (LDs) under normal/fed conditions. Lipid droplets are dynamic organelles consist of a hydrophobic lipid core surrounded by a hydrophilic outer structure. Triglycerides (TAGs) are the main lipids in the hydrophobic core of LDs and are considered as the major source of energy storage in both flies and mammals. In addition to TAGs, ipid droplets contain other esterified lipids such as cholesterol. The outer hydrophobic layer is composed of a single layer of phospholipids, which is decorated by several lipid droplet-associated proteins. TAGs are not only the major form of stored lipids but also play an important role in whole-body functions by providing structural lipids and signaling ligands (like FFAs) (Arrese et al., 2014). It is shown that the proper metabolism of TAGs is required for oogenesis and embryogenesis of *Drosophila*. In larva and adult flies, TAG storage in

the fat body is the main source of energy during non-feeding stage/food scarcity (Canavoso et al., 2001; Kuhnlein, 2012). Furthermore, the excessive carbon gained through food will turn into TAGs. This process prevents cytotoxicity imposed by lipotoxic or glucotoxic metabolic intermediates (Musselman et al., 2013; Zechner et al., 2017). The function and metabolism of TAGs are similar in *Drosophila* and mammals, therefore *Drosophila* has emerged as a useful model organism to study lipid metabolism.

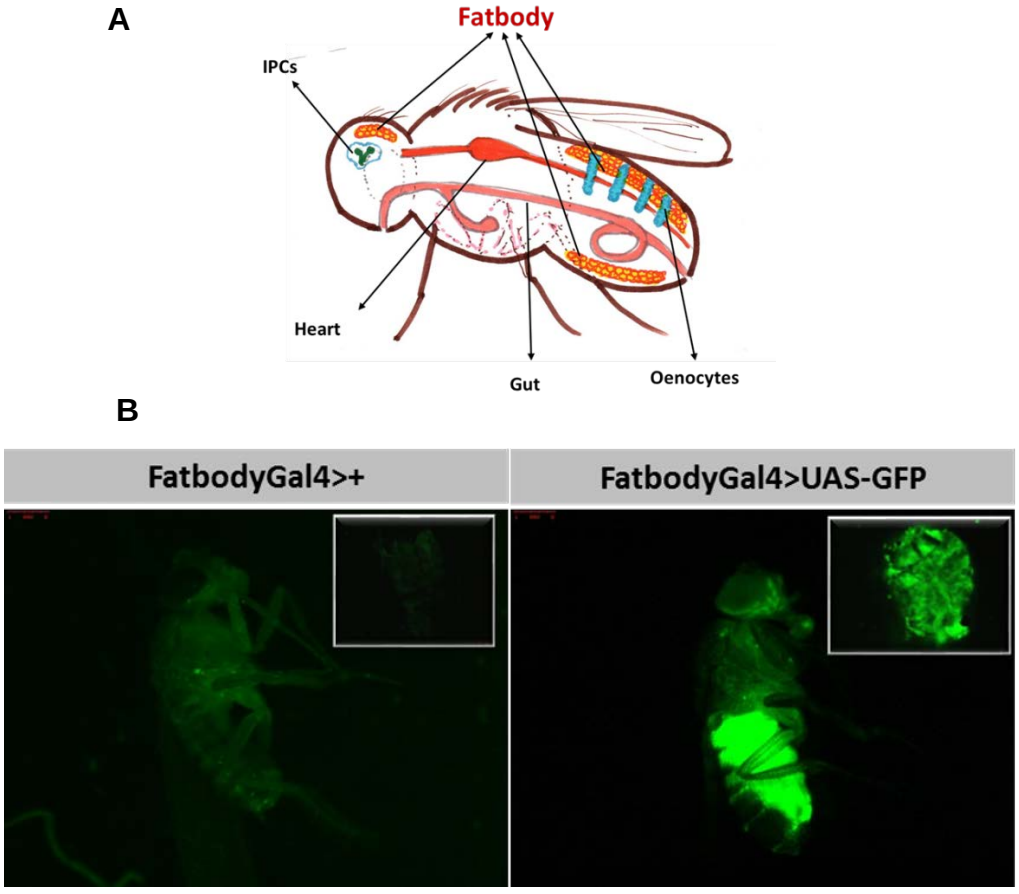

Figure 1.4 The location of the fat body in adult *Drosophila*. (A) Schematic diagram of fat body, brain, heart and intestine in adult *Drosophila*. (B) Fat body-induced GFP in the right panel. A dissected fat body is shown at the top right of the panel.

1.3.2 Triglyceride metabolism in flies

After a meal, dietary TAGs are digested to fatty acids in the midgut lumen of flies. Enterocytes can absorb fatty acid from the lumen. These cells also produce de-novo fatty acids from acety-CoA precursors. This lipogenesis process requires several enzymatic reactions. First, an enzyme called ACC converts acetyl-CoA to malonyl-CoA. Subsequently, malonyl-CoA produces fatty acid during a reaction mediated by FASN enzyme. In the enterocytes, the fatty acids from diet or de-novo synthesis turn into TAG or DAGs. TAGs play as energy storage in enterocytes and will be broken up to DAGs and fatty acid when required. DAGs are exported to the hemolymph in order to transport to other tissues such as fat body (Heier and Kuhnlein, 2018). Indeed, the majority of circulating lipids in flies are in the form of DAG and attached to Lpp (*Drosophila* lipoprotein) (Palm et al., 2012) .

The fat body can perform both lipolysis and lipogenesis, according to nutritional condition. As mentioned before, TAGs in the fat body are packed into LDs. In *Drosophila*, several LD-associated proteins have been reported to be involved in the regulation of TAG metabolism, including Brummer (Bmm), lipid storage droplet-1 (Lsd1 or PLIN1) and Lipid storage droplet-2 (Lsd2 or PLIN 2) (both belong to perilipin family) (Arrese and Soulages, 2010).

It is shown that Plin1 and Plin2 play an opposite and redundant role in *Drosophila* lipolysis. Plin1 is mainly expressed in the fat body and typically is associated with enhanced lipolysis. More precisely, in large lipid droplets, Plin1 promotes lipolysis. Phosphorylation of Plin1 stimulates lipolysis through AKH/AKHR/PKA pathway and, therefore promotes lipolysis by HSL. It is shown that mutation of Plin1 results in impaired lipolysis and promotes obesity. However, in small lipid droplets, it can prevent lipolysis. Plin 2 inhibits lipolysis mediated by Bmm. Therefore,

it promotes lipid accumulation. This protein is detected in the fat body during larval development and is required for the storage of fat (Bi et al., 2012).

Brummer (Bmm) is the orthologue of mammalian ATGL and act as the major triglyceride lipase in both mammals and flies. It promotes lipolysis by hydrolyzing TAGs to DAGs and plays critical role in the regulation of systemic TAG levels in adult flies. It is shown that mutation of Bmm leads to impaired lipid homeostasis. Increases in Bmm/ATGL lead to increases in lipolysis and decreases in fat storage, and decreases in Bmm/ATGL limit lipolysis and lead to obesity (Gronke et al., 2005). Also, Bmm-HSL double mutant flies promotes obesity in flies (Gronke et al., 2005; Gronke et al., 2007).

The DAGs produced by Bmm can be exported to peripheral tissues or undergo the second and third hydrolysis (possibly catalyzed by HSL) to produce more fatty acids and glycerol. Later on, fatty acids undergo β-oxidation to produce acetyl-CoA. β-oxidation of flies requires several enzymes such as Pdgy (activates FAs by adding CoA) and Yip2 (thiolase, acety-CoA acyltransferase). Acetyl-CoA then enters the citric acid cycle to produce NADH and $FADH_2$. Eventually, these coenzymes fuel electron chain in order to generate ATP required for physiological processes of cells. In addition to Bmm/ATGL and HSL flies have some proteins with predicted lipase activity such as Lip4 and CG5966. It is shown that these predicted lipases are expressed in the fat body. However, their physiological function and roles are not fully understood (Heier and Kuhnlein, 2018).

Similar to mammals, TAG metabolism in flies is also regulated by hormonal pathways, including insulin and adipokinetic hormone (Akh). *Drosophila* carries several insulin-like peptides (Dilps). Dilps are produced by IPCs insulin-producing cells (IPCs) located in the brain (Figure

1.4) and can stimulate insulin receptor (InR). The insulin pathway is conserved between flies and mammals in both components and functions. Stimulation of InR by Dilps results to activation of PI3K92E (orthologue of mammalian PI3K), and subsequently activation of Akt1. Akt is involved in phosphorylation and regulation of several downstream proteins. One of the major targets of Akt1 is dFoxO transcription factor. Akt inhibits dFoxO function by phosphorylation and cytoplasmic retention of this TF, while insulin pathway is induced. Upon, starvation, when insulin signaling is reduced, the inhibitory effect of Akt on FoxO is removed, therefore, FoxO can translocate into the nucleus. As in mammals, FoxO can induce the expression of several metabolic genes in response to dietary deprivation, including Bmm/ATGL (Figure 1.5). This process allows the breakdown of TAGs to FFAs and DAGs. Fatty acids later undergo β- oxidation and eventually provide ATP for the organism (Varma et al., 2014; Vihervaara and Puig, 2008).

Akh is a glucagon-like peptide in *Drosophila* and can stimulate lipolysis (TAG mobilization). Neuroendocrine cells in the corpora cardiaca[5] (CC) secret this hormone to hemolymph (Kim and Rulifson, 2004; Park et al., 2011). Fat body cells carry G protein-coupled Akh receptors (AkhR). Activation of the AkhR receptor transfers the signal to the variety of downstream targets (transcription factors, kinases, and lipid droplet associated proteins) through G protein/cAMP/PKA pathway. This pathway is involved in the regulation of lipolysis by phosphorylation of Plin1 in flies. Phosphorylation of Plin1, in turn, facilitates the activity of HSL and results in the induction of lipolysis (Figure 1.6) (Lee et al., 2018b; Musselman and Kuhnlein, 2018; Patel et al., 2005).

[5] Corpoa cardiaca (CC) consist of neuroendocrine cells and serve as functional orthologues of vertebrate pancreatic α-calls. It is involved in systemic glucose homeostasis.

AkhR can also, turn on PLC which results in increased Ca^{2+} through several enzymes and mediators. It has been shown that this increase in CA^{2+} promotes TAG hydrolysis by the mechanism that is not understood. It is known that knocking down the Akh or AkhR causes obesity. Double mutation of Bmm/ATGL and AkhR promotes extreme obesity and defective lipid mobilization. Therefore, AkhR and Bmm both can promote lipolysis by different mechanisms (Gronke et al., 2007; Sajwan et al., 2015). Notably, studies suggest that there are some interactions between Akh and insulin pathways (Kim and Neufeld, 2015; Rajan et al., 2017). Furthermore, Akh can regulate the expression of Bmm by removing the inhibitory effect of Sik3 on HDAC4, which allows the nuclear localization of HDAC4 (Choi et al., 2015). HDAC4 is the activator of FoxO transcription factor. Therefore, Akh stimulation can indirectly increase the expression of Bmm/ATGL in flies (Wang et al., 2011) (Figure 1.6).

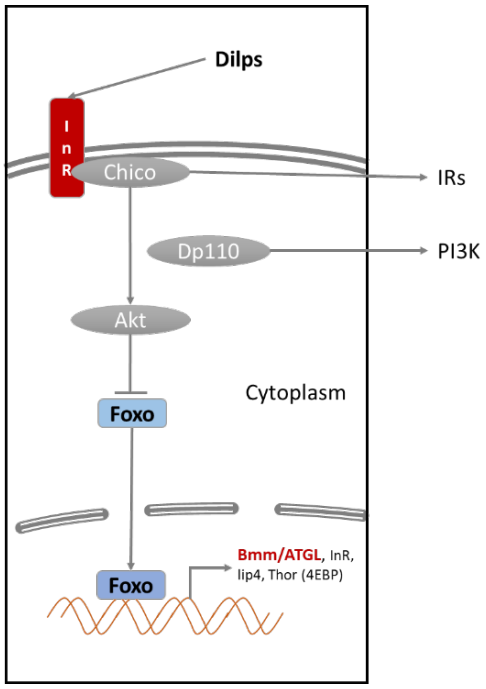

Figure 1.5 Regulation of Bmm/ATGL by insulin and FoxO.

Similar to mammals, high sugar diet leads to obesity and insulin resistance in *Drosophila*. During lipogenesis in fat body, the excessive dietary glucose can turn into acetyl- CoA that is the precursor of fatty acids and eventually produces TAG. This process protects flies against the harmful effect of excessive glucose (Musselman et al., 2013).

In *Drosophila* adults and larva there are cluster and ribbons of oenocytes in-between fat boy cells. Oenocyts are involved in fatty acids and hydrocarbon metabolisms. In larva, the very-long-fatty acids produced by oenocytes are required to waterproof the lining of tracheal. In adults, they are involved in desiccation resistance and pheromonal communications by producing cuticular hydrocarbons (Makki et al., 2014). Some studies suggest that oenocytes are hepatocyte-like cells that are involved in the regulation of lipid mobilization under starvation, acting downstream of the fat body. Interestingly, these cells develop large lipid vesicles upon starvation or local activation of Bmm/ATGL-mediated lipolysis, while under the fed condition they are almost empty of lipids (Arquier and Leopold, 2007; Gutierrez et al., 2007; Makki et al., 2014).

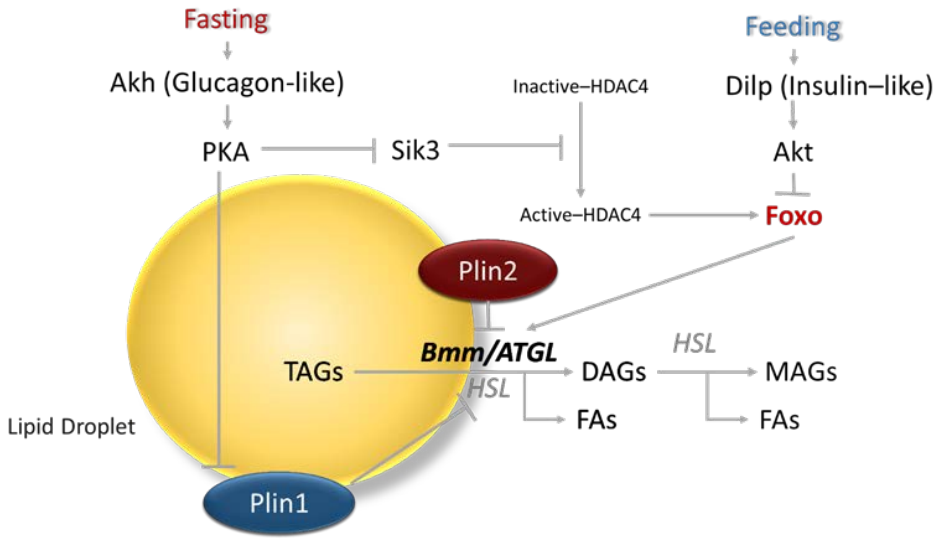

Figure 1.6 Hormonal regulation of TAG metabolism.

1.3.3 Innate immunity in flies

As opposed to vertebrates that possess both innate and adaptive immunity, insects only rely on innate immunity to combat infection. In *Drosophila*, epithelia provide the first barrier against infection. Insects also have chitin (polymer of *N*-acetyl-glucosamine) based layer (exoskeleton/cuticle) that covers external surfaces of their body (including tracheal tubes, foregut, and hindgut) and provides the first physical protective barrier against microorganisms. The second layer of protection in epithelia is chemical barrier. In the digestive tract of *Drosophila*, reactive oxygen species (ROS) cooperate with antimicrobial peptides (AMPs) to eliminate infection. The release of nucleotide uracil (U) by invading bacteria leads to induction of dual oxidase (DUOX) which is the first line of defense against enteric infection. DUOX is a member of NADPH oxidase family and can eliminate many of bacteria by producing microbicidal ROS (this process consumes NADPH). The basal levels of DUOX in gut kill yeast in the taken food while retaining the microbiota (Lemaitre and Hoffmann, 2007).

Interestingly, it is shown that enteric infection induces a metabolic reprogramming in the intestine, promoting lipolysis and limiting lipogenesis. This infection-induced lipolysis provides NADPH required for sustained DUOX activity and therefore, allows maintaining the immune response in the gut during enteric infection (Lee et al., 2018a).

Those microorganisms that overcome the epithelial barrier and enter the body cavity (hemocoel) encounter humoral and cellular immune responses. The cellular response of insect includes phagocytosis, melanization, and coagulation. *Drosophila* contains three different cell type (hemocytes) involved in immunity: plasmocytes, crystal cells, and lamellocytes. All these cells

have functional and morphological characteristic similar to vertebrate myeloid lineage (Lemaitre and Hoffmann, 2007).

Plasmatocytes are the majority of hemocytes (90-95%), they are round cells enriched in endoplasmic reticulum and lysosome. These cells are equivalent to mammalian macrophages and their major role in phagocytosis of dead cells, debris and invading pathogens. They are also involved in encapsulation and coagulation of foreign bodies (microbes) and produce AMPs (Gold and Bruckner, 2015). Furthermore, during infection, plasmatocytes can secrete Upd-3 (*Drosophila* cytokine implicated to septic injury) and therefore, activate JAK/STAT pathway, which is also linked to immune response against wasp infection (Dostert et al., 2005; Woodcock et al., 2015; Yang and Hultmark, 2017).

Another mechanism of defense in flies is RNA interference. This pathway is involved in the antiviral immunity against double stranded RNA viruses. In this pathway, double-stranded viral RNA is first cleaved by Dicer-2, then loaded onto Argonaute (AGO2), and eventually, targeted to degradation. This pathway provides a specific response to viruses and is required for removing viruses. (Galiana-Arnoux et al., 2006) Interestingly, it is shown that in mosquitos the RNAi pathway can lead to production of Vago molecules. Vago in turn induces JAK/STAT pathway, through an unknown receptor, and provides immunity in un-infected cells by induction of Vir-1 and some other uncharacterized antiviral factors (Paradkar et al., 2012).

Two major immune pathways conduct the humoral immunity of *Drosophila*: Imd and Toll (Figure 1.7). Induction of these pathways by various pathogens (gram-positive, gram-negative, or fungus) leads to activation of NF-κB transcription factors family. *Drosophila* genome encodes three NF-κB proteins. Dorsal, DIF (dorsal-related immunity factor) and Relish. All these proteins

contain a Rel homology domain (REL or RHD), which is conserved in mammals and flies, and Nuclear localization signal (NLS). Dif and Dorsal are 70kD proteins. Their REL homology domain has 45% similarities with their mammalian counterparts c-REL, Rel A, and Rel B (REL subfamily of NF-κB family) (Gilmore, 2006; Meng et al., 1999).

Dif and Dorsal both are involved in Toll pathway and under normal conditions are retained in cytoplasm by a protein named Cactus. Cactus is a 54kDa protein carrying ankyrin inhibitory repeats and is the orthologue of mammalian IκBs (inhibitor of NF-κB). Relish is a 100 kDa protein. The C-terminal of Relish contains ankyrin repeats, REL-49, which is similar to cactus and mammalian IκBs and inhibits nuclear localization of N-terminal REL homology domain (REL-68). Relish has the most similarities to mammalian p100 and p105 NF-κB family members (NF-κB subfamily of NF-κB family) (Gilmore, 2006; Stoven et al., 2000). A proteolytic cleavage removes C-terminal and results in its activation of Relish upon infection (Hultmark, 2003).

In non-infected cells, NF-κB TF family are retained in the cytosol by conserved ankyrin repeats (in cactus or Rel-49). Upon infection, degradation/cleavage of ankyrin repeats allows the release and nuclear translocation of NF-κB TFs. In the nucleus, NF-κB TFs induce transcription of multiple antimicrobial peptides (AMPs) (Hetru and Hoffmann, 2009). AMPs are secreted to hemolymph and play crucial role in host defense. Each organism has a repertoire of AMPs that may act on pathogen cell walls or intracellular compartments. Insects possess two major groups of AMPs: alpha-helical cecropin that fights against Gram-negative bacteria, and disulfide-bridge defensins that are effective on gram-positive bacteria. *Drosophila melanogaster* also produces drosomycin (Drs) which is an antifungal peptide (Lemaitre and Hoffmann, 2007).

In *Drosophila*, fungi and gram-positive bacteria (and gram-negative bacteria to a lower degree) activate Toll pathway (named after transmembrane receptor Toll) through spätzle cytokine (a neurotrophin-like cytokine that acts as Toll receptor ligand). Upon sensing nonself-components such as YS type peptidoglycan or β-glucan by peptidoglycan recognition receptors (PPARs), a protease cascade converts pro-spätzle to active spätzle that can bind to Toll receptor. Through several mediator/adaptors including MyD88, activation of Toll receptor leads to phosphorylation and degradation of Cactus inhibitory protein (homologous of mammalian IκB, NF-κB inhibitor). The degradation of cactus allows the Dif/Dorsal NF-κB transcription factor to translocate to the nucleus. In the nucleus Dif/Dorsal can bind to corresponding Dif/Dorsal target genes including drosomycin (Drs), defensin (Def) and several other AMPs and upregulate their transcription (Valanne et al., 2011) (Figure 1.7A).

Imd pathway (named after immune deficiency (Imd) gene) is activated by gram-negative bacteria as well as some gram-positive bacteria. In this pathway, PGRPs (peptidoglycan recognition protein) can sense meso-diaminopimelic acid (DAP)-type peptidoglycan that presents in cell wall of the most gram-negative bacteria. PGRP-LC is a transmembrane receptor that senses poly peptidoglycans (poly PGN). While PGRP-LE is an intracellular receptor that can respond to monomeric peptidoglycan (Royet, 2004). PGRP receptors activation initiate the activation and nuclear localization of NF-κB Relish Transcription factor. This process involves several molecules such as immune deficiency (Imd) and Fas-associated protein with dead domain (FADD) mediators, dead –related ced-3/Nedd2-like (DREDD) caspase, TAK1 associated binding protein 1 (TAB2), transforming growth factor β (TGF-β)-activated kinase 1 (TAK1) and inhibitor of κB kinase (IKK) complex/signalosome (Myllymaki et al., 2014).

PGRP receptors bind to Imd mediator upon infection. Imd is itself associated with FADD mediator and DREDD caspase. Dredd can cleave Imd. Then, the cleaved Imd promotes the recruitment of TAB1/TAK1 complex and activation of TAK1. In fact, Activation of TAK1 and IKK signalosome requires the activity of FADD and DREDD caspase. TAK1 (along with E3 ubiquitin ligase Uev1A/Ubc13) activates IKK (IκB kinase) complex. IKK complex/signalosome consist of IKK-β (Ird5) which is a kinase, and its regulatory subunit, IKK-γ (Key or Kenny). IKK-β (Ird5) promotes proteolytic cleavage of ankyrin repeats of NF-κB Relish by Dredd caspase, through phosphorylation of ankyrin repeats presents in inactive form of NF-κB Relish (Stoven et al., 2000). Cleaved NF-κB Relish (Rel-68) then can translocate into the nucleus, where it can bind to NF-κB response elements and induce the expression of several AMPs including diptericin (Dpt) and drosocin (Dro) (Myllymaki et al., 2014) (Figure 1.7B).

Imd and Toll pathway are conserved and have remarkable similarities to mammalian TLR/IL-1R (interlukin-1 receptors) and TNFR (TNF-α receptor) pathways (Hetru and Hoffmann, 2009).

Fat body is defined as the main tissue secreting AMPs into hemolymph (systemic immune response) via activation of Imd and Toll pathways. However, Imd pathway is also described in other tissues such as gut, trachea, and brain. Activation of Dredd (independent of upstream signaling) in the brain, leads to Relish-mediated-AMP production that can be involved in neurodegeneration. In the gut, several negative regulators such as Pirk (interacts with the receptor and Imd) and Caudal (Cad, intestinal homeobox gene) prevent extensive activation of Imd pathway which might be mediated by gut microbiota. These negative regulators play an important role in

maintaining immune tolerance in the gut. However, pathogens are still capable of inducing Imd pathway due to producing more PGN (Kleino et al., 2008; Ryu et al., 2008).

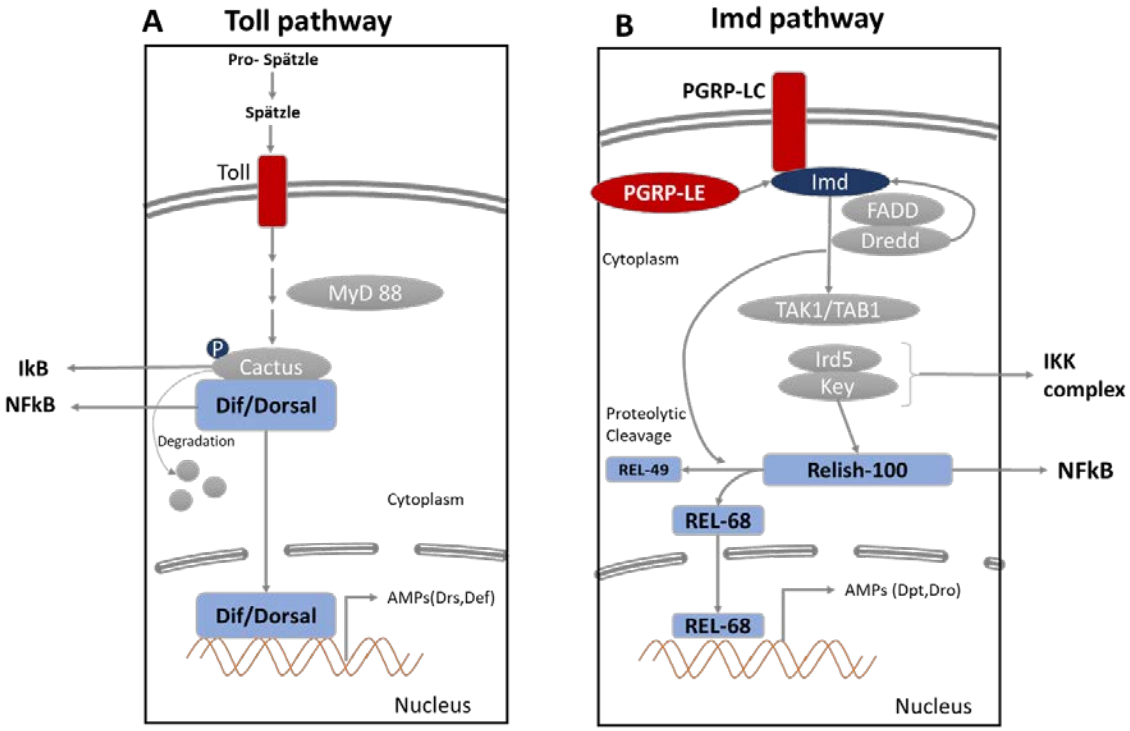

Figure 1.7 Innate immune signaling pathways in *Drosophila*.

1.4 NF-κB signaling pathway

1.4.1 An overview

The NF-κB signaling pathway is the main regulator of innate immunity in both mammals and flies (Silverman and Maniatis, 2001). In addition to immune response, this pathway plays role in the regulation of different processes such as promotion of cell proliferation, inhibition of apoptosis, cell migration and invasion, and metabolism (Gilmore, 2006).

Mammalian genomes carry five different NF-κB proteins: RelA (p65), RelB, c-Rel, NF-κB1 (p105/p50) and NF-κB2 (p100/p52) (Tieri et al., 2012). *Drosophila* genome encodes only 3

types of NF-κB molecules: Relish, Dorsal and Dif. Relish has similarities to mammalian p105 and p100. Indeed, they all carry ankyrin inhibitory repeats and undergo a proteolytic cleavage prior to nuclear localization. While Dorsal/Dif shares more similarities with RelA (p65), RelB, c-Rel. All NF-κB molecules carry conserved Rel-homology domain which is required for DNA binding and dimerization (Hetru and Hoffmann, 2009). These molecules can shape varieties of dimers. However, the most common type of dimers in mammals are p50/RelA and p52/RelB (Gilmore and Wolenski, 2012).

NF-κB pathway can be induced by several stimuli such as bacteria, viruses, oxidative stress (ozone, hydrogen peroxide, butyl peroxide), physical stress, physiological stress (hyperglycemia, hyperoxia), cytokines, physiological mediators (L-glutamate, lysophosphatidylcholine), DNA damage, and growth factors. NF-κB transcription factors have more than 150 target genes including cytokines, chemokines, antioxidant and stress response genes, immune receptors and growth factors (Pahl, 1999; Tieri et al., 2012). However, clearly, not all of these genes are expressed in all cells. This can be due to combinatorial response of promoter/enhancer regions as well as selective activation/dimerization and binding of NF-κB proteins. In addition, other factors and regulators such as TFs and epigenetic modifications assist NF-κB in the regulation of genes. Regulation of many of NF-κB target genes requires the collaboration of NF-κB with another transcription factor. Several studies have reported co-regulation of NF-κB target genes with STAT, AP1, and IRFs (Grivennikov and Karin, 2010; Oeckinghaus et al., 2011; Zhong et al., 2006).

Induction of pattern recognition receptors (PRRs) such as Toll-like receptors (TLRs) by different NF-κB ligands leads to the activation of NF-κB signaling pathway. For example, LPS of gram-negative bacteria can activate TLR4, which is a receptor involved in NF-κB classical

pathway. This signal is transferred to IKK complex through several mediators including MyD88. IKK complex consists of three subunits: IKKα and IKKβ are regulatory subunits, while IKKγ (also known as NEMO) serves as catabolic subunits and has protein phosphorylation activity. IKK (IκB kinase) activates NF-κB TFs by phosphorylation of IκB α inhibitory protein (containing Ankyrin repeats). This phosphorylation leads to degradation of IkB α protein and therefore, allows the release and nuclear translocation of NF-κB TF (Gilmore and Wolenski, 2012)(Figure 1.8).

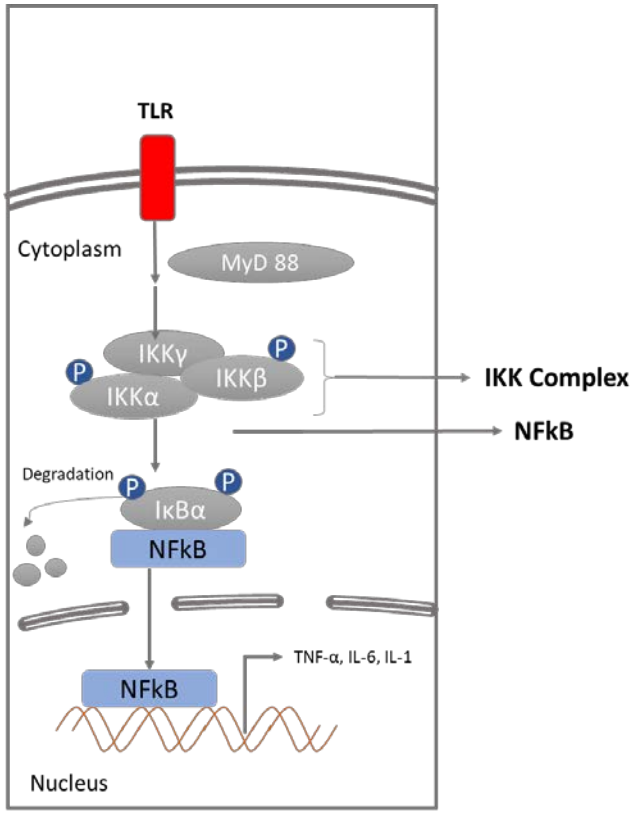

Figure 1.8 Classical NF-κB signaling pathway in mammals.

1.4.2 NF-κB signaling pathway and metabolism

An overwhelming number of studies have demonstrated that NF-κB pathway can affect metabolism in both health and disease condition. Most of the reported cases are through the role

of NF-κB in the inflammation and insulin resistance (Baker et al., 2011; Tornatore et al., 2012). However, recently, more direct mechanisms of the interaction of NF-κB pathway and metabolic system have reported. Some of these studies are discussed here.

Insulin resistance: NF-κB pathway can act as a nutritional sensor. Induction of NF-κB pathway by fatty acids, chronic overnutrition or high sugar diet, IL-1, TNF-α, or LPS lead to the expression of inflammatory cytokines including TNF-α and IL-6. These inflammatory cytokines then reduce insulin sensitivity by phosphorylation of insulin receptor (IRS) (Tornatore et al., 2012). Additionally, IL-6 can decrease the expression of glucose transporter- 4 (GLUT-4) and IRS-1 through activation of JAK-STAT signaling pathway (a cytokine-activated pathway involved in cell proliferation, differentiation, and apoptosis). This decrease leads to less sensitivity to insulin. Also, in muscle IL-6 can induce the expression of TLR-4 which is the receptor involved in the NF-κB pathway (Chen et al., 2015; Henstridge et al., 2012; Kim et al., 2013; Lukic et al., 2014).

Toll-like receptors (TLRs) play an important role in obesity- and diet-induced insulin resistance. These upstream receptors of NF-κB signaling pathway can be activated by several ligands including pattern-associated molecular receptors (PAMPs), endogenous ligands (saturated fatty acids, Ox-LDL) and LPS. Induction of TLR4 with fatty acids has been linked to insulin resistance-associated inflammation. This effect is through increasing the expression of IKKβ (IκB kinase), NF-κB TFs and pro-inflammatory mediators such as MCP1, IL-6, and IL-1β in adipose tissue macrophages. These changes lead to induction of M1 macrophages phenotype and eventually development of insulin resistance. The increased levels of TLR4 and TLR2 mRNA as

well as increased TLR4 signaling has been reported in obesity and type 2 diabetes (Jialal et al., 2014; Lee et al., 2003; Yin et al., 2014)

Similar to mammals, *Drosophila* can develop both systemic and tissue-specific insulin resistance in response to high sugar diet (HSD). In both mammals and flies, obesity-induced insulin resistance leads to more infection susceptibility. This effect in *Drosophila* is associated with regulation of insulin receptor (InR) in the fat body. Activation of insulin signaling can reduce immune response (AMP gene expression), while the host resistance and expression of immune genes are increased upon insulin signaling inactivation (Musselman et al., 2018).

Studies in *Drosophila* have linked insulin resistance to Imd/Relish pathway. Downregulation of PGRP-SB2 (negative regulator of Imd/Relish pathway) in the fat body can protect flies against obesity-induced insulin resistance (Musselman et al., 2017, 2018).

Mitochondrial function: Several studies have linked NF-κB to metabolism through regulation of mitochondrial function. Indeed, NF-κB plays role in creating a balance between glycolysis and oxidative phosphorylation. Interestingly, a crosstalk between NF-κB and p53 in the context of metabolism in cancer cells has been reported. For example, it is shown that NF-κB can upregulate expression of synthesis of cytochrome c oxidase 2 (SCO2), a subunit of complex IV of the electron chain in mitochondria. This upregulation stimulates mitochondrial respiration (Mauro et al., 2011). However, in P53 deficient cells, NF-κB facilitates glycolysis through induction of GLUT3 (SLC2A3). GLUT3 expression leads to enhanced glucose uptake and glycolytic flux. It

also inhibits oxidative phosphorylation and promotes the development of Warburg effect[6]. In addition, during a positive feedback loop, produced O-linked β-N-acetyl glucosamine activates IKKβ/NF-κB pathway (Johnson and Perkins, 2012; Johnson et al., 2011; Mauro et al., 2011).

In the context of cancer, NF-κB also is linked to cachexia. Cancer cachexia is a multifactorial wasting syndrome characterized by anorexia and weight loss. It is shown that attenuation of NF-κB activity ameliorates cachexia in cancerous mice by decreasing IL-6 and TNF-α activity (Kuroda et al., 2007; Zhou et al., 2003).

NF-κB and lipid metabolism: NF-κB is involved in the regulation of lipid metabolism through its effect on PPAR-γ[7]. NF-κB can inhibit PPAR-γ activity through several mechanisms. It is shown that chronic activation of NF-κB results in suppression of expression of PPAR-γ gene (decreased transcription) (Nunn et al., 2007). On the other hand, acute activation of NF-κB leads to activation of TNF-α which in turn inhibits PPAR-γ transcriptional activity by recruiting HDAC3 to the nucleus. HDAC3 is one of the co-repressors of PPAR-γ transcriptional activity. Therefore, translocation of HDAC3 can decrease the function of this PPAR-γ without affecting its DNA binding affinity (Gao et al., 2006). Additionally, fatty acids can modulate NF-κB pathway through TLR 2 and TLR4 receptors (Lee et al., 2003; Yin et al., 2014).

---

[6] Warburg effect is the usage of glycolysis (glucose fermentation/anaerobic metabolism) to produce energy (even when oxygen is available) rather than oxidative phosphorylation which is used by other normal cells. Indeed, this seems to favor and provide benefits for the development of cancer.

[7] PPAR-γ is linked to adipocyte differentiation and hypertrophy as well as glucose and lipid metabolic disorders in cancer and inflammation conditions. This nuclear receptor decreases the production of pro-inflammatory cytokines and NFkB transcriptional activity. It also, can increase the expression of IRS proteins, therefore, limits inflammation and improve insulin sensitivity.

1.4.3 NF-κB and regulation of gene expression

NF-κB transcription factors are involved in both activation and repression of genes. More than 150 target genes are reported for NF-κB transcription factors. In addition to direct regulation of the genes, these TFs can also affect expression of more genes through crosstalk with other pathways and signaling molecules. Also, combinatorial regulation of genes with other TFs are reported. For example, it is shown that NF-κB pathway can interaction with STAT3, p53, IRF, NRF2, JNK, WNT, and notch (Oeckinghaus et al., 2011). These crosstalk and co-regulations allow more complex and precise regulation of genes in different cell types and tissues according to different inputs, and create a complex NF-κB interactome (Oeckinghaus et al., 2011; Taniguchi and Karin, 2018; Tieri et al., 2012).

NF-κB TFs also contribute to the regulation of the genes via expression or repression of miRNAs (Boldin and Baltimore, 2012; Mann et al., 2017; Markopoulos et al., 2018). This effect on miRNA levels can be direct or indirect (through induction of other inhibitors). For example, it is shown that NF-κB can regulate expression of let-7 miRNA (inhibitor of IL-6 mRNA) indirectly through expression of Lin-28B. Lin-28B is an inhibitor of Let-7 expression. It can also regulate Let-7 at posttranscriptional level (Iliopoulos et al., 2009).

Another level of complexity of NF-κB interactome has arisen from recruitment and utilization of coactivators and corepressors. These coregulators of transcription are molecules that lack DNA-binding activity/specificity. Therefore, they need to bind to special chromatin modifications or transcription factors or other regulatory proteins in order to play their role in the regulation of the target genes. Several coactivators and corepressors assist NF-κB in the regulation of different genes. Examples of coactivators are P300/CBP, p/CA and p160 proteins (SRC 1-3).

These coactivators facilitate transcription by opening chromatin structure, which is induced by their histone acetylation activity. It is known that acetylation of histones is associated with open chromatin and increased expression of the genes (Gao et al., 2005).

Amongst co-repressors there are HDAC1-3 (class I histone deacetylases), SMRT and NCoR. These corepressors can shape different complexes such as HDAC1/SMRT and HDAC3/NCoR. In flies, SMRTER (EcR-interacting protein) is functional homolog of vertebrates SMRT and NCor co-repressors. SMRTER forms a complex with Sin3A repressor, which in turn interacts with Rpd3 (HDAC1). These co-repressors are involved in the repression of NF-κB target genes through catalyzing histone deacetylation at regulatory regions of genome (Ashburner et al., 2001).

In contrast to histone acetylation, non-acetylated histones are representative of compact regions of genome with none or less transcription. Furthermore, these regions are usually characterized by DNA hyper-methylation (epigenetic mark involved in regulation of genes) at CpG islands too (Gao et al., 2005; Guzik and Cosentino, 2018; Shakespear et al., 2011).

Notably, in addition to histones, some non-histone proteins are the targets of HDACs. Several studies have shown that HDACs are involved in the regulation of immune and metabolic pathways (Shakespear et al., 2011; Toubal et al., 2013). For example, HDAC2 and HADC3 are reported to be involved in the regulation of inflammatory genes. Indeed, HADC3 contributes to the expression of inflammatory cytokines in macrophages. It is shown that HDAC3-deficient macrophages are unable to induce some of inflammatory cytokines. This effect is due to loss of expression of IFN-β (Chen et al., 2012b). In contrast, HDAC2 (recruited by Tet2) acts as a repressor of inflammation via inhibiting IL-6 pro-inflammatory cytokine (Zhang et al., 2015).

Interestingly, a study in mouse using NF-κB p65 mutant (carrying alanine instead of serine at position 276) has shown that unphosphorylated NF-κB p65 contributes to the repression of the genes that are not normally regulated by this transcription factor. In fact, this unphosphorylated NF-κB binds to NF-κB binding motif and recruits HDAC3 instead of CBP/p300, which results in the direct repression of NF-κB target genes as well as, epigenetically repression of some other genes, such as pax6 (Dong et al., 2008).

Related to infection, it is shown that NF-κB is involved in the HDACs-dependent repression of mir-424 and mir-503 in response to microbial challenge. Upon C. parvum infection, NF-κB and HDAC1/2 are recruited to the promoter region of mir-424 and mir-503. This results in a decrease in histone acetylation and therefore, decrease in the expression of these genes (Zhou et al., 2013).

Another example of NF-κB/HDAC1-dependent repression is reported in IL-1β-mediated repression of gastrin, which is an acid modifying hormone in the intestine. In IL-1β-untreated AGS cell (human gastric cancer cell line), NF-κB (p50/p65 dimer) can activate the expression of gastrin by recruitment of p300 coactivator. However, after IL-1β treatment, NF-κB inhibits expression of gastrin by recruiting HDAC1/NcoR corepressors rather than p300 (Datta De et al., 2013).

Recruitment of HDACs in order to repress the expression of NF-κB target genes might be indirect and through other factors. For example, in *Drosophila* it is shown that pickle (an IκB protein) can bind to Relish homodimer at the promoter region of some immune genes and repress their expression by recruiting HDAC1(upd3). This inhibitory effect of pickle on immune genes is

important in maintaining proper immune response in the gut while preventing the over-activation of immune genes which might be harmful for the organism (Morris et al., 2016).

Similarly, in mammals it is reported that IκBα (an upstream component of NF-κB pathway) can mediate translocation of HDAC3 in response to TNF-α induction. This recruitment of HDAC3 inhibits the transcriptional activity of PPARɣ without affecting its DNA binding affinity (Gao et al., 2006).

Notably, it has been shown that different genes are regulated by different corepressors or coactivators and not all factors are involved in the regulation of a single gene. In addition, corepressors and coactivators might be recruited to promoter simultaneously and in oscillation trend. Furthermore, the repression of genes by transcription factors is context-dependent. This allows the precise and specific regulation of NF-κB target genes in different tissues (van Dijk et al., 2017).

1.5 Summary

Starvation and infection are two primitive challenges in multicellular organisms. In order to combat these ancient stressors, organisms have developed integrated and co-regulated innate immune and metabolic signaling pathways. The crosstalk between these systems is vital to maintain homeostasis while encountering different immune or metabolic stressors. While these pathways share regulatory axes and nodes in order to coordinate their responses, misregulation of these pathways arisen from over-nutrition or mutation may lead to the development of pathologies such as systemic inflammation, obesity, insulin resistance, and fatty liver.

Many studies have linked NF-κB signaling pathway, the main regulator of innate immunity in both mammals and flies, to metabolism, particularly through its role in inflammation. In addition, recently, some studies provide more evidence on the more intimate relationship and direct regulation of metabolic genes by NF-κB transcription factors, such as its role in regulation of GLUT3 and SCO2. Altogether, these studies provide evidence that NF-κB serves as a central node in the bidirectional communication of innate immune and metabolic pathways. Therefore, there is a critical need to further uncover tissue and cell-autonomous mechanism by which NF-κB may affect metabolic homeostasis.

However, due to the extreme complexity of immune and metabolic pathways, uncovering the underlying mechanism is difficult in mammals. Herein, *Drosophila melanogaster* has emerged as an invaluable model organism to study the integration of innate immune and metabolic systems. While innate immune and metabolic pathways are more primitive in flies compared to mammals, they still share conserved fundamental components and domains. Furthermore, fat body (equivalent to mammalian adipose tissue and liver) in *Drosophila* carries on both innate immune and metabolic function. Therefore, this tissue provides a unique model to study the integration of these pathways.

My research aimed to first, explore the effect of NF-κB on lipid homeostasis, and subsequently, uncover the potential tissue and cell-autonomous mechanism of this effect. Uncovering this effect and mechanism will help us to better understand the underlying mechanism of NF-κB-associated disease, and eventually, will open new avenues for innovation of medications aimed to target proper molecules in order to cure these disorders.

2. MATERIALS AND METHODS[8]

2.1 *Drosophila* Husbandry and Strains

A detailed list of fly strains used for these studies is provided in Table 2.1. All flies were reared on standard yeast and cornmeal-based diet at 25°C and 65% humidity on a 12 hr light/dark cycle, unless otherwise indicated. A standard lab diet (cornmeal-based) for rearing was made with the following protocol: 14g Agar/165.4g Malt Extract/ 41.4g Dry yeast/ 78.2g Cornmeal/ 4.7ml propionic acid/ 3g Methyl 4-Hydroxybenzoate/ 1.5L water.

In order to standardize metabolic results, 2-3 days after eclosion, mated adult flies were placed on a simple sugar-yeast (SY) diet for 5 days. The standard SY diet was made with the following protocol: 1.0g agar/10g sucrose/ 10g yeast/ 0.3 ml propionic acid/ 100 ml water/ 1.5 mL Methyl 4-Hydroxybenzoate. Ingredients were combined, heated to at least 102°C, and cooled before pouring. The high sugar diet (Figure 3.2B) was prepared as follows: 1.5 g agar/30 g sucrose/10 g yeast/0.3 ml propionic acid/100 ml water.

For RU486 food, RU486 or vehicle (ethanol 80%) was mixed with food (SY diet), resulting in a 200 uM concentration of RU486 in the food, unless otherwise indicated.

All experiments presented in the results were done utilizing female flies 7 days old post-eclosion (following dietary protocol referenced above) with the exception of data from males (also 7 days old post-eclosion) presented in Figure 3.7.

---

[8] Reprinted with permission from Molaei, M., C. Vandehoef, and J. Karpac, "NF-kappaB Shapes Metabolic Adaptation by Attenuating Foxo-Mediated Lipolysis in Drosophila." Dev Cell, 2019. 49(5): p. 802-810 e6. Copyright 2019 Elsevier.

The UAS-Relish^{RNAi} (both trangenic lines), UAS-FoxO^{RNAi}, UAS-Kenny^{RNAi}, UAS-Dredd^{RNAi}, UAS-Bmm^{RNAi}, UAS-PGRP-LC^{RNAi}, UAS-PGRP-LE^{RNAi}, CGGal4, PplGal4, and HmlGal4 lines used throughout the paper were backcrossed 8-10X into the w^{1118} background that was used as a control strain. The ebony mutation/marker e^{S} was removed from the rel^{E20} mutant background, with the rel^{E20} mutation finally outcrossed into a wild-type (OreR) background.

The efficiency of transgenic RNAi lines UAS-Relish^{RNAi} (VDRC: 108469 (KK) and VDRC: 49413 (GD)), UAS-Kenny^{RNAi} (VDRC: 7723 (GD)) and UAS-Dredd^{RNAi} (VDRC: 104726 (KK)) were confirmed in this study. The efficiency of transgenic RNAi lines UAS-FoxO^{RNAi} (VDRC: 106097 (KK)), UAS-Bmm^{RNAi} (VDRC: 37877 (GD)), UAS-PGRP-LC^{RNAi} (VDRC: 101636 (KK)), UAS-PGRP-LE^{RNAi} (VDRC: 23664 (GD)), and UAS-Rpd3^{RNAi} (TRiP: 36800) were confirmed in previous studies.

Table 2.1 The list of fly lines used in this study

Fly Line	Source	Identifier
D. melanogaster: w^{1118}	Bloomington *Drosophila* Stock Center	BDSC: 3605; FlyBase: FBst0003605
D. melanogaster: w*; P{ppl-GAL4.P}2	Bloomington *Drosophila* Stock Center	BDSC: 58768; FlyBase: FBst0058768
D. melanogaster: UAS- luciferase RNAi (y^1v^1; P{TRiP.JF01355}attP2)	Bloomington *Drosophila* Stock Center	BDSC: 31603; FlyBase: FBst0031603
D. melanogaster: w*;; *FoxO$^{\Delta 94}$*/TM6B, Tb1 *(w^{1118}; FoxOΔ94/TM6B, Tb1)*	Bloomington *Drosophila* Stock Center	BDSC: 42220; FlyBase: FBst0042220
D. melanogaster: UAS-FoxO RNAi (y^1w*; P{**KK**108485}VIE-260B)	Vienna *Drosophila* RNAi Center	VDRC: 106097; FlyBase: FBst0477923
D. melanogaster: w*; P{CG-GAL4.A}	(Hennig et al., 2006)	N/A
w^*;; *rel^{E20}*, *e^s*	Bloomington *Drosophila* Stock Center	BDSC: 9457; FlyBase: FBst0009457
D. melanogaster: w^-; UAS-Relish (w^{1118}; P{UAS-Rel.His6}2; l(3)**/TM3, Sb1)	Bloomington *Drosophila* Stock Center	BDSC: 9459; FlyBase: FBst0009459
w^-;; *$FoxO^{w24}$* / TM3	(Weber et al., 2005)	N/A
y^1w^-; TubGeneSwitch/ CyO	(Sykiotis and Bohmann, 2008)	N/A

Table 2.1 Continued

Fly Line	Source	Identifier
w*; UAS FLAG-Rel 68 (w*; P{UAS-FLAG-Rel.68}i21-B; TM2/TM6C, Sb1)	Bloomington *Drosophila* Stock Center	BDSC: 55778; FlyBase: FBst0055778
D. melanogaster: UAS-Bmm RNAi (GD) (w*; P{**GD**5139}v37877)	Vienna *Drosophila* RNAi Center	VDRC:37877; FlyBase: FBst0462214
D. melanogaster: UAS-Key RNAi (GD) (w*; P{**GD**1249}v7723)	Vienna *Drosophila* RNAi Center	VDRC:7723; FlyBase: FBst0470808
D. melanogaster: UAS-Dredd RNAi (KK) (P{**KK**110428}VIE-260B)	Vienna *Drosophila* RNAi Center	VDRC: 104726; FlyBase: FBst0476565
D. melanogaster: UAS-Rel RNAi (GD) (w*; P{**GD**1199}v49413)	Vienna *Drosophila* RNAi Center	VDRC:49413; FlyBase:FBst0468440
D. melanogaster: UAS-Rel RNAi (KK) (w*; P{**KK**109851}VIE-260B)	Vienna *Drosophila* RNAi Center	VDRC: 108469; FlyBase: FBst0480279
D. melanogaster: UAS-Rpd3 RNAi (y^1 sc^* v^1; P{TRiP.GL01005}attP40)	Bloomington *Drosophila* Stock Center	BDSC: 36800; FlyBase: FBst0036800
OreR (Oregon-R-C)	Bloomington *Drosophila* Stock Center	BDSC: 5
w^{1118}; Bmm_Int_Δ1-RFP	This study	N/A
w^{1118}; Bmm_Int_WT-RFP	This study	N/A
D. melanogaster: UAS-PGRL-LC RNAi (KK) (P{**KK**105287}VIE-260B)	Vienna *Drosophila* RNAi Center	VDRC: 101636; FlyBase: FBst0473509
D. melanogaster: UAS-PGRL-LE RNAi (GD) (w^{1118}; P{**GD**14089}v23664)	Vienna *Drosophila* RNAi Center	VDRC: 23664; FlyBase: FBst0455134
D. melanogaster: UAS-Sir2 RNAi (GD) (w^{1118}; P{**GD**11580}v23201)	Vienna *Drosophila* RNAi Center	VDRC: 23201; FlyBase: FBst0454875
D. melanogaster: UAS-AMPKalpha RNAi (GD) (w^{1118}; P{**GD**736}v1827)	Vienna *Drosophila* RNAi Center	VDRC:1827; FlyBase: FBst0453086
D. melanogaster: w*; Hml-Gal4 (Delta) (w^{1118}; P{Hml-GAL4.Δ}2)	Bloomington *Drosophila* Stock Center	BDSC: 30139; FlyBase: FBst0030139

2.2 Generation of Transgenic Flies

To create transgenic flies carrying Brummer/NF-κB expression reporters (Bmm_Int_WT-RFP and Bmm_Int_Δ1-RFP), 300 bp of Bmm/ATGL locus containing κB binding site was selected. The DNA fragment carrying wild-type or mutated (6 bp deletion) κB binding site were synthesized using gBlock technology (Integrated DNA Technology) and cloned into a ϕ31-based

DsRed (Chatterjee and Bohmann, 2012).T4 plasmid reporter system. Finally, the constructs were injected into w^-, attP40 embryos (Rainbow Transgenic Flies, Inc) (Table 2.5).

Bmm/ATGL intronic region containing wild type κB binding site:

GCATGCACGCATTGAATTGAATTTTATTGATAAGCTTGTTTGCGTTTGTAGGT
CGCTAGGAAGTCAATGGGGATCTTTCATAATTGACTGCGATAGTGTGTGTGTTTT
TGGGCGTGTTTGTCCAATTTCGAAGGGGGCTCGTCCCATCCGCTCAAAAGAAAACTG
CGGCGCAGTTGAAAAACCTTACGAAAACAGAAAAACAAGTTTCGTATGCCCGGGAC
AACGCACTTTTGTAAAGCGGCACCCGAATATATGGGCAAATGGTTGGGCACAGCGG
TGGGTATATGAATAGCAACGCAGTCCGAAAACATTTCATCAAACTCGAG

Bmm/ATGL intronic region containing mutant κB binding site:

GCATGCACGCATTGAATTGAATTTTATTGATAAGCTTGTTTGCGTTTGTAGGT
CGCTAGGAAGTCAATGTTTCATAATTGACTGCGATAGTGTGTGTGTTTTTGGGCG
TGTTTGTCCAATTTCGAAGGGGGCTCGTCCCATCCGCTCAAAAGAAAACTGCGGCGC
AGTTGAAAAACCTTACGAAAACAGAAAAACAAGTTTCGTATGCCCGGGACAACGCA
CTTTTGTAAAGCGGCACCCGAATATATGGGCAAATGGTTGGGCACAGCGGTGGGTA
TATGAATAGCAACGCAGTCCGAAAACATTTCATCAAACTCGAG

2.3 *de novo* Lipid Synthesis Analysis

After 5 days of feeding on standard diet, 200 female flies were transferred to a bottle containing standard diet with 2μCi of ^{14}C-labeled glucose (thatched into the top of food). After 1.5 hrs or 16 hrs feeding, total lipid was extracted from 5 flies for each sample (Fed samples). The

other half were transferred to starvation vials (water only) and total lipids were extracted immediately after 12 hrs of fasting (Fasted samples). For extraction of total lipids, 5 flies for each sample were homogenized in 2 ml Folch reagent ($CHCl_3$: MeOH 1:1 v/v). Then, 0.4 mL of cold 0.1 M KCl was added, thoroughly mixed by 1 min vortexing and then spun down at 3000 rpm, 4°C for 5 min. The lower phase was transferred to a glass tube and dried down. Dried lipids were re-suspended in 3 ml of scintillation fluid and CPM was counted using a liquid scintillation analyzer (Packard- 2500 TR). Fed samples were indicative of the rate of incorporation of glucose into lipids and Fasted samples were indicative of the breakdown of the labeled lipids.

2.4 Analysis of Gene Expression

Total RNA from the whole bodies or dissected fat body/carcass (with all of the eggs and intestines removed) of flies were extracted using Trizol and complementary DNAs were synthesized using Superscript III (Invitrogen). Quantitative Real-Time PCR (qRT-PCR) was performed using SYBR Green, the Applied Biosystems StepOnePlus Real-Time PCR system, and the primer sets described in Table 2.2. Results are the average ± standard error of at least three independent biological samples, and quantification of gene expression levels calculated using the ΔCt method and normalized to *actin5C* expression levels.

2.5 Metabolite Measurements

For triglyceride (TAG) assays, five beheaded adult females were homogenized in 200 µl of PBST (PBS, 0.1% Tween 20) and heated at 70°C for 5 min to inactivate endogenous enzymes. Samples were centrifuged at 4000 rpm for 3 min at 4 °C and 10 uL of the cleared extract were

used to measure triglycerides (StanBio Liquicolor Triglycerides Kit) or protein concentrations (Bio-Rad Protein Assay Kit) according to the manufacturer instructions. TAG levels were normalized to weight or protein levels depending on genotype (some genotyped reveal drastic changes in wet weight after starvation that limits interpretation of normalized metabolite data). Note: The kit measures glycerol cleaved from TAG and diacylglycerol (DAG), as well as minimal amounts of free glycerol; the majority of neutral lipids extracted from whole flies are TAG.

The levels of free fatty acids (FFAs) were measured using the Free Fatty Acid Quantification Kit (Sigma-Aldrich), following the manufacturer's instruction. Metabolite samples preparation was the same as described for TAG measurements.

Table 2.2 List of primer used in qRT-PCR

Gene	Forward	Reverse
Relish	CATCAGGAGACAGAGCGTGA	CCGACTTGCGGTTATTGATT
Kenny	TGACAAGGTCAACCAAACCA	CCTGCTCCTTTAGCCTGATG
Dredd	CAGGAGATCCACTTCGCTTC	CGACTGCTGGTTATCCGATT
Brummer	CAATAAGGGTCTGGCCAACTGGAT	TAAGTCCTCCACCATTACTCTGGC
dHSL	ATGAGTGGCTTTCCCAACTG	CATGGCTTCGTTGGATAACA
dLip4	TGGATAGCTCAGCCACTT	GCGGGTATATCATGCTTTCC
CG5966	CTGCAATCACATTCGCAGTC	TGCTCCTGGTAATCCTCCTG
YIP2	CGGTCTTAAGGGTGAGCAA	ACATTACGGGCAATGAAAGG
dACC	CTATCGCTATGGTTACCTGCCGTA	AACATGATCTGTGTGCCACCCAA
dFASN1	TGATGGCCGGTATTCTGGAAGAGA	ATTGCTCATCAGCTCAGCGAACCT
Dipt	TTCATTGGACTGGCTTGTGCCTTC	TGAGGCTCAGATCGAATCCTTGCT
Drs	AAGTACTTGGCCCTCTTCGCT	TCCTTCGCACCAGCACTTCAGACT
FoxO	TCTCGCCGAACTCAGTAACC	CCTCCAGGCATTGTCCTATC
Thor	CACTTGCGGAAGGGAGTACG	TAGCGAACAGCCAACGGTG
Actin5c	CTCGCCACTTGCGTTTACAGT	TCCATATCGTCCCAGTTGGTC

2.6 Oil Red O staining

Intestines and fat body/carcasses (with all of the eggs and intestines removed) of flies were dissected in PBS and fixed in 4% paraformaldehyde for 20 min, then washed twice with PBS, incubated for 20 min in fresh Oil Red O solution (6 ml of 0.1% Oil Red O in isopropanol and 4 ml distilled water, and passed through a 0.45 µm syringe), followed by rinsing with distilled water. Bright-field images were collected using a Leica M165 FluoCombi stereoscope system (utilizing a single focal plane) and processed using Leica software and Adobe Photoshop. Note: Contrast (red – neutral lipids vs. yellow/black – cuticle) was enhanced using Adobe Photoshop (equal for all images) in order to better visualize the red stain.

2.7 Nile Red staining

Fat body/carcasses were dissected in PBS (with all of the eggs and intact intestines removed) and fixed in 4% paraformaldehyde for 20 min. Fixed carcasses were then washed twice with PBS, incubated for 30 min in fresh Nile Red solution with DAPI (1µl of 0.004% Nile Red Solution in 500 µl PBS), followed by rinsing with distilled water. Confocal images were collected using a Nikon Eclipse Ti confocal system (utilizing a single focal plane) and processed using Nikon software and Adobe Photoshop.

2.8 Immunostaining and Microscopy

Flies were dissected in PBS and fat body/carcasses were fixed with 4% paraformaldehyde containing 0.1% Tween-20 and 0.1% Triton X-100 for 10 min at room temperature, washed 2 times with PBS containing 0.1% Triton X-100 (PBST) and then blocked in blocking buffer (PBST

containing 0.1% BSA and 0.0025 Sodium Azide) for 1 h. The primary antibody Rabbit anti-Relish (RayBiotech, RB-14-0004) (1:500) was applied overnight at 4°C. Alexa Fluor 488-conjugated anti-Rabbit IgG antibody (Jackson Immunoresearch, 1:500) was incubated for 2 h at room temperature. Hoechst was used to counterstain DNA. Confocal images were collected using a Nikon Eclipse Ti confocal system (utilizing a single focal plane) and processed using the Nikon software and Adobe Photoshop.

2.9 Feeding Behavior

The CAFE assay was performed as follows: Briefly, a single fly was transferred from SY standard food to vials filled with 5 ml of 1.5% agar that maintains internal humidity and serves as a water source. Flies were fed with 5% sucrose solution and maintained in 5 ul capillaries (VWR, #53432-706). After twelve hours habituation, the old capillaries were replaced with a new one at the start of the assay. The amount of liquid food consumed was recorded after 24 hr and corrected on the basis of the evaporation (typically < 10% of ingested volumes) observed the identical vials without flies.

Feeding assays on blue dye-labeled food were performed as follows: 30 flies were transferred from standard food to vials filled with identical medium containing 0.5% brilliant blue. Feeding was interrupted after 1h and 5 flies each were transferred to 50 µl 1 x PBS containing 0.1% Triton X-100 (PBST) and homogenized immediately. Blue dye consumption was quantified by measuring the absorbance of the supernatant at 630 nm (A630). Various amounts of dye-containing food were weighed, homogenized in PBST, and measured (A630) in order to create a standard curve used to quantify blue dye food consumption of flies.

2.10 Chromatin Immunoprecipitation (ChIP)

Approximately 100 adult female flies (5-10 days old post-eclosion) were ground in liquid nitrogen then homogenized and cross-linked (10 minutes at RT) in 600 uL of 1xPBS containing 1% formaldehyde, 1mM PMSF and 1x Protease Inhibitor cocktail (Thermo Scientific). The homogenate was centrifuged for 20 min at 12000 x rpm (4^{o} C). The pellet was washed twice by resuspending in 600 uL of 1x PBS containing 1mM PMSF and 1x Protease Inhibitor cocktail and centrifuged at 12000 x rpm for 20 min (4^{o} C). To lyse tissue and cells, the pellet was resuspended in 600 uL of RIPA buffer (10 mM Tris-HCl, pH 7.6, 1 mM EDTA, 0.1% SDS, 0.1% Na-Deoxycholate, 1% Triton X-100, 1mM PMSF and 1x Protease Inhibitor cocktail) then incubated at RT for 30 min.

The chromatin was sheared to 500-1000 bp DNA fragments using a Diagenode sonicator (20 min sonication, highest power, 30 sec sonication, 30 sec rest). After sonication, the sheared chromatin was centrifuged for 20 min at 12000x rpm, 4^{o} C. The supernatant was collected, aliquoted, snap-frozen, and stored at -80^{0} C.

For immunoprecipitation, 40 uL of protein A magnetic beads (Thermos Scientific) were conjugated (4 hours incubation at 4^{0} C) with 10 uL of Normal Goat Serum (Rockland, used as control), 10 uL of Rabbit anti-Relish (RayBiotech, RB-14-0004), or 2 uL of anti-Histone H3 (acetyl 9) antibody (abcam, ab4441). After applying beads to the magnet and removing supernatant, 100 uL of chromatin was diluted 1:10 with dilution buffer (20 mM Tris-HCl, pH 8, 2 mM EDTA, pH 8, 150 mM NaCl, 1% Triton X-100) and incubated overnight with beads. Beads were washed with following buffers at 4^{o} C, for 10 min each: 2x with 1mL of RIPA buffer + 1mM

PMSF + 1x protease inhibitor; 2x with 1mL of RIPA buffer + 0.3 M NaCl; 2x with 1mL of LiCl buffer (0.25 M LiCl, 0.5% Triton X-100, 0.5% NADOC); 1x with 1 mL of 1x TE + 0.2 Triton X-100; 1x with 1mL of 1x TE.

To reverse crosslink, beads were re-suspended in 100uL of 1x TE + 3 uL 10% SDS + 5 uL of 20mg/mL Proteinase K (VWR) and incubated at 65^{o} C overnight. Beads were applied to the magnet and supernatant was transferred to a PCR purification column (Qiagen PCR purification kit) to purify DNA. To prepare Input (chromatin extract without Immunoprecipitation), 10 uL of chromatin extract were incubated with proteinase K then applied to PCR purification column. For all Immunoprecipitated (IP) and Input samples, DNA was eluted in 30 uL of water, and 2uL of that was used as template for qRT-PCR (see Table S2 for primer sets). The upstream region of the actin5c gene (Act5C^{P}) and Normal Goat Serum were used as controls.

To assess enrichment, %Input was calculated first (between ChIP DNA and input DNA for each primer set). Then the fold change in enrichment was calculated by dividing %Input of each primer set to %Input of a negative control primer set designed for *Drosophila* (*Drosophila* Negative Control primer set 1, Active Motif, 71028).

Table 2.3 List of primers used in ChIP analysis

Gene	Forward	Reverse
R1 (Bmm locus)	GCTTGTTTGCGTTTGTAGGTC	TTCGAAATTGGACAAACACG
R2 (Bmm locus)	TGTCGCTGACAATCAAAAGC	TTCTGGGTGGAGTTTGGAAC
Act5c^{P}	AACCCCCAAATTGAATCACA	GAGAATTTCCTCCGCAACTG
Dipt^{P}	AAGAAAGATCCCCTGGTGGT	TTTTATAGGCCGCTTTCCAA
FR1 (Bmm locus)	CACCGCGCCGCAATGAATGTATAA	TTCAATCACTGTTTGTCGGTCGGC
Drosophila Negative Control Primer Set 1	Active Motif	71028

2.11 Generating Germ-Free Animals

Female adult flies were fed Penicillin/Streptomycin for 5 days to remove bacteria from the gut. Then single flies were washed with 70% ethanol (to remove bacteria from cuticle), dried completely and ground in 200 uL of sterile LB broth and quickly spun down. 10 uL of the supernatant was cultured on Nutrient agar plates. Colonies were counted after 2 days incubation at 29^{o} C.

2.12 Starvation Sensitivity Analysis

Adult flies (20-25 flies per vial/cohort) were provided with only water (absolutely no food) on filter paper with a KimWipe, ensuring water was present throughout the analysis. The number of dead flies in each vial was recorded every 12 hours, and data is presented as the mean survival of cohorts.

2.13 Septic/Systemic Infection Assay

To induce systemic infection, 5-10 days adult female flies of indicated genotypes were pocked in their thorax with a sterilized tungsten needle dipped into a concentrated overnight culture of *Ecc15* (Erwinia carotovora carotovora 15, gram-negative bacteria, OD_{600} ~ 300). The pocked flies were incubated at 25^{o} C and total RNA and metabolite samples were collected from the whole body of flies at 16 hours and 40 hours after septic infection, as well as from unchallenged flies. Heat-killed bacteria were inactivated by incubating a 1 mL aliquot of the bacterial suspension at 65^{o} C for 20 mins before poking.

2.14 Quantification and Statistical Analysis

All p-values were calculated using the Student's t test with unpaired samples. All error bars represent standard error.

2.15 Key resources, reagents and services

Table 2.4 List of antibodies used for ChIP and immunostaining assays

Antibody	Source	Identifier
Normal Goat serum	Rockland	B304
Anti-Relish	RayBiotech	RB-14-0004
Anti-Histone H3 (acetyl K9)	abcam	ab4441
Alexa Flour 488-conjugated Anti-Rabbit IgG	Jackson Immunoresearch	119191
Anti-dFoxO	(Kang et al., 2017)	N/A

Table 2.5 Software and services

Software and services	Source	Identifier
FlyBase		https://flybase.org/
gBlock Gene Fragments	Integrated DNA Technology	https://www.idtdna.com/pages
DNA Sequencing	Eton Bioscience	https://www.etonbio.com/
Transgenic Flies	Rainbow Transgenic Flies	https://www.rainbowgene.com/
Clover Software	(Frith et al., 2004)	N/A

Table 2.6 List of equipment

Equipment and other	Source	Identifier
StepOnePlus Real-Time PCR systems	Applied Biosystems	N/A
Leica M165FC system	Leica	N/A
Nikon Eclipse Ti confocal system	Nikon	N/A
Capillaries	VWR	53432-706
Bioruptor/sonicator	Diagenode	UCD-200
96-well EIA/RIA plate	VWR	29442-322
Pierce Protein A magnetic beads	Thermo Fisher Scientific	88845

Table 2.7 List of chemicals, peptides and recombinant proteins

Chemicals, Peptides, and Recombinant Proteins	Source	Identifier
^{14}C-labeled Glucose (Glucose, D-[^{14}C(U)])	PerkinElmer	NEC042X050UC
Alexa Fluor 488 Phalloidin	Thermo Fisher Scientific	A12379
DAPI (4',6-Diamidino-2-Phenylindole, Dihydrochloride)	Thermo Fisher Scientific	D1306
Drosophila Agar, Type II	Genesee	66-103
Malt Extract	Genesee	62-110
Inactive Dry yeast	Genesee	62-106
Cornmeal	Genesee	62-101
Propionic acid	VWR	TCP0500-500mL
Methyl 4-Hydroxybenzoate	VWR	97061-946
Sucrose	VWR	97063-788
Folch reagent	This paper	N/A
Trizol	Life Technologies	15596018
Superscript III Reverse Transcriptase	Life Technologies	18080-044
iTaq Universal SYBR Green Supermix	Biorad	1725121
DreamTaq PCR Master Mix	Thermo Fisher Scientific	K1081
Sph I-HF	New England BioLab	R3182S
Xho I	New England BioLab	R0146S
CutSmart Buffer	New England BioLab	B7202S
T4 DNA Ligase	New England BioLab	M0202T
RNase A	QIAGEN	19101
Oil Red O	abcam	ab150678
Nile Red	Life Technologies	N1142
Phosphoric acid	VWR	97064-780
Brilliant blue	Sigma-Aldrich	B0149
Protease Inhibitor Cocktail	Thermo Fisher Scientfic	78440
Proteinase K	VWR	0706
LB Agar	BD	244520
LB Broth	BD	244620
LiCl	Amresco	0416-100G
KCl	J.T.Baker	3052-01
CaCl2	Macron	4160-12
PMSF	Thermo Fisher Scientific	36978
Sodium Deoxycholate	Alfa Aesar (by Thermo Fisher Scientific)	J622-88
Penicillin/ Streptomycin	Gibco	15140-122
Ampicillin	Sigma-Aldrich	A0166

3. RESULTS[9]

3.1 Relish Function in Fat body Directs Lipid Metabolism in Response to Metabolic Adaptation

In order to explore mechanistic connections between NF-κB and various metabolic control networks, we first assessed lipid homeostasis in *Drosophila* lacking functional Relish (utilizing the rel^{E20} allele) independent of pathogenic infection. Relish is similar to mammalian p100/p105 NF-κB proteins and contains a Rel-homology domain (N-terminal, involved in DNA binding and dimerization, as well as ankyrin repeats (C-terminal) (found in mammalian inhibitory IκBs) (Buchon et al., 2014; Hetru and Hoffmann, 2009). During *ad libitum* feeding, NF-κB/Rel mutant adult female flies (rel^{E20} / rel^{E20}) had significantly less organismal triglycerides (TAGs) compared to genetically matched controls (either OreR or rel^{E20} / + heterozygote flies, 7 days old post-eclosion; (Figure 3.1A) and (Rynes et al., 2012)).

However, these changes in TAG correlated with decreases in acute and chronic feeding (Figure 3.2A), and can be rescued by high-calorie (sugar) diets (Figure 3.2B), suggesting that steady-state differences in lipid homeostasis are potentially driven by changes in feeding behavior.

Assaying the major fat storage tissues, we also found that TAG level reduction in mutant animals correlates with strong, but variable, decreases in neutral lipid content in fat body/adipose, but not in the intestine (Figure 3.3 and (Kamareddine et al., 2018)).

[9] Reprinted with permission from Molaei, M., C. Vandehoef, and J. Karpac, "NF-kappaB Shapes Metabolic Adaptation by Attenuating Foxo-Mediated Lipolysis in Drosophila." Dev Cell, 2019. 49(5): p. 802-810 e6. Copyright 2019 Elsevier.

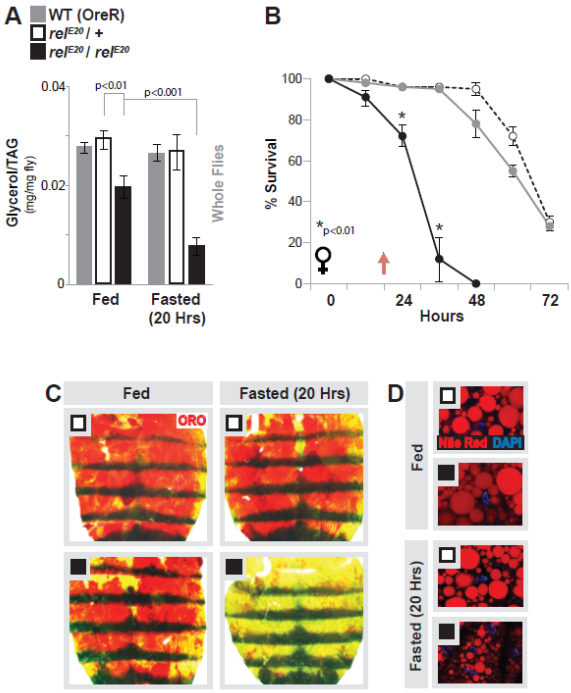

Figure 3.1 Relish-dependent changes in lipid metabolism and survival in response to fasting. (A) Total triglyceride (TAG) levels of whole flies (OreR (WT-wild type) control, relE20/+ (heterozygote control), or relE20/relE20 (mutant) genotypes) before and after fasting (20 hours). n = 4-5 samples. (B) Starvation resistance of female flies. n = 5 cohorts (total 87-95 flies). The red arrow indicates time-point of fasting assays. (C) Oil Red O (ORO) and (D) Nile red stain of dissected carcass/ fat body before and after fasting (20 hours). Nile red (neutral lipids; red) and DAPI (DNA; blue) detected by fluorescent histochemistry. All bars and line graph markers represent mean±SE. All flies were 7 days old post-eclosion.

Since *ad libitum* effects on lipid homeostasis appear to correspond with feeding deficits (i.e. are potentially indirect), we next assayed changes in fat metabolism in Relish mutant animals during metabolic adaptation to fasting. rel^{E20}/rel^{E20} mutant flies are sensitive to starvation compared to control flies (Figure 3.1B). Furthermore, Relish-deficient animals display accelerated decreases in organismal TAG levels during acute fasting (at time-points before significant death occurs), while controls flies show little to no change at these same time-points (always comparing within sibling genotypes, Figure 3.1A). These changes in TAG levels correlate with a strong

reduction of stored neutral lipids/lipid droplets in carcass fat body (Figure 3.1C-D), suggesting that there is enhanced or accelerated lipid breakdown during metabolic adaptation in these animals.

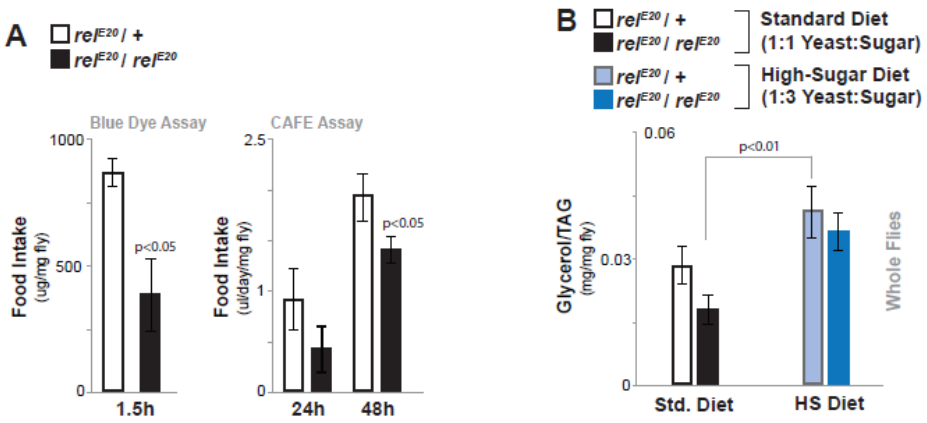

Figure 3.2 Feeding behavior and the effect of diet(A)Relish-dependent changes in feeding behavior. relE20/relE20 (mutant) female flies display decreases in food intake using both the Blue Dye feeding assay (n=3-6 cohorts of 5 flies, measured ZT(8-10) after 1.5 hours feeding) and the CAFE assay (n=7 samples measured after 24 hours and 48 hours); compared to relE20/+ controls. Note: relE20/relE20 mutant show stronger decreases in acute food intake (Blue Dye, 1.5 hours) as opposed to chronic (CAFE, 48 hours). (B) Relish-dependent (relE20/relE20 mutant) changes in total triglyceride (TAG) levels (whole flies) during ad libitum feeding (compared to relE20/+ controls) can be minimized by feeding a high calorie/high sugar diet (n = 5 samples). Bars represent mean ± SE. All flies were 7 days old post-eclosion.

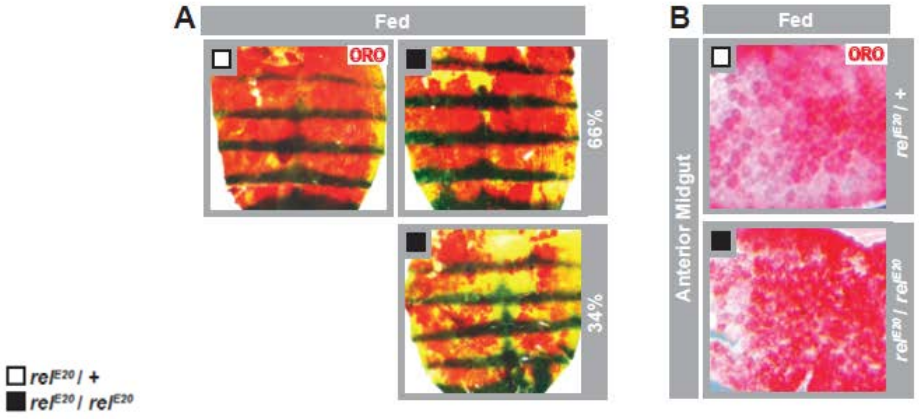

Figure 3.3 Relish-dependent changes in lipid content in fat body compared to intestine. Oil red O (ORO) neutral lipid stain in dissected (A) fat body/carcass and (B) intestine from relE20/relE20 (mutant) female flies compared to relE20/+ control flies. Images from intestine taken from anterior midgut. Note: relE20/relE20 mutant show variable decreases in lipid storage in fat body, but not in the intestine. Percentages represent relative contribution of mild (top panel) or strong (bottom panel) lipid storage defects from 45 unique fat body/carcass dissections from multiple, independent experiments. All flies were 7 days old post-eclosion.

Since Relish in involved in the immune response against infection, we measured TAGs levels in both standard reared flies and germ-free reared flies. rel^{E20}/rel^{E20} mutant flies had less organismal TAGs level compared to control flies ($rel^{E20}/+$) in both standard and germ-free conditions. However, there was no significant difference between standard and the germ-free condition within the control or within mutant groups, suggesting that Reslih-dependent changes in TAGs levels are not due to microbial dysbiosis (Figure 3.4).

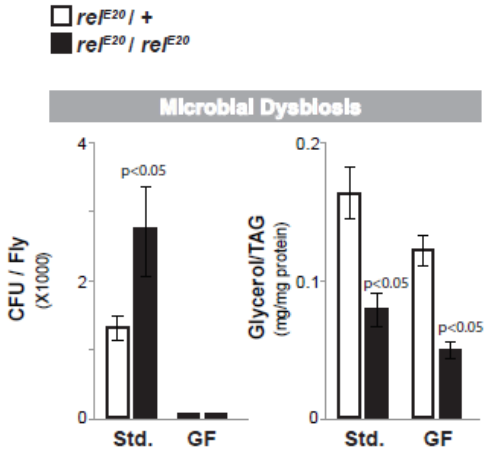

Figure 3.4 The effect of microbial dysbiosis on lipid content of flies. Relish-dependent changes in triglyceride levels during *ad libitum* feeding are not caused by microbial dysbiosis. Colony forming units (CFU per fly, n = 4) and total triglyceride (TAG) levels of whole flies (n = 4 samples) in standard rearing conditions (Std.) or germ-free rearing conditions (GF); genotypes *relE20*/+ (control) or *relE20*/*relE20* (mutant). Bars represent mean ± SE. All flies were 7 days old post-eclosion.

The insect fat body acts as a key sensor to link nutrient status and energy expenditure, and as such is the major lipid depository (mainly triglycerides) that combines energy storage, de novo synthesis, and breakdown functions of vertebrate adipose and hepatic tissues (Arrese and Soulages, 2010; Canavoso et al., 2001; Kuhnlein, 2012). This tissue is also essential for Toll and Relish mediated innate immune responses to bacterial infection (Buchon et al., 2014; Hetru and

Hoffmann, 2009; Lemaitre and Hoffmann, 2007). Critically, fat body is integral to properly balance lipid catabolism and anabolism in order to modulate organismal energy homeostasis (through lipid supply to other tissues) in response to metabolic or dietary adaptation (Arrese and Soulages, 2010; Kuhnlein, 2012). Expression of full-length Relish in fat body (CGGal4>UAS-Rel) can rescue reduced starvation survival rates and the accelerated loss of lipid storage in rel^{E20} / rel^{E20} mutant flies during fasting (

Figure 3.5). These data suggest that Relish function in fat body is required to acutely maintain lipid homeostasis throughout the course of metabolic adaptation.

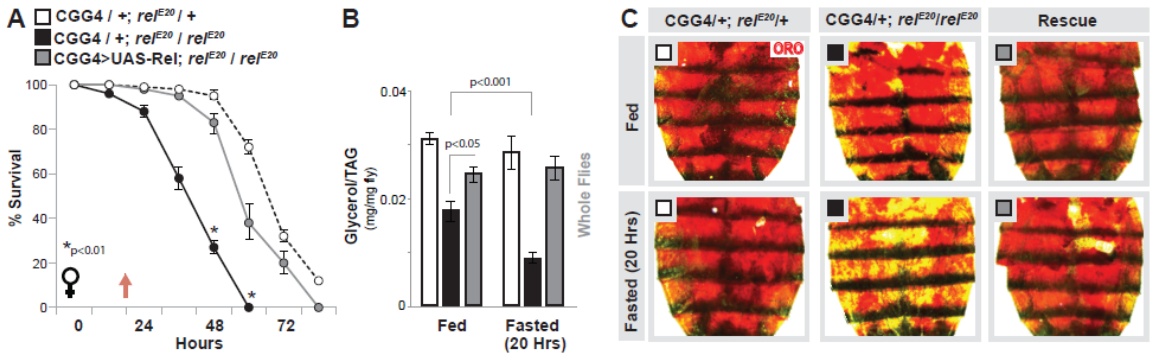

Figure 3.5 Re-expressing Relish in fat body of Relish-deficient flies restores metabolic adaptation responses.(A) Starvation resistance of female flies (CGGal4/+; rel^{E20}/+ (control), CGGal4/+; rel^{E20}/rel^{E20} (mutant), or CGGal4/UAS-Rel; rel^{E20}/rel^{E20} (Rescue)). n = 5 cohorts (total 79-98 flies). The red arrow indicates time-point of fasting assays. (B) Total TAG levels of whole flies (n = 4-5 samples) and (C) ORO stain of dissected carcass/ fat body before and after fasting (20 hours). All bars and line graph markers represent mean±SE. All flies were 7 days old post-eclosion.

To further confirm an autonomous and potentially direct role for Relish in the regulation of fasting-mediated changes in lipid metabolism, we inhibited Relish specifically in fat body (using multiple, independent RNAi lines; UAS-Rel^{RNAi} KK and GD). First, we examined the efficiency of these RNAi lines using a Tubulin-GeneSwitch-Gal4 (TubGS, a ubiquitous driver that is induced

by RU486 drug). Flies carrying RNAi lines (TubGS>UAS-Rel^{RNAi} KK and UAS-Rel^{RNAi} GD) had lower levels of Relish mRNA compared to control flies (TubGS> W^{1118}), confirming that these RNA lines can efficiently attenuate Relish activity (Figure 3.6A).

Attenuating Relish in fat body of female flies (CGGal4>UAS-Rel^{RNAi}) leads to starvation sensitivity, as well as accelerated loss of organismal TAG levels and fat body lipid storage in response to fasting (compared to control flies (CGGal4>*w^{1118}*) (Figure 3.6B-D). As expected, fasting-induced changes in fat body lipid storage occur before significant decreases in total TAG levels of whole animals are observed (Figure 3.6).

The observed phenotypes were confirmed with an independent fat body driver (PplGal4; Figure 3.6E-G), and similar results were found utilizing males (Figure 3.7) but not when utilizing another immune cell (hemocyte) driver (HmlGal4Figure 3.8). Conversely, over-expressing full-length Relish (CGGal4>UAS-Rel) or a constitutively active N-terminal fragment (CGGal4>UAS-Rel.68) in fat body significantly limits fasting-mediated decreases in lipids compared to controls (CGGal4>+ (W^{1118}) (Figure 3.9).

In order to confirm that observed lipid phenotypes are due to attenuation of Relish activity, and not the mere effect of different genetic background of fly lines, we performed additional control experiments. Organismal TAG levels, as well as starvation sensitivity of UAS-RelRNAi KK/+ and UAS-RelRNAi GD/+ flies, were similar to control (+/+ (W^{1118})), ruling out the effect of genetic background or or UAS-Rel NAi transgenes on the lipid homeostasis. (Figure 3.10).

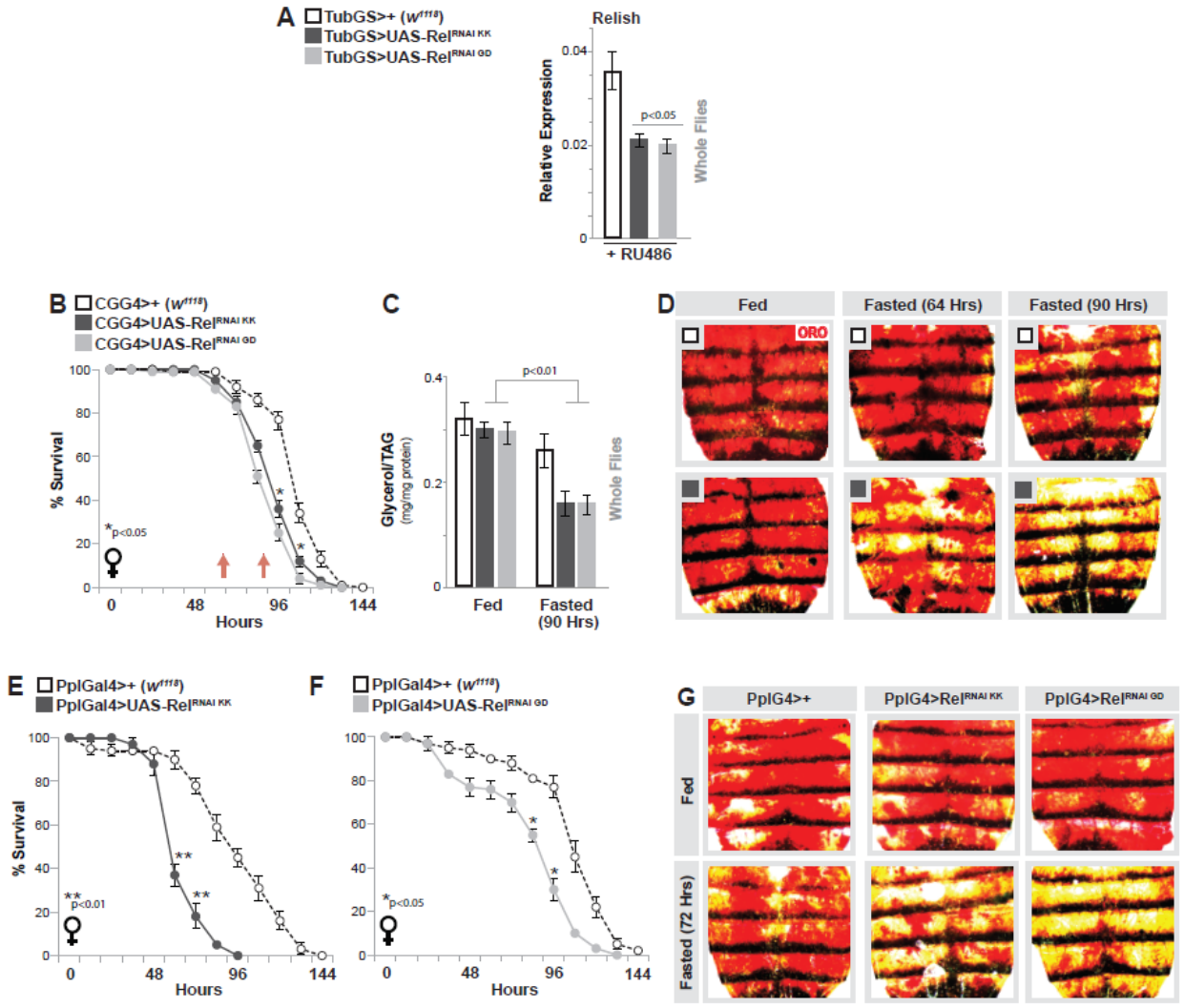

Figure 3.6 Relish function in fat body directs lipid metabolism in response to metabolic adaptation. (A) UAS-Rel RNAi efficiency. Changes in *relish* transcription (measured by qRT-PCR in whole flies) upon ubiquitous Relish depletion (RNAi line v108469-KK and v49413-GD) using Tubulin-GeneSwitch-Gal4 (TubGS) after 5 days feeding RU486; compared to controls (TubGS>+(w^{1118})). n = 4 samples. (B-D) Changes in lipid metabolism and survival upon Relish depletion (RNAi lines v108469-KK and v49413-GD) in fat body (CGGal4). (B) Starvation resistance of female flies. n = 6 cohorts (total 139-149 flies). The red arrow indicates time-point of fasting assays. (C) Total TAG levels of whole flies (n = 4-5 samples) and (D) ORO stain of dissected carcass/ fat body (only RNAi v108469-KK shown) before and after fasting (64 and/or 90 hours). (E-G) Changes in lipid metabolism and survival upon Relish depletion (RNAi lines v108469-KK and v49413-GD) in fat body (PplGal4). (E-F) Starvation resistance of female flies. n = 6 cohorts (total 110-141 flies). (G) Oil Red O (ORO) neutral lipid stain of dissected carcass/ fat body before and after fasting (72 hours). All bars and line graph markers represent mean±SE. All flies were 7 days old post-eclosion.

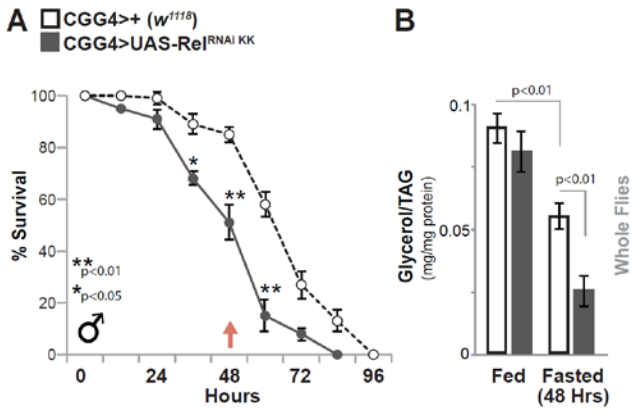

Figure 3.7 Changes in lipid metabolism and survival upon Relish depletion in fat body of male flies. (A) Starvation resistance of male flies. n = 5 cohorts (total 90-95 flies). (B) Total triglyceride (TAG) levels of whole male flies (n=5 samples, before and after fasting (48 hours)). All bars and line graph markers represent mean±SE. All flies were 7 days old post-eclosion.

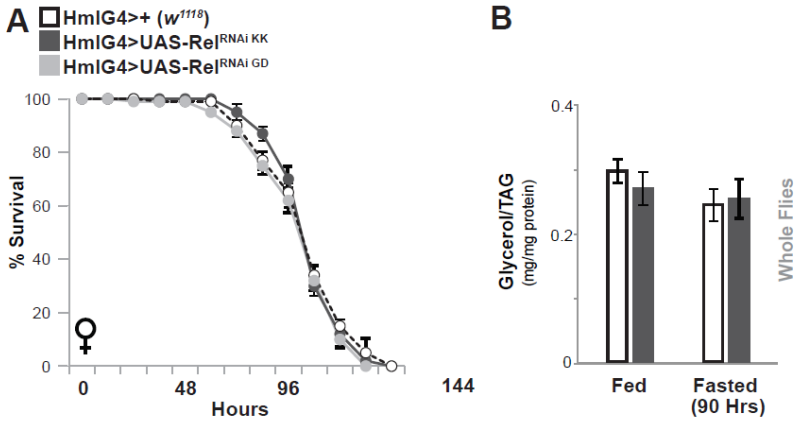

Figure 3.8 Absence of changes in lipid metabolism and survival upon Relish depletion in hemocytes of female flies.(A) Starvation resistance of female flies. n = 4 cohorts (total 77-80 flies). (B) Total triglyceride (TAG) levels of whole male flies (n=3 samples, before and after fasting (90 hours)). All bars and line graph markers represent mean±SE. All flies were 7 days old post-eclosion

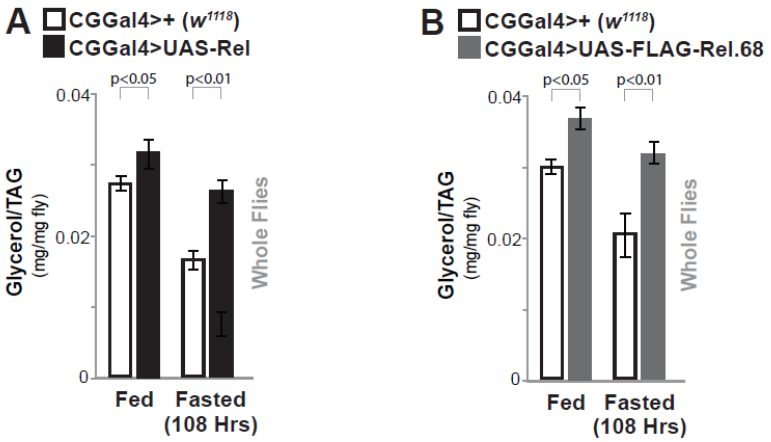

Figure 3.9 Changes in fasting-induced lipid metabolism upon Relish over-expression. (A) Full-length Relish (UAS-Rel) and (B) The tagged N-terminal active fragment (UAS-FLAG-Rel.68)) in fat body (CGGal4). Total TAG levels of whole female flies (n=5 samples, before and after fasting (108 hours)). Control genotype CGGal4/+ (w^{1118}). Bars represent mean ± SE. All flies were 7 days old post-eclosion.

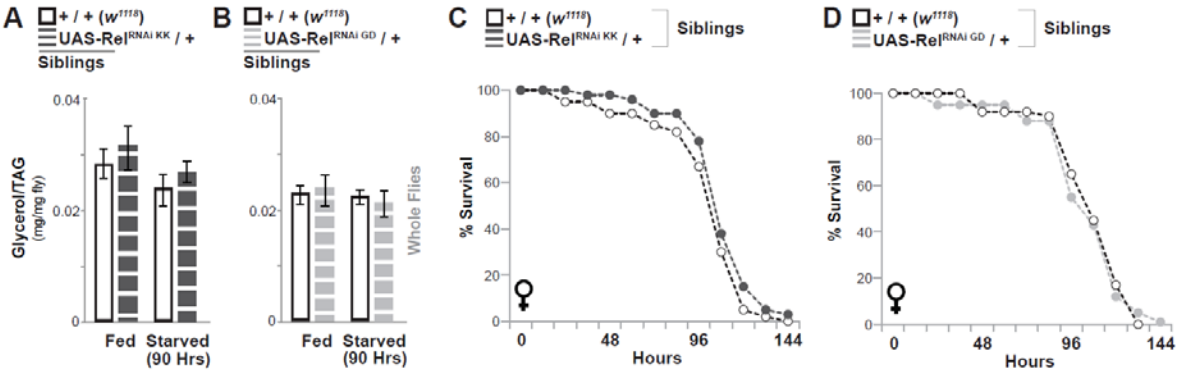

Figure 3.10 UAS-Rel RNAi transgenes alone do not affect fasting-induced triglyceride metabolism or survival during metabolic adaptation. (A-B) Total TAG levels of whole female flies (n=5 samples, before and after fasting (90 hours)) and (C-D) starvation resistance of female flies (n = 5 cohorts, total 89-96 flies) from UAS-Rel RNAi/+(w^{1118}) and +/+(w^{1118}) female siblings. All bars and line graph markers represent mean±SE. All flies were 7 days old post-eclosion.

Furthermore, attenuation of upstream components of the Relish signaling pathway phenocopies these Relish loss-of-function effects on lipid metabolism during metabolic adaption (Figure 3.11). Relish is governed by conserved regulators TAK1 and the IKK (IκB Kinase)

signalosome (which consists of homologs of both IKKβ (*Drosophila* Ird5) and IKKϒ/NEMO (*Drosophila* Kenny (key)) (Ganesan et al., 2011; Hetru and Hoffmann, 2009)), while the apical caspase DREDD is required for the proteolytic cleavage of the IkB domain, allowing for nuclear translocation (Hetru and Hoffmann, 2009).

First, we assessed the efficiency of UAS-Key^{RNAi} and UAS-DREDD^{RNAi} in attenuating the correspondence mRNA level (same method that was used for UAS-REL^{RNAi} lines) (Figure 3.11A)

Inhibiting Kenny or DREDD in fat body of female flies (CGGal4>UAS-DREDD^{RNAi} or Key^{RNAi}) leads to starvation sensitivity, as well as the accelerated loss of organismal TAG levels and fat body lipid storage in response to fasting (compared to control flies (CGGal4>w^{1118}, Figure 3.11B-E). Similarly, attenuating upstream receptors usually required for NF-κB/Relish activation (PGRP family members PGRP-LC (trans-membrane) or PGRP-LE (cytoplasmic)) also leads to decreased lipid storage in fat body after starvation (Figure 3.11F), suggesting that at least part of the canonical innate immune pathway is required for these metabolic phenotypes.

Taken together, these data show that Relish can autonomously regulate lipid metabolism in fat body during metabolic adaptation, and suggest that Relish may direct specific metabolic responses to control the breakdown of triglycerides.

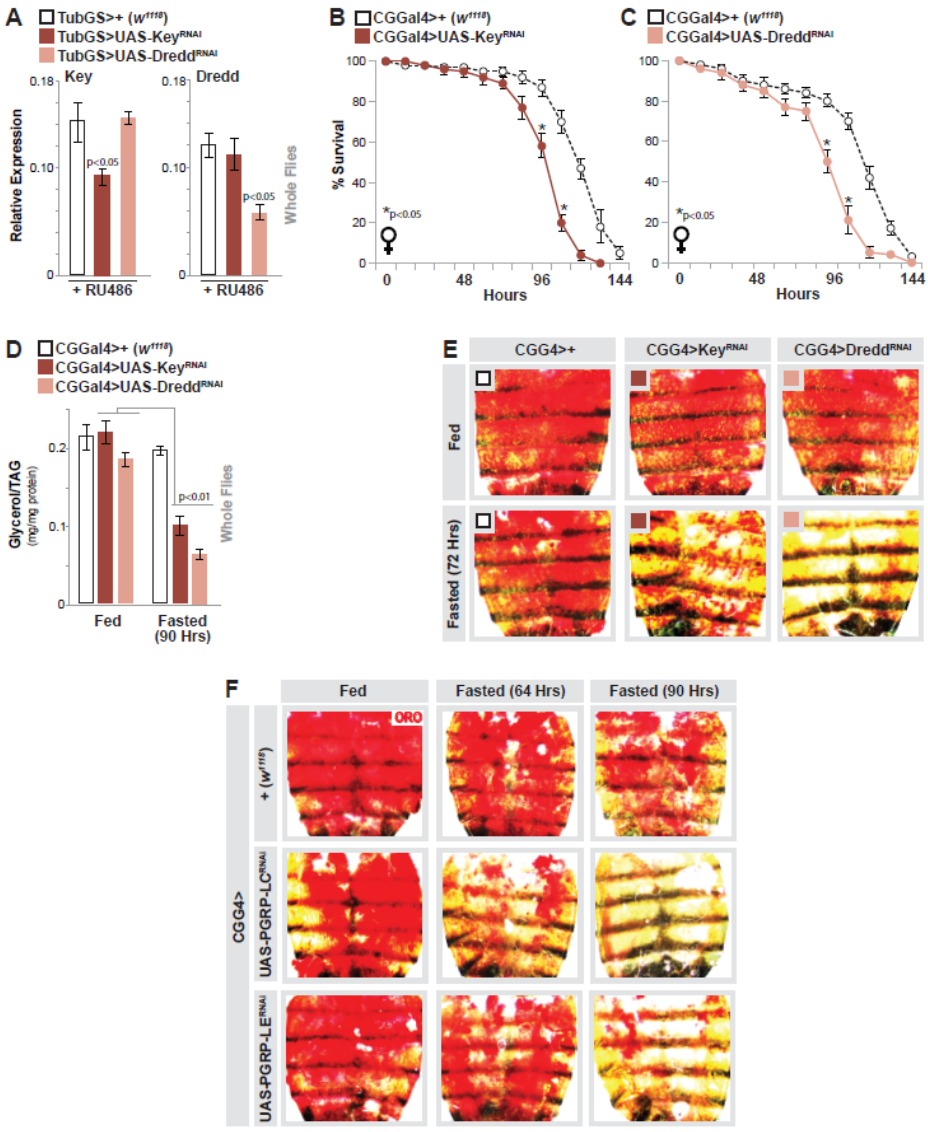

Figure 3.11 The effect of upstream components of Relish/Imd pathway on lipid metabolism in response to metabolic adaptation.(A) RNAi efficiency. Changes in *kenny or dredd* transcription (measured by qRT-PCR in whole flies) upon ubiquitous depletion (Kenny (Key) RNAi line v7723-GD and Dredd RNAi line v104725-KK) using Tubulin-GeneSwitch-Gal4 (TubGS) after 5 days feeding RU486; compared to controls (TubGS>+(w^{1118})). n = 4 samples. (B-E) Changes in lipid metabolism and survival upon Kenny or Dredd depletion (RNAi lines v7723-GD (Key) and v104726-KK (Dredd)) in fat body (CGGal4) of female flies. (B-C) Starvation resistance of female flies. n = 7 cohorts (total 140-149 flies). (D) Total triglyceride (TAG) levels of whole female flies (n=5 samples, before and after fasting (90 hours)) and (E) Oil Red O (ORO) neutral lipid stain of dissected carcass/ fat body before and after fasting (72 hours). Control genotype CGGal4/+ (w^{1118}). (F) Changes in lipid metabolism upon PGRP-LC or PGRP-LE depletion (RNAi lines v101636-KK (LC) and v23664-GD (LE)) in fat body (CGGal4) of female flies. Oil Red O (ORO) neutral lipid stain of dissected carcass/ fat body before and after fasting (64 and 90 hours). Control genotype CGGal4/+ (w^{1118}). Bars and line graph markers represent mean ± SE. All flies were 7 days old post-eclosion.

3.2 Relish Controls Fasting-induced Lipolysis and Bmm Triglyceride Lipase Gene Expression

Properly balancing energy homeostasis in response to metabolic adaptation depends on the ability to coordinate storage, breakdown, and mobilization of lipids, primarily TAG. This coordination requires precise control of metabolic response networks, including changes in metabolic gene expression. To determine potential mechanisms by which the Relish transcription factor could direct cellular triglyceride metabolism during fasting, we assayed transcriptional changes of various metabolic genes related to lipid catabolism or anabolism in Relish-deficient animals (a subset is shown in Figure 3.12).

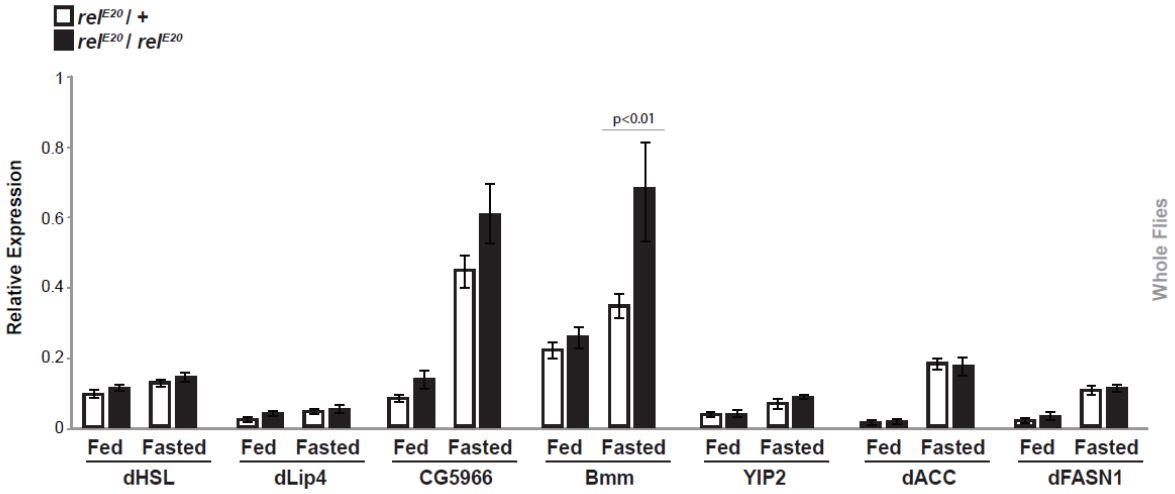

Figure 3.12 Relish-dependent changes in the expression of metabolic genes in response to metabolic adaptation. *Drosophila* HSL (dHSL), lip4, CG5966, bmm, YIP2 (yippee interacting protein 2/thiolase), ACC (acetyl-CoA carboxylase), and FASN1 (fatty acid synthase) transcription (measured by qRT-PCR in whole flies) before and after fasting (20 hours). relE20/+ (heterozygote control), or relE20/relE20 (mutant) genotypes. n = 3 samples. Bars represent mean ± SE. All flies were 7 days old post-eclosion.

Specifically, we identified the lipase Brummer (Bmm) as being regulated by Relish (Figure 3.12 and Figure 3.13A). Bmm is the *Drosophila* homolog of mammalian adipose triglyceride

lipase (ATGL), an enzyme that is critical for lipolysis (Gronke et al., 2005). Bmm plays an essential and conserved role in TAG breakdown, and subsequently fatty acid mobilization, from lipid droplets in fat storage tissues during metabolic adaptation (Gronke et al., 2007). In control flies, *bmm* transcription is mildly induced during acute fasting, but in rel^{E20} / rel^{E20} mutant flies *bmm* expression is strongly up regulated (from whole flies). These Relish-dependent changes in *bmm* transcription appear unique, as Relish-deficiency does not impact fasting-induced changes in other lipases such as *Drosophila* hormone-sensitive lipase (dHSL), *Drosophila* lipase 4 (dLip4) or CG5966 (Figure 3.13A).

In addition, similar results were found in dissected fat body with specific attenuation of NF-κB/Relish in this same tissue (CGGal4>UAS-$Rel^{RNAi\ KK}$, Figure 3.13B-C). These results suggest that Relish function is required to repress or limit Bmm expression in response to metabolic adaptation, and subsequently restrain triglyceride breakdown.

To correlate this difference in gene expression to differences in lipolysis, we next employed an assay to measure dynamic changes in lipid content based on the incorporation of radiolabeled glucose (^{14}C-glucose) into lipids during fatty acid synthesis *in vivo*. After acute feeding (1.5 hours) of a diet containing ^{14}C-glucose, Relish mutant flies show drastic changes in glucose-incorporation (synthesis) that is likely due to changes in feeding behavior (Figure 3.13D and Figure 3.2). Sixteen hours of feeding minimized these differences in synthesis, and subsequent analysis of newly synthesized ^{14}C-labeled lipids during fasting showed an increased rate of breakdown in rel^{E20} / rel^{E20} mutant flies (47% in mutants compared to 20% in controls, Figure 3.13D). This change in the rate of breakdown correlated with increases in free fatty acids (Figure 3.13E).

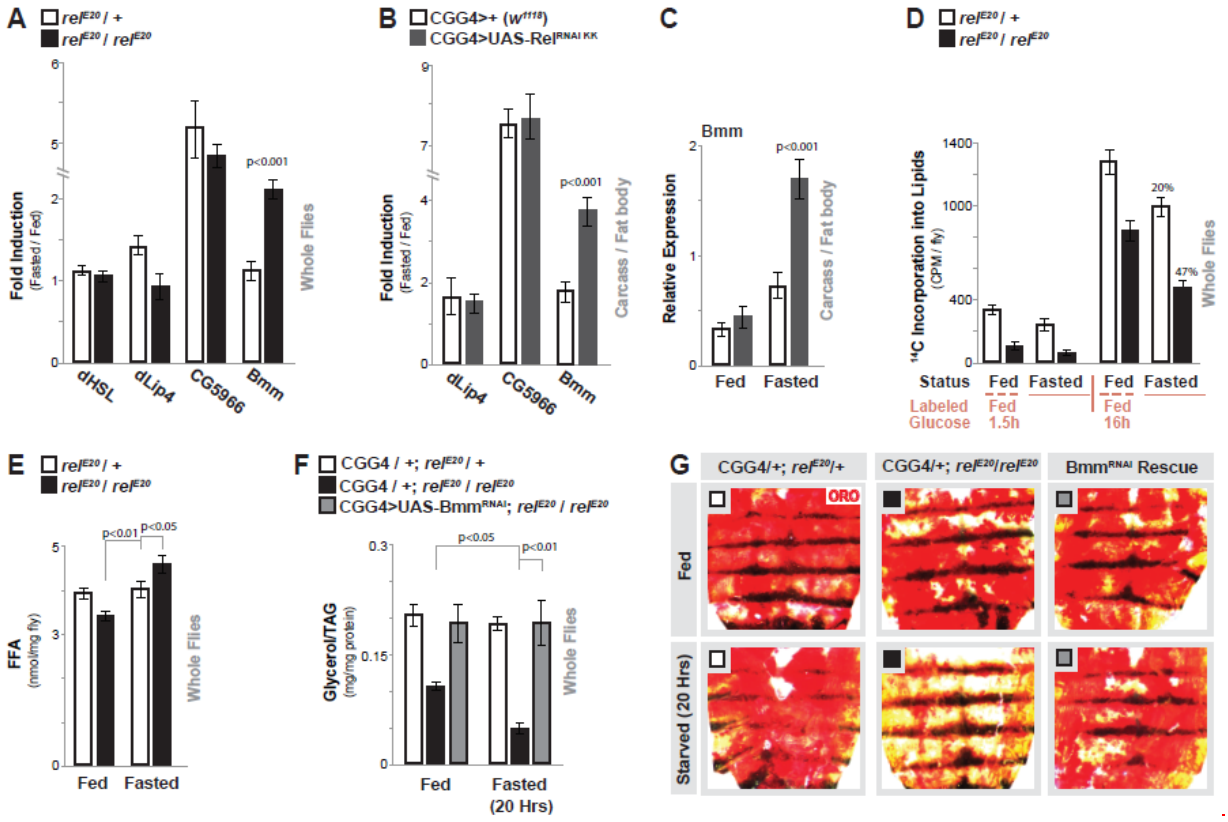

Figure 3.13 Relish controls fasting-induced triglyceride lipase Bmm transcription and lipolysis. (A) *Drosophila HSL*, *lip4*, *CG5966*, and *bmm* transcription (measured by qRT-PCR in whole flies, plotted as fold induction (20 hours fasted/fed) of relative expression). rel^{E20}/+ (heterozygote control), or rel^{E20}/rel^{E20} (mutant) genotypes. n = 3 samples. (B-C) Changes in *lip4*, *CG5966*, and *bmm* transcription (measured by qRT-PCR in dissected carcass / fat body, plotted as fold induction (64 hours fasted/fed) of relative expression) upon Relish depletion (RNAi line v108469-KK) in fat body (CGGal4). (C) Relative expression values (from (B)) for *bmm* transcription. n = 3-4 samples. (D) Quantification of lipid breakdown. Incorporation of ^{14}C-labeled glucose into total lipids (from whole flies) from labeled-glucose fed (1.5 hours or 16 hours) or fasted (20 hours) flies are shown. Percent change in loss of ^{14}C-labeled lipids after fasting is also shown. n = 3-4 samples. (E) Free fatty acid (FFA) levels measured in whole flies before and after fasting (20 hours). n = 4 samples. (F-G) Attenuating Bmm (RNAi line v37877) in fat body (CGGal4) of Relish-deficient flies restores metabolic adaptation responses. (F) Total TAG levels of whole flies (n = 3-4 samples) and (G) Oil Red O stain of dissected carcass/ fat body before and after fasting (20 hours, CGGal4/+; rel^{E20}/+ (control), CGGal4/+; rel^{E20}/rel^{E20} (mutant), or CGGal4/UAS-Bmm RNAi; rel^{E20}/rel^{E20} (Rescue)). Bars represent mean ± SE. All flies were 7 days old post-eclosion.

Finally, genetically attenuating Bmm lipase in fat body (CGGal4>UAS-Bmm^{RNAi}, (Baumbach et al., 2014)) can rescue the accelerated loss of lipid storage/triglycerides in rel^{E20} / rel^{E20} mutant flies during fasting (Figure 3.13F-G).

These data collectively reveal that Relish function is required to limit fasting-induced Bmm gene expression and subsequently restrain triglyceride lipolysis during metabolic adaptation.

Following these results, we wanted to further explore the mechanism by which the Relish transcription factor can context-dependently attenuate Bmm expression. Utilizing Clover (Cis-element OVERrepresentation) software (Frith et al., 2004), we identified conserved NF-κB DNA binding motifs (κB sequence sites identified as GGG R N YYYYY, (Busse et al., 2007)) throughout the first intron of the Bmm locus (Fig. 3.14A).

To assess binding, we used a previously characterized Relish antibody to perform chromatin immunoprecipitation (ChIP)-qPCR experiments (Ji et al., 2016). Relish binding in fed or fasted wild type flies is significantly enriched (compared to IP's using serum controls) at binding motif(s) approximately 1 kB downstream from the transcriptional start site (R1, Figure 3.14A).

We also cloned this putative Bmm regulatory region upstream of RFP in order to generate *in vivo* expression reporters (individual transgenic flies carrying either a wild type reporter (endogenous locus, Bmm_Int_WT-RFP) or a reporter with a deletion in the Relish DNA binding site (Bmm_Int_Δ1-RFP), Figure 3.14B). While the unaltered region only slightly influenced RFP reporter activity in fed or fasted conditions, eliminating the Relish binding site leads to minimal enhanced reporter activity under fed conditions and strong increases in RFP activity during fasting (primarily in fat body of carcass and head, Figure 3.14B). Thus, this Relish binding site within the first Bmm intron acts as an important regulatory region to limit induced gene expression.

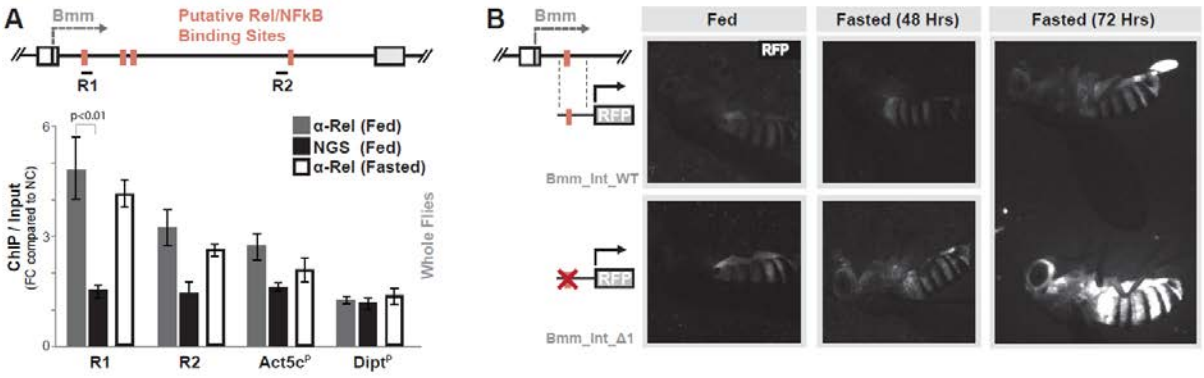

Figure 3.14 Relish binds to the regulatory region in Bmm locus. (A) Schematic shows Bmm locus (focusing on first intron proximal to transcription start site) and putative NF-κB/Rel binding motifs (identified by Clover). R1 and R2 represent regional target sites (and corresponding primer sets) tested in ChIP-qPCR analysis. The histogram represents ChIP-qPCR analysis of Relish binding to the Bmm locus (compared to the Actin5c promoter ($Act5c^P$) and the Diptericin promoter ($Dipt^P$) in fed or fasted (20 hours) conditions. ChIP-qPCR analysis with normal goat serum (NGS) is included as a control. Plotted as fold change (FC) of indicated PCR primer sets compared to a negative control (NC) primer set. n = 3 biological replicates. (B) Requirement of Bmm locus Rel binding site in limiting induced gene expression measured by RFP fluorescence in transgenic flies carrying indicated reporters (during fed and fasted (48 or 72 hours) conditions). Bars represent mean ± SE. All flies were 7 days old post-eclosion.

Relish binding at this region is similar in fed and fasted states (Figure 3.14A). We also did not find any evidence of classical Relish transcriptional activation function during acute fasting. First, innate immune target gene expression (Drosomycin and Diptericin) and Relish DNA binding to innate immune gene promoters (Diptericin) were not changed during fasting (Figure 3.15A and Figure 3.14A). Second, metabolic adaptation did not significantly alter nuclear localization of Relish in fat body (Figure 3.15B). Thus, in order to explore how Relish limits or represses fasting-induced Bmm expression, despite its constitutive binding to DNA and distinct from its transcriptional activation function, we assessed histone/chromatin changes in Relish-deficient flies. Histone deacetylases (HDACs) have been shown to accumulate in the nucleus during metabolic adaptation, influencing gene expression in a fasting-dependent manner through

chromatin regulation and transcription factor deacetylation (Mihaylova et al., 2011; Nakajima et al., 2016; Wang et al., 2011). Furthermore, previous studies have linked interactions of NF-κB transcription factors and HDACs with NF-κB-dependent transcriptional repression (Ashburner et al., 2001; Dong et al., 2008; Morris et al., 2016). We thus hypothesized that Relish might repress Bmm gene expression through influencing histone modifications during fasting, when histone modifiers (such as HDACs) in the nucleus are elevated. Using ChIP-qPCR, we monitored histone 3 lysine 9 acetylation (H3K9ac, a post-translational modification generally associated with transcriptional activation) at this Bmm regulatory region in Relish-deficient animals and controls. During feeding, there is no change in H3K9ac enrichment at this locus between genotypes (Fig. 3C). However, during fasting rel^{E20} / rel^{E20} mutant flies display a significant enrichment (compared to controls) of H3K9ac at the site of Relish binding (Figure 3.16A), indicative of promoter or enhancer activation. Analysis of modEncode ChIP-Seq. databases associated with histone modifications (in adult female flies) also revealed that this site is generally enriched for other modifications linked to gene expression regulation (such as H3K27ac, H3K4me3, and H3K4me1), further indicating that this locus is an important regulatory region (Contrino et al., 2012). Additionally, inhibiting a single HDAC in fat body (Rpd3 (*Drosophila* HDAC1), CGGal4>UAS-$Rpd3^{RNAi}$) can drive small, but significant, increases in fasting-induced Bmm transcription (from whole flies,Figure 3.16B) and accelerate fat body lipid usage (Figure 3.16C).

Taken together, these data show that Relish can bind to a putative regulatory region within the Bmm locus during both feeding and fasting. In response to fasting, the presence of Relish can influence fasting-dependent histone acetylation and chromatin changes that are consistent with transcriptional repression.

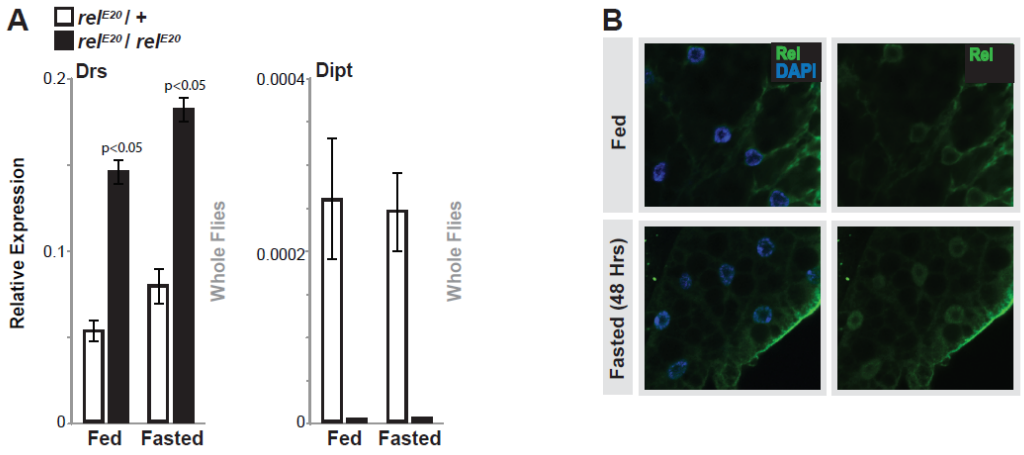

Figure 3.15 Relish transcriptional activation function is not elevated during fasting. (A) *Drosophila drs* (Drosomycin) and *dipt* (Diptericin) transcription (measured by qRT-PCR in whole flies) before and after fasting (20 hours). *relE20*/+ (heterozygote control), or *relE20*/*relE20* (mutant) genotypes. n = 4 samples. (B) Relish immunostaining in carcass/fat body before and after fasting (20 hours; OreR female flies). Stained with anti-Rel and nuclei visualized with DAPI (blue). Weak Rel signal is detected in the nucleus during fed and fasted conditions, however, the staining is slightly more perinuclear during *ad libitum* feeding (upper right panel). Bars represent mean ± SE. All flies were 7 days old post-eclosion.

3.3 FoxO and Relish Antagonism Dictates Fasting-induced Bmm Transcription and Lipolysis

The unique ability of Relish to limit or repress fasting-induced Bmm transcription correlates with attenuation of H3K9ac at Bmm regulatory regions. We thus hypothesized that Relish binding to the Bmm locus leads to fasting-dependent chromatin changes, which subsequently limit transcription activation function of other factors that are induced during metabolic adaptation (Figure 3.17A). We assessed various metabolic transcription factors and found that FoxO, a critical regulator of lipolysis and catabolism in general, is required for Relish-dependent changes in ATGL/Bmm expression during metabolic adaptation (Figure 3.18). Firstly, FoxO (of which there is a single ortholog in *Drosophila*) is activated during metabolic adaptation and required for fasting-induced ATGL/Bmm expression across taxa, including in the fly fat body

(Figure 3.18C-D (from dissected fat body) and (Chakrabarti and Kandror, 2009; Kang et al., 2017; Wang et al., 2011)).

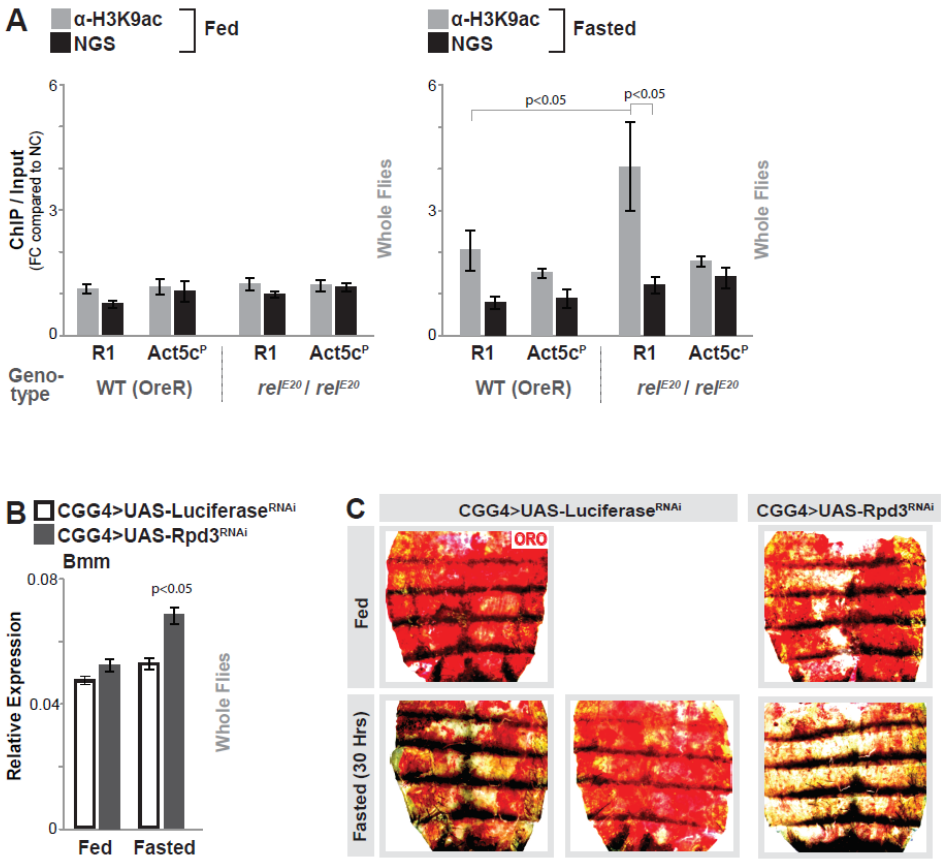

Figure 3.16 Relish regulates Bmm expression though modifying histone acetylation of Bmm regulatory region. (A) ChIP-PCR analysis of H3K9ac enrichment in R1/Relish-binding region of the Bmm locus in wild type (WT; OreR) and rel^{E20}/rel^{E20} (mutant) genotypes before and after fasting (20 hours). n = 3 biological replicates. (B) Changes *bmm* transcription (measured by qRT-PCR in whole flies) before and after fasting (20 hours) upon Rpd3 depletion (RNAi line TRiP 36800) in fat body (CGGal4). Controls are a genetically matched RNAi targeting luciferase. n = 4-6 samples. (C) Changes in lipid metabolism upon Rpd3 depletion (RNAi TRiP 36800) in fat body (CGGal4) of female flies. Oil Red O (ORO) neutral lipid stain of dissected carcass/ fat body before and after fasting (30 hours). Control genotype CGGal4>UAS-Luciferase RNAi (slight variation in control phenotype after fasting is highlighted with two independent images). Bars represent mean ± SE. All flies were 7 days old post-eclosion.

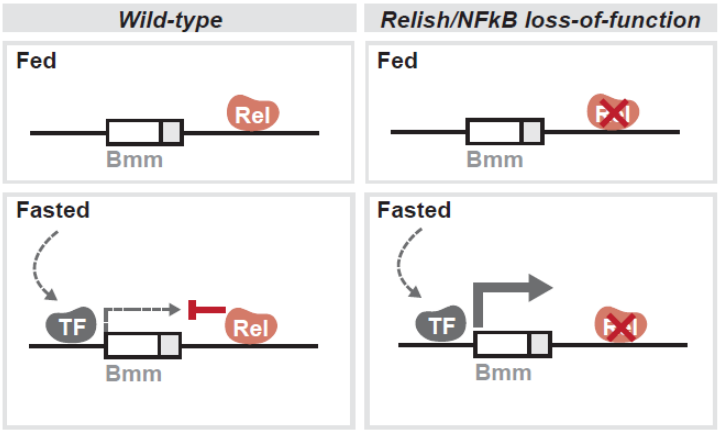

Figure 3.17 Putative model highlighting the integration of Relish (Rel) and other fasting-induced transcription factors (TF)

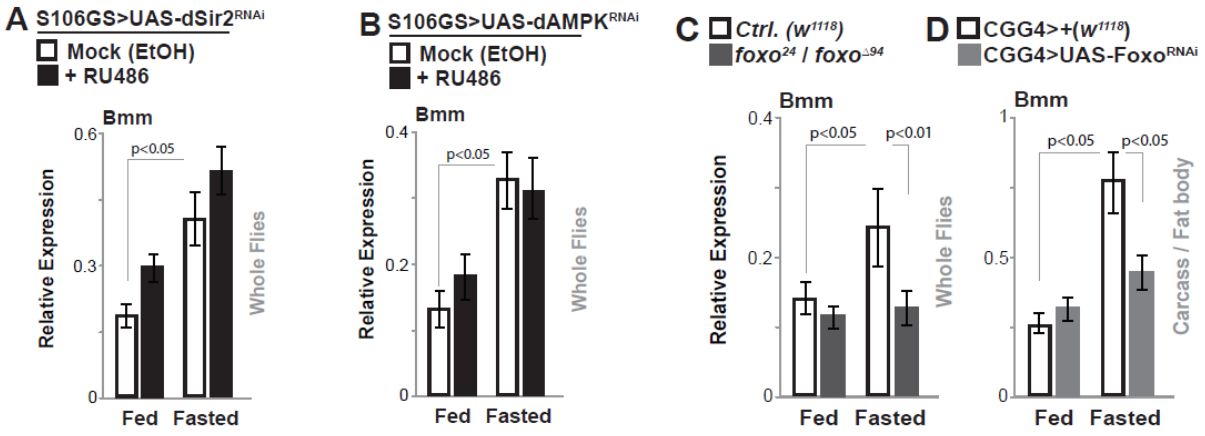

Figure 3.18 Upregulation of Bmm in response to fasting is FoxO-dependent. (A-B) Changes in *bmm* transcription (measured by qRT-PCR in whole flies) upon fat body-specific depletion of *Drosophila* (A) AMPKα (RNAi line v1827-GD) and (B) Sir2 (homolog of SIRT1; dSir2 RNAi line v23201-GD) using S106-GeneSwitch-Gal4 after 5 days feeding RU486; compared to controls (mock (EtOH) treated siblings) before and after fasting (90 hours). n = 4-5 samples. (C-D) Changes in *bmm* transcription (measured by qRT-PCR in whole flies or dissected fat body) before and after fasting (64 hours) in (C) FoxO mutant (w^{1118};; $FoxO^{24}/FoxO^{\Delta 94}$) and control ($w^{1118}$) genotypes, as well as upon (D) FoxO depletion (RNAi line v106097) in fat body (CGGal4). n = 4 samples. Bars represent mean ± SE. All flies were 7 days old post-eclosion.

Full Relish/FoxO double mutant animals (using the $FoxO^{24}$ allele) are synthetic lethal during metamorphosis (rel^{E20}, $FoxO^{24}$ / rel^{E20}, $FoxO^{24}$, Figure 3.19A). However, simply reducing

FoxO gene-dose in NF-κB/Relish mutant flies (*rel*^{E20}, *FoxO*^{24} / *rel*^{E20}) completely rescues fasting-dependent increases in Bmm expression (from whole flies), starvation survival rates, and increases in lipolysis (accelerated loss of lipid storage) in Relish-deficient flies during metabolic adaptation (Figure 3.19B-D). Furthermore, attenuating FoxO specifically in fat body (CGGal4>UAS-FoxO^{RNAi}, (Zhao and Karpac, 2017)) rescues the enhanced depletion of triglycerides/lipid storage and starvation sensitivity associated with *rel*^{E20} / *rel*^{E20} mutant flies during fasting (Figure 3.19E-G).

Molecular analysis of FoxO transcription activation function also showed that FoxO binding to the Bmm promoter is slightly, but significantly, elevated in Relish-deficient flies only during fasting (Figure 3.20A), while the expression of FoxO is not Relish dependent (3.20B). FoxO transcription activation function is thus required for Relish-dependent changes in lipid metabolism, highlighting that Relish/FoxO integration and antagonism is critical to maintain triglyceride metabolism throughout the course of metabolic adaptation.

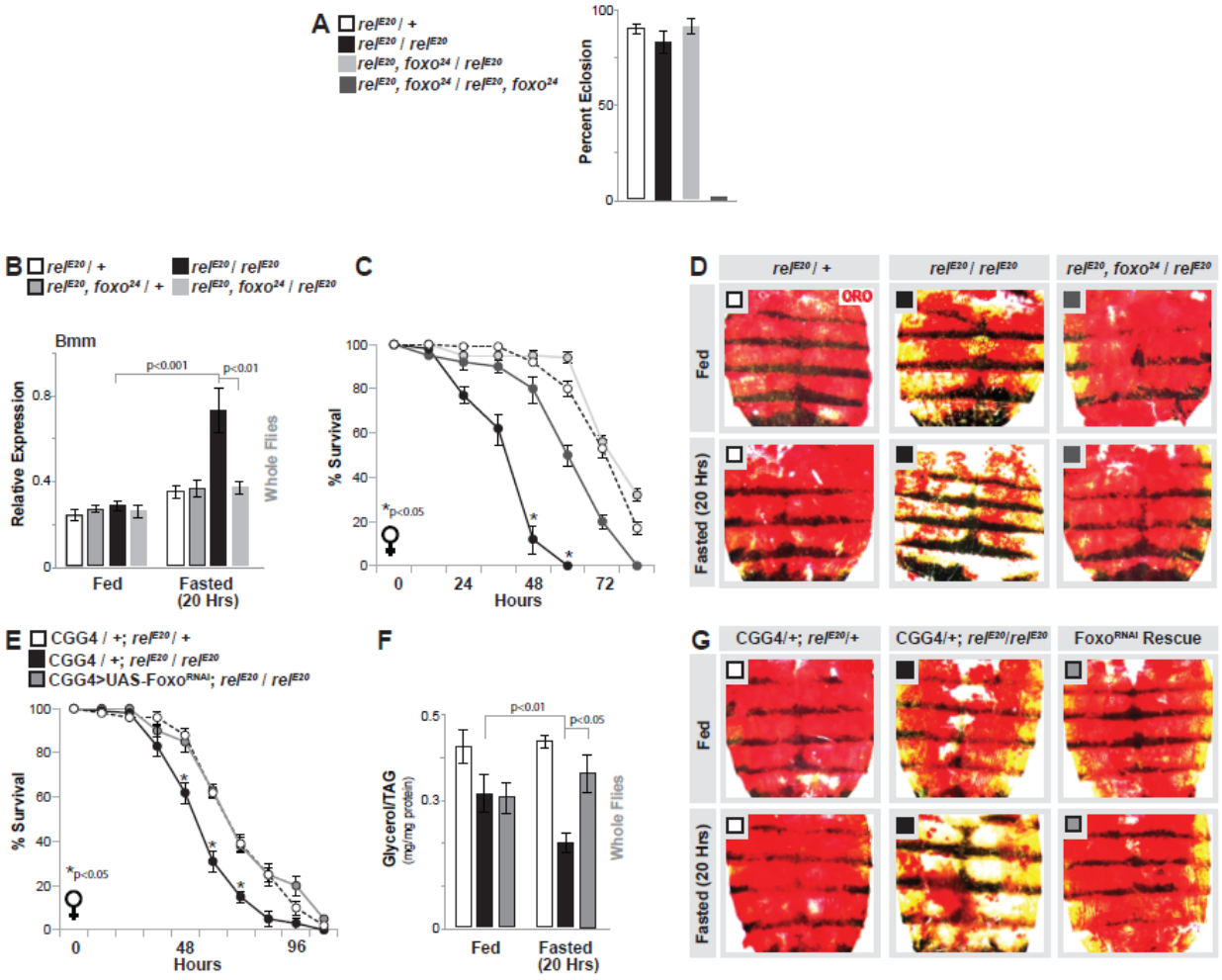

Figure 3.19 FoxO and Relish antagonism dictate fasting-induced Bmm transcription and lipolysis. (A) Percent eclosion of adult animals of indicated mutants / double mutants. n = 67-90 animals. (B) Changes in *bmm* transcription (measured by qRT-PCR in whole flies) before and after fasting (20 hours) in controls (rel^{E20}/+ and rel^{E20}, $FoxO^{24}$/+), mutant (rel^{E20}/rel^{E20}) and mutant with reduction in FoxO gene dose (rel^{E20}, $FoxO^{24}/rel^{E20}$) genotypes. n = 3 samples. (C) Starvation resistance of Relish-deficient female flies with reduction in FoxO gene dose (n = 4 cohorts (total 68-78 flies)), and (D) ORO stain of dissected carcass/ fat body before and after fasting (20 hours). (E-G) Attenuating FoxO (RNAi line v106097) in fat body (CGGal4) of Relish-deficient flies restores metabolic adaptation responses. (E) Starvation resistance of female flies (CGGal4/+; rel^{E20}/+ (control), CGGal4/+; rel^{E20}/rel^{E20} (mutant), or CGGal4/UAS-FoxO RNAi; rel^{E20}/rel^{E20} (Rescue)). n = 6 cohorts (total 117-140 flies). The red arrow indicates time-point of fasting assays. (F) Total TAG levels of whole flies (n = 5 samples) and (G) ORO stain of dissected carcass/ fat body before and after fasting (20 hours).

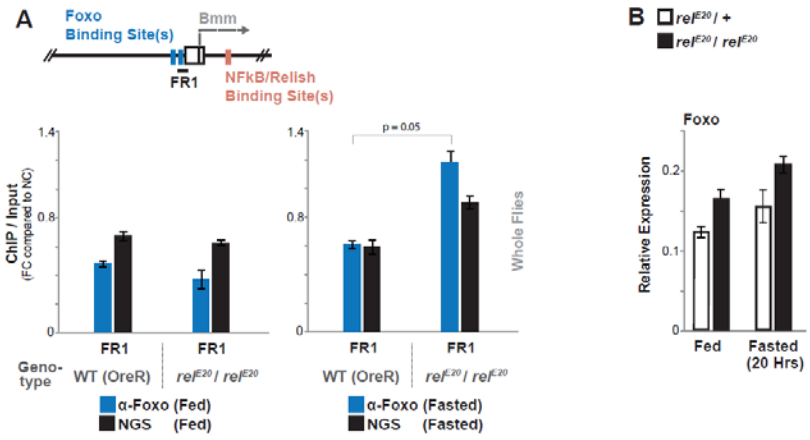

Figure 3.20 Binding of FoxO TF to Bmm locus is enhanced upon fasting. (A) Schematic shows Bmm locus (focusing on the upstream promoter and first intron proximal to transcription start site), as well as FoxO and NF-κB/Rel binding motifs. FR1 represents regional target site of FoxO binding (and corresponding primer set) tested in ChIP-qPCR analysis. The histogram represents ChIP-qPCR analysis of FoxO binding to the Bmm promoter/locus in fed (left panel) and fasted (20 hours; right panel) conditions. ChIP-qPCR analysis with normal goat serum (NGS) is included as a control. Plotted as fold change (FC) of indicated PCR primer sets compared to a negative control (NC) primer set. n = 3 samples. (B) *Drosophila FoxO* transcription (measured by qRT-PCR in whole flies) before and after fasting (20 hours). *relE20*/+ (heterozygote control), or *relE20*/*relE20* (mutant) genotypes. n = 3 samples. All bars and line graph markers represent mean±SE. All flies were 7 days old post-eclosion.

4. CONCLUSIONS AND FUTURE DIRECTION

This study aimed to uncover the role of Relish innate immune transcription factor, the orthologue of mammalian NF-κB, in the control of cellular lipid homeostasis. Our lipid analysis and starvation sensitivity assays (Figures 3.1, 3.5 and 3.6) revealed that Relish in the fat body plays an important role in the regulation of lipid homeostasis during metabolic adaptation. More precisely, Relish prevents excessive triglyceride hydrolysis during fasting and therefore, is required for maintaining lipid storage in fat body. Consistent with our findings, the effect of Relish on the triglyceride content of flies was previously reported by Rynes et al. (Rynes et al., 2012). NF-κB signaling pathway is also linked to lipid metabolism in mammals, through its regulatory effect on PPAR-ɣ[10] (Gao et al., 2006; Kim et al., 2006; Nunn et al., 2007). However, it is not clear whether NF-κB can directly affect lipid storage/content in mammals. Also, we would like to mention that the methods used in our study (TAGs measurement kit, ORO and Nile staining (described in sections 2.5-7)) are incapable of distinguishing the different types of TAGs (different number of carbon, short-chain versus long-chain, and saturated versus unsaturated fatty acids) or other esterified lipids such as cholesterol. Therefore, a future direction would be performing lipidomics analysis in order to explore how elevated Bmm expression in Relish deficient flies may influence specific types of TAGs or other esterified lipids. This analysis can be particularly important to determine whether there is a Relish-dependent change in the amount of signaling lipids stored in the lipid droplets such as eicosanoids.

[10] PPARɣ is a major regulator of lipid metabolism. A study suggested that it is involved in transactivation of ATGL.

Our feeding behavior assays (Figure 3.2) suggested that Relish positively impacts appetite. In mammals, several studies have also linked NF-κB pathway to the regulation of feed intake. However, in contrast to our results, mammalian studies have highlighted the anorexic effect of NF-κB. For example, upregulation of IL-1 α and IL-1β, both targets of NF-κB transcription factor, is associated with anorexia in cancer, a condition in which NF-κB is elevated and promotes inflammation (Gupta et al., 2011). In addition, it is known that activation of NF-κB in hypothalamus (by LPS or leptin) leads to anorexia through induction of POMC (pro-opiomelanocortin, a precursor of anorexigenic melanocortin) (Jang et al., 2010). In central nervous system (CNS), MyD88, an upstream component of NF-κB pathway, is responsible for inhibition of leptin in response to diet-induced obesity (Kleinridders et al., 2009). Similarly, overnutrition/obesity-induced TLR signaling in adipose tissue leads to disruption of leptin function[11] through IKKβ (Baker et al., 2011). This controversial observation might be due to the effect of upregulated NF-κB in disease condition (obesity, inflammation, and cancer in mammalian studies) versus the steady-state function of NF-κB in healthy organisms under normal conditions (our study). In other words, NF-κB pathway may promote or inhibit appetite according to the organism's condition and tissue. Another possible explanation is the diverged mechanism of food intake in mammals and flies due to the more complexity of organs in mammals.

Transcriptional analysis of several lipases and rescue experiments (Figures 3.12 and 3.13) provided evidence that inhibitory effect of Relish on fasting-induced lipolysis is through specific repression of Bmm, the orthologue of mammalian ATGL lipase. ATGL/Bmm is the major

[11] Leptin inhibits food intake/appetite through its effect on hypothalamus.

triglyceride lipase, initiating and rate-limiting component of the lipolysis process in both mammals and flies (Gronke et al., 2005; Schreiber et al., 2019). It is shown that decreased activity of this lipase leads to increased fat storage and obesity, and enhanced activity is associated with weight loss and lean animals (Gronke et al., 2007; Haemmerle et al., 2006). Thus, it is quite possible that the dramatic decrease in lipid storage observed upon fasting in our study is due to overexpression of Bmm in Relish-deficient flies.

Interestingly, the maximum of only two-fold induction of Bmm expression was observed in our study (Figures 3.12, and 3.13), which led to a dramatic decrease in lipid content of Relish deficient flies (Figures 3.1, 3.5, 3.6, and 3.13). These results suggest that Bmm is a non-processive enzyme with a tight threshold of induction, and requires precise regulation in order to maintain lipid homeostasis. Therefore, Relish might be required to limit the gene inducibility of Bmm. Further research needs to determine whether Relish plays role in limiting the gene inducibility of other metabolic genes with a tight induction threshold.

Transcription binding site analysis (using clover software), in vitro transcription reporter assay (using transgenic flies), ChIP assays (using Relish and H3K9Ac antibodies) (Figures 3.14 and 3.16) and analysis of Bmm expression in HDAC1-attenuated flies (Figure 3.16) revealed that NF-κB binds to a region within the first intron of Bmm gene in both fasted and fed condition. Furthermore, upon fasting, Relish can repress the expression of Bmm by decreasing the acetylation of Histone 3 at Lysine 9 (H3K9Ac)[12] within Bmm locus, likely through recruiting Rpd3 (*Drosophila* HDAC1). In line with our results, previous studies demonstrated that NF-κB could

[12] An epigenetic marker that is associated with open chromatin and enhanced expression of genes.

repress the expression of genes by recruiting HDACs (histone acetylases). These HDACs act as co-repressors of NF-κB transcription factors (Gao et al., 2005). For instance, NF-κB/HDAC1 can repress the expression of mir-424, mir-503, and gastrin (Datta De et al., 2013; Zhou et al., 2013). In addition, IκBα (upstream component of NF-κB pathway) can inhibit PPAR-γ activity by promoting nuclear translocation of HDAC3 in response to TNF-α. Indeed, the inhibition of PPAR-γ by TNF-α is not through decreasing the DNA binding activity of this TF but through IκBα-dependent translocation of HDAC3 (Gao et al., 2006).

Dong et al. reported that un-phosphorylated NF-κB /p65 represses the expression of genes by recruiting HDAC1. They proposed a model in which un-phosphorylated NF-κB has the ability to bind to NF-κB binding motif but is inefficient at recruiting CBP/p300 coactivator. Instead, it recruits HDAC1, which leads to the repression of a subset of genes (Dong et al., 2008). Their model, in fact, has some similarities to our observations. In our study, NF-κB/Relish binds to the Bmm region in both fed and fasted conditions; however, binding of Relish does not impose any detectable positive regulation during feeding/basal condition. Although our analysis using upstream components of Relish pathway (Figure 3.11) suggest that proteolytic cleavage of Relish is required for its effect on lipid metabolism, the Relish antibody used in this research (Table 2.4) can detect both cleaved and un-cleaved form of Relish (Figure 3.14A). Therefore, we are not able to determine if Relish attached to Bmm locus is the active cleaved form capable of inducing gene expression or not.

Some studies have reported the assisted-recruitment and/or function of HDAC1. For instance, in *Drosophila* recruitment of HDAC1 to the promoter of Relish target genes is mediated by an IκB protein named pickle (Morris et al., 2016). Moreover, it is shown that HDAC1 can make

a complex with SMRT (Gao et al., 2005). Hence, future studies should investigate whether Relish directly recruits HDAC1 or some other proteins such as pickle are involved as well. Also, if HDAC1/Rpd3 creates a complex with SMRTE (orthologue of mammalian SMRT).

While we only assessed the H3K9 acetylation state of Bmm locus, and its regulatory effect on Bmm expression, analysis of modEncode ChIP-Seq. database (Contrino et al., 2012) suggests that other epigenetic markers such as H3K27ac, H3K4me3, and H3K4me1 might be involved in the regulation of Bmm as well. Additionally, non-acetylated histones are usually characterized by DNA hyper-methylation at CpG islands (Gao et al., 2005; Guzik and Cosentino, 2018; Shakespear et al., 2011). Thus, researchers may further examine the effect of these epigenetic markers, in order to better understand the complexity of Bmm transcription.

Analysis of the mRNA level of Bmm in response to attenuation of different metabolic factors/TFs (figure3.18) combined with the results of our rescue experiments (figure3.19) provided evidence that Relish antagonizes FoxO transcriptional activity on Bmm locus. FoxO is a major metabolic transcription factor. Induction of ATGL and Bmm by FoxO in response to starvation is previously stablished (Chakrabarti and Kandror, 2009; Zhang et al., 2016). Furthermore, similar to our findings, previous researches have demonstrated that regulation of many of NF-κB target genes requires the collaboration of NF-κB with another transcription factors such as STAT, AP1, and IRFs (Grivennikov and Karin, 2010; Oeckinghaus et al., 2011; Zhong et al., 2006).

Our research shows that the deacetylation of Bmm locus, likely by HDAC1 leads to limited FoxO-mediated transcription. The association of FoxO TFs and HDACs has been reported in previous studies, although not in the same context and direction. For example, HDAC4 acts as a coactivator of FoxO in response to fasting-induced Akh signaling. Association of FoxO with

HDAC4 promotes expression of Bmm and lipolysis in flies (Choi et al., 2015; Wang et al., 2011). In mammalian skeletal muscles, HDAC1 and HDAC2 deacetylate FoxO3a. This deacetylation results in enhanced nuclear localization and transcriptional activity of FoxO3a and promotes muscle atrophy (Beharry et al., 2014). While these researches are not in the same direction and context of our study, they still highlight the importance of HDACs in the regulation of FoxO transcriptional activity. These differences in the function of HDAC1 are likely due to acetylation of FoxO proteins versus histones located at FoxO target genes as well as, tissue and gene specificity of FoxO-dependent transcription. Furthermore, it is plausible that this opposite function of HDAC1 is required for the proper balancing of FoxO function.

Researchers have indicated that AMPK and SIRT1 may serve as upstream regulators of FoxO and ATGL (Chen et al., 2012a; Lo et al., 2019). However, we did not observe the AMPK-dependent or dSir2 (orthologue of SIRT1)-dependent changes in bmm expression upon fasting (Figure 3.18). Additionally, the expression of Lip4 (Figures 3.12 and 3.13), another FoxO target gene, as well as FoxO TF itself (Figure 3.20) were not Relish-dependent. Collectively, these data confirm that firstly, Relish represses Bmm expression by limiting FoxO-dependent transcription, and secondly, this effect of Relish is not due to decreasing global activity of FoxO but more likely through local chromatin/histone modifications at Bmm locus. Having that said, it is known that NF-κB TFs also contribute to the regulation of the genes via expression or repression of miRNAs (Boldin and Baltimore, 2012; Mann et al., 2017; Markopoulos et al., 2018). Therefore, the question remains if Relish regulates Bmm by induction of a specific miRNA in addition to histone acetylation.

Our research revealed that Relish regulates expression of Bmm, which is a FoxO target gene. Interestingly, FoxO transcription factor is also involved in the regulation of immune genes independent of infection and according to energy (Wang et al., 2014). Indeed, FoxO can induce expression of Relish, Dredd, Key (Dredd and Key are upstream components of Relish pathway), and some Relish-target AMPs. The promoter of these AMPs carries FoxO binding motif, which allows regulation of these immune genes by FoxO and according to nutritional condition (Becker et al., 2010; Li et al., 2012; Varma et al., 2014). In addition, in the intestine of flies, FoxO can repress PGRP-SC2, which is the inhibitor of Imd/Relish pathway (Guo et al., 2014). This function of FoxO is important in maintaining immune homeostasis while the organism is facing energy changes. Collectively, our study, combined with previous reports regarding the effect of FoxO on immunity, suggests that FoxO and Relish collaboration is required to maintain both immune and lipid homeostasis. However, future studies need to explore whether other metabolic FoxO target genes are regulated by Relish.

Another intriguing question that might be addressed in the future is how the organism may benefit from the inhibitory effect of NF-κB on lipolysis. It is known that fatty acids act as an inducer of NF-κB pathway (Lee et al., 2003; Yin et al., 2014). Therefore, one plausible answer is that NF-κB indeed tries to block a positive feedback loop, and therefore prevents inflammation and avoids spending of energy on immune response during fasting, when, in fact, energy is more required for dormancy (energy-preserving catabolic metabolism). While our current data is not supporting this hypothesis, since we did not observe upregulation of Dpt during acute fasting (Figure 3.15), this hypothesis might still be valid during chronic low energy intake, or in regard to other targets of Relish.

Triglyceride form the main part of lipid droplets. During fasting, triglycerides in the lipid droplets undergo hydrolysis to provide energy for energy-consuming organs. In addition to TAGs, lipid droplets contain esterified lipids such as cholesterol and are sites for synthesis and/or storage of eicosanoids and some other signaling lipids as well as some transcription factors. Interestingly, these dynamic organelles also serve as a repertoire of antiviral and antibacterial proteins and therefore, play a role in immune responses (Arrese et al., 2014; den Brok et al., 2018; Welte, 2015). Our data demonstrated that attenuation of Relish function leads to less and smaller lipid droplets in the fat body of adult flies (Figure 3.1D). Thus, one can argue that Relish strives to maintain the immune function, as well as the potential signaling transduction function of lipid droplets by repressing fasting-induced lipolysis. In order to better dissect the role of Relish in signaling and distinguish the immune and metabolic function of this transcription factor, we are considering two approaches. Firstly, as previously mentioned, performing lipidomic and proteomic analysis of lipid droplets will help to determine whether there is a change in the amount of signaling molecules (protein or lipids) that reside in the lipid droplets. Secondly, we are planning to create transgenic flies with a mutated NF-κB binding site at Bmm locus, using CRISPR/Cas9 technology. Afterward, we will examine the effect of this single mutation at the Bmm locus on immunity of flies. Using this approach would be extremely beneficial for distinguishing the immune and metabolic effects of Relish-dependent repression of Bmm expression.

In summary, using *Drosophila* we uncovered a role for the innate immune transcription factor Relish in governing lipid metabolism during metabolic adaptation. Relish is required to limit triglyceride hydrolysis during fasting and therefore, maintains lipid storage. Figure 4.1 represents our proposed model for the regulation of Bmm by FoxO and Relish. In this model, Relish binds to

Bmm locus in both fed and fasted conditions. Upon fasting Relish inhibits FoxO-dependent transcription of Bmm by recruiting HDAC1 and modifying histone acetylation state of Bmm locus.

Lastly, we would like to mention that conservation of fundamental components of innate immune and lipid metabolism system (such as NF-κB, FoxO, and ATGL), as well as the existence of NF-κB binding motif within mice ATGL locus, suggest that similar mechanism is involved in the regulation of lipolysis in mammals. However, due to more complexity of pathways and organs in mammals, our model cannot be simply generalized to mammalian systems. Therefore, more studies need to be done in order to investigate the involvement of the same mechanism in the regulation of lipid metabolism in mammals. In addition, studying different species that are between Drosophila and mammals in the phylogenetic tree (such as fish, amphibians, and bird) may provide a better insight into the coevolution of immune and metabolic pathways and the conservation of the particular mechanism discovered in our study.

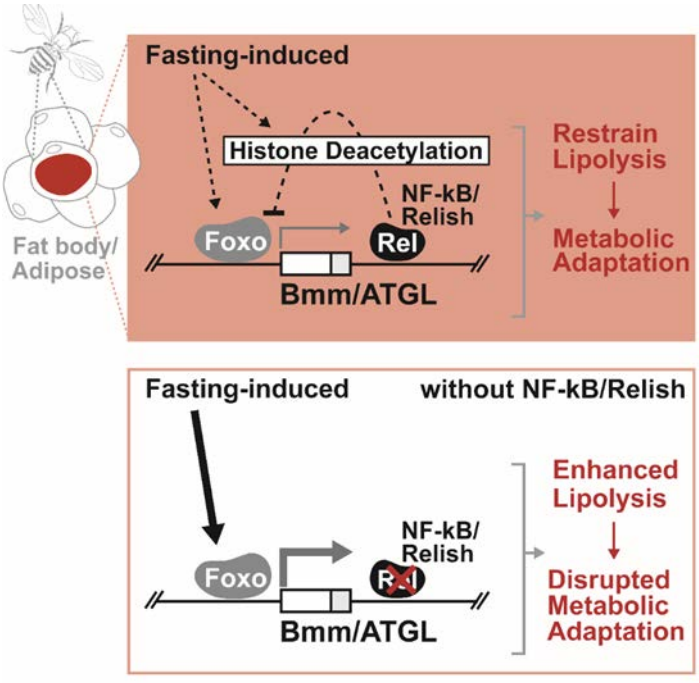

Figure 4.1 Upon fasting, Relish inhibits FoxO-mediated expression of Bmm through the recruitment of HDAC1.

REFERENCES

Ahmadian, M., Abbott, M.J., Tang, T., Hudak, C.S., Kim, Y., Bruss, M., Hellerstein, M.K., Lee, H.Y., Samuel, V.T., Shulman, G.I., et al. (2011). Desnutrin/ATGL is regulated by AMPK and is required for a brown adipose phenotype. Cell Metab *13*, 739-748.

Arner, P., Bernard, S., Salehpour, M., Possnert, G., Liebl, J., Steier, P., Buchholz, B.A., Eriksson, M., Arner, E., Hauner, H., et al. (2011). Dynamics of human adipose lipid turnover in health and metabolic disease. Nature *478*, 110-113.

Arquier, N., and Leopold, P. (2007). Fly foie gras: modeling fatty liver in Drosophila. Cell Metab *5*, 83-85.

Arrese, E.L., Saudale, F.Z., and Soulages, J.L. (2014). Lipid Droplets as Signaling Platforms Linking Metabolic and Cellular Functions. Lipid Insights *7*, 7-16.

Arrese, E.L., and Soulages, J.L. (2010). Insect fat body: energy, metabolism, and regulation. Annual review of entomology *55*, 207-225.

Ashburner, B.P., Westerheide, S.D., and Baldwin, A.S., Jr. (2001). The p65 (RelA) subunit of NF-kappaB interacts with the histone deacetylase (HDAC) corepressors HDAC1 and HDAC2 to negatively regulate gene expression. Mol Cell Biol *21*, 7065-7077.

Baker, R.G., Hayden, M.S., and Ghosh, S. (2011). NF-kappaB, inflammation, and metabolic disease. Cell Metab *13*, 11-22.

Baumbach, J., Hummel, P., Bickmeyer, I., Kowalczyk, K.M., Frank, M., Knorr, K., Hildebrandt, A., Riedel, D., Jackle, H., and Kuhnlein, R.P. (2014). A Drosophila in vivo screen identifies store-operated calcium entry as a key regulator of adiposity. Cell Metab *19*, 331-343.

Becker, T., Loch, G., Beyer, M., Zinke, I., Aschenbrenner, A.C., Carrera, P., Inhester, T., Schultze, J.L., and Hoch, M. (2010). FOXO-dependent regulation of innate immune homeostasis. Nature *463*, 369-373.

Beharry, A.W., Sandesara, P.B., Roberts, B.M., Ferreira, L.F., Senf, S.M., and Judge, A.R. (2014). HDAC1 activates FoxO and is both sufficient and required for skeletal muscle atrophy. J Cell Sci *127*, 1441-1453.

Bi, J., Xiang, Y., Chen, H., Liu, Z., Gronke, S., Kuhnlein, R.P., and Huang, X. (2012). Opposite and redundant roles of the two Drosophila perilipins in lipid mobilization. J Cell Sci *125*, 3568-3577.

Boldin, M.P., and Baltimore, D. (2012). MicroRNAs, new effectors and regulators of NF-kappaB. Immunol Rev *246*, 205-220.

Boutens, L., and Stienstra, R. (2016). Adipose tissue macrophages: going off track during obesity. Diabetologia *59*, 879-894.

Brown, A.K., and Webb, A.E. (2018). Regulation of FOXO Factors in Mammalian Cells. Curr Top Dev Biol *127*, 165-192.

Buchon, N., Silverman, N., and Cherry, S. (2014). Immunity in Drosophila melanogaster--from microbial recognition to whole-organism physiology. Nat Rev Immunol *14*, 796-810.

Busse, M.S., Arnold, C.P., Towb, P., Katrivesis, J., and Wasserman, S.A. (2007). A kappaB sequence code for pathway-specific innate immune responses. EMBO J *26*, 3826-3835.

Cai, D., Yuan, M., Frantz, D.F., Melendez, P.A., Hansen, L., Lee, J., and Shoelson, S.E. (2005). Local and systemic insulin resistance resulting from hepatic activation of IKK-beta and NF-kappaB. Nat Med *11*, 183-190.

Canavoso, L.E., Jouni, Z.E., Karnas, K.J., Pennington, J.E., and Wells, M.A. (2001). Fat metabolism in insects. Annu Rev Nutr *21*, 23-46.

Chakrabarti, P., English, T., Karki, S., Qiang, L., Tao, R., Kim, J., Luo, Z., Farmer, S.R., and Kandror, K.V. (2011). SIRT1 controls lipolysis in adipocytes via FOXO1-mediated expression of ATGL. J Lipid Res *52*, 1693-1701.

Chakrabarti, P., and Kandror, K.V. (2009). FoxO1 controls insulin-dependent adipose triglyceride lipase (ATGL) expression and lipolysis in adipocytes. The Journal of biological chemistry *284*, 13296-13300.

Chatterjee, N., and Bohmann, D. (2012). A versatile PhiC31 based reporter system for measuring AP-1 and Nrf2 signaling in Drosophila and in tissue culture. PLoS One *7*, e34063.

Chen, L., Chen, R., Wang, H., and Liang, F. (2015). Mechanisms Linking Inflammation to Insulin Resistance. Int J Endocrinol *2015*, 508409.

Chen, W.L., Chen, Y.L., Chiang, Y.M., Wang, S.G., and Lee, H.M. (2012a). Fenofibrate lowers lipid accumulation in myotubes by modulating the PPARalpha/AMPK/FoxO1/ATGL pathway. Biochem Pharmacol *84*, 522-531.

Chen, X., Barozzi, I., Termanini, A., Prosperini, E., Recchiuti, A., Dalli, J., Mietton, F., Matteoli, G., Hiebert, S., and Natoli, G. (2012b). Requirement for the histone deacetylase Hdac3 for the inflammatory gene expression program in macrophages. Proc Natl Acad Sci U S A *109*, E2865-2874.

Choi, S., Lim, D.S., and Chung, J. (2015). Feeding and Fasting Signals Converge on the LKB1-SIK3 Pathway to Regulate Lipid Metabolism in Drosophila. PLoS Genet *11*, e1005263.

Clark, R.I., Tan, S.W., Pean, C.B., Roostalu, U., Vivancos, V., Bronda, K., Pilatova, M., Fu, J., Walker, D.W., Berdeaux, R., et al. (2013). MEF2 is an in vivo immune-metabolic switch. Cell *155*, 435-447.

Contrino, S., Smith, R.N., Butano, D., Carr, A., Hu, F., Lyne, R., Rutherford, K., Kalderimis, A., Sullivan, J., Carbon, S., et al. (2012). modMine: flexible access to modENCODE data. Nucleic Acids Res *40*, D1082-1088.

Datta De, D., Datta, A., Bhattacharjya, S., and Roychoudhury, S. (2013). NF-kappaB mediated transcriptional repression of acid modifying hormone gastrin. PLoS One *8*, e73409.

Daval, M., Diot-Dupuy, F., Bazin, R., Hainault, I., Viollet, B., Vaulont, S., Hajduch, E., Ferre, P., and Foufelle, F. (2005). Anti-lipolytic action of AMP-activated protein kinase in rodent adipocytes. J Biol Chem *280*, 25250-25257.

den Brok, M.H., Raaijmakers, T.K., Collado-Camps, E., and Adema, G.J. (2018). Lipid Droplets as Immune Modulators in Myeloid Cells. Trends Immunol *39*, 380-392.

Dionne, M. (2014). Immune-metabolic interaction in Drosophila. Fly (Austin) *8*, 75-79.

Dominguez-Andres, J., Joosten, L.A., and Netea, M.G. (2018). Induction of innate immune memory: the role of cellular metabolism. Curr Opin Immunol *56*, 10-16.

Dong, J., Jimi, E., Zhong, H., Hayden, M.S., and Ghosh, S. (2008). Repression of gene expression by unphosphorylated NF-kappaB p65 through epigenetic mechanisms. Genes Dev *22*, 1159-1173.

Dostert, C., Jouanguy, E., Irving, P., Troxler, L., Galiana-Arnoux, D., Hetru, C., Hoffmann, J.A., and Imler, J.L. (2005). The Jak-STAT signaling pathway is required but not sufficient for the antiviral response of drosophila. Nat Immunol *6*, 946-953.

Eguchi, J., Kong, X., Tenta, M., Wang, X., Kang, S., and Rosen, E.D. (2013). Interferon regulatory factor 4 regulates obesity-induced inflammation through regulation of adipose tissue macrophage polarization. Diabetes *62*, 3394-3403.

Frith, M.C., Fu, Y., Yu, L., Chen, J.F., Hansen, U., and Weng, Z. (2004). Detection of functional DNA motifs via statistical over-representation. Nucleic Acids Res *32*, 1372-1381.

Gaidhu, M.P., Fediuc, S., Anthony, N.M., So, M., Mirpourian, M., Perry, R.L., and Ceddia, R.B. (2009). Prolonged AICAR-induced AMP-kinase activation promotes energy dissipation in white adipocytes: novel mechanisms integrating HSL and ATGL. J Lipid Res *50*, 704-715.

Galenza, A., and Foley, E. (2019). Immunometabolism: Insights from the Drosophila model. Dev Comp Immunol *94*, 22-34.

Galiana-Arnoux, D., Dostert, C., Schneemann, A., Hoffmann, J.A., and Imler, J.L. (2006). Essential function in vivo for Dicer-2 in host defense against RNA viruses in drosophila. Nat Immunol *7*, 590-597.

Ganesan, S., Aggarwal, K., Paquette, N., and Silverman, N. (2011). NF-kappaB/Rel proteins and the humoral immune responses of Drosophila melanogaster. Curr Top Microbiol Immunol *349*, 25-60.

Gao, Z., Chiao, P., Zhang, X., Zhang, X., Lazar, M.A., Seto, E., Young, H.A., and Ye, J. (2005). Coactivators and corepressors of NF-kappaB in IkappaB alpha gene promoter. J Biol Chem *280*, 21091-21098.

Gao, Z., He, Q., Peng, B., Chiao, P.J., and Ye, J. (2006). Regulation of nuclear translocation of HDAC3 by IkappaBalpha is required for tumor necrosis factor inhibition of peroxisome proliferator-activated receptor gamma function. J Biol Chem *281*, 4540-4547.

Gao, Z., Zhang, X., Zuberi, A., Hwang, D., Quon, M.J., Lefevre, M., and Ye, J. (2004). Inhibition of insulin sensitivity by free fatty acids requires activation of multiple serine kinases in 3T3-L1 adipocytes. Mol Endocrinol *18*, 2024-2034.

Gilmore, T.D. (2006). Introduction to NF-kappaB: players, pathways, perspectives. Oncogene *25*, 6680-6684.

Gilmore, T.D., and Wolenski, F.S. (2012). NF-kappaB: where did it come from and why? Immunol Rev *246*, 14-35.

Glass, C.K., and Olefsky, J.M. (2012). Inflammation and lipid signaling in the etiology of insulin resistance. Cell Metab *15*, 635-645.

Gold, K.S., and Bruckner, K. (2015). Macrophages and cellular immunity in Drosophila melanogaster. Semin Immunol *27*, 357-368.

Grahn, T.H., Kaur, R., Yin, J., Schweiger, M., Sharma, V.M., Lee, M.J., Ido, Y., Smas, C.M., Zechner, R., Lass, A., et al. (2014). Fat-specific protein 27 (FSP27) interacts with adipose triglyceride lipase (ATGL) to regulate lipolysis and insulin sensitivity in human adipocytes. J Biol Chem *289*, 12029-12039.

Grivennikov, S.I., and Karin, M. (2010). Dangerous liaisons: STAT3 and NF-kappaB collaboration and crosstalk in cancer. Cytokine Growth Factor Rev *21*, 11-19.

Gronke, S., Mildner, A., Fellert, S., Tennagels, N., Petry, S., Muller, G., Jackle, H., and Kuhnlein, R.P. (2005). Brummer lipase is an evolutionary conserved fat storage regulator in Drosophila. Cell Metab *1*, 323-330.

Gronke, S., Muller, G., Hirsch, J., Fellert, S., Andreou, A., Haase, T., Jackle, H., and Kuhnlein, R.P. (2007). Dual lipolytic control of body fat storage and mobilization in Drosophila. PLoS biology *5*, e137.

Guo, L., Karpac, J., Tran, S.L., and Jasper, H. (2014). PGRP-SC2 promotes gut immune homeostasis to limit commensal dysbiosis and extend lifespan. Cell *156*, 109-122.

Gupta, S.C., Kim, J.H., Kannappan, R., Reuter, S., Dougherty, P.M., and Aggarwal, B.B. (2011). Role of nuclear factor kappaB-mediated inflammatory pathways in cancer-related symptoms and their regulation by nutritional agents. Exp Biol Med (Maywood) *236*, 658-671.

Gutierrez, E., Wiggins, D., Fielding, B., and Gould, A.P. (2007). Specialized hepatocyte-like cells regulate Drosophila lipid metabolism. Nature *445*, 275-280.

Guzik, T.J., and Cosentino, F. (2018). Epigenetics and Immunometabolism in Diabetes and Aging. Antioxid Redox Signal *29*, 257-274.

Haemmerle, G., Lass, A., Zimmermann, R., Gorkiewicz, G., Meyer, C., Rozman, J., Heldmaier, G., Maier, R., Theussl, C., Eder, S., et al. (2006). Defective lipolysis and altered energy metabolism in mice lacking adipose triglyceride lipase. Science *312*, 734-737.

Heier, C., and Kuhnlein, R.P. (2018). Triacylglycerol Metabolism in Drosophila melanogaster. Genetics *210*, 1163-1184.

Hennig, K.M., Colombani, J., and Neufeld, T.P. (2006). TOR coordinates bulk and targeted endocytosis in the Drosophila melanogaster fat body to regulate cell growth. J Cell Biol *173*, 963-974.

Henstridge, D.C., Bruce, C.R., Pang, C.P., Lancaster, G.I., Allen, T.L., Estevez, E., Gardner, T., Weir, J.M., Meikle, P.J., Lam, K.S.L., et al. (2012). Skeletal muscle-specific overproduction of constitutively activated c-Jun N-terminal kinase (JNK) induces insulin resistance in mice. Diabetologia *55*, 2769-2778.

Hetru, C., and Hoffmann, J.A. (2009). NF-kappaB in the immune response of Drosophila. Cold Spring Harb Perspect Biol *1*, a000232.

Hotamisligil, G.S. (2017a). Foundations of Immunometabolism and Implications for Metabolic Health and Disease. Immunity *47*, 406-420.

Hotamisligil, G.S. (2017b). Inflammation, metaflammation and immunometabolic disorders. Nature *542*, 177-185.

Hultmark, D. (2003). Drosophila immunity: paths and patterns. Curr Opin Immunol *15*, 12-19.

Iliopoulos, D., Hirsch, H.A., and Struhl, K. (2009). An epigenetic switch involving NF-kappaB, Lin28, Let-7 MicroRNA, and IL6 links inflammation to cell transformation. Cell *139*, 693-706.

Jang, P.G., Namkoong, C., Kang, G.M., Hur, M.W., Kim, S.W., Kim, G.H., Kang, Y., Jeon, M.J., Kim, E.H., Lee, M.S., et al. (2010). NF-kappaB activation in hypothalamic pro-opiomelanocortin neurons is essential in illness- and leptin-induced anorexia. J Biol Chem *285*, 9706-9715.

Ji, Y., Thomas, C., Tulin, N., Lodhi, N., Boamah, E., Kolenko, V., and Tulin, A.V. (2016). Charon Mediates Immune Deficiency-Driven PARP-1-Dependent Immune Responses in Drosophila. Journal of immunology *197*, 2382-2389.

Jialal, I., Kaur, H., and Devaraj, S. (2014). Toll-like receptor status in obesity and metabolic syndrome: a translational perspective. J Clin Endocrinol Metab *99*, 39-48.

Johnson, R.F., and Perkins, N.D. (2012). Nuclear factor-kappaB, p53, and mitochondria: regulation of cellular metabolism and the Warburg effect. Trends Biochem Sci *37*, 317-324.

Johnson, R.F., Witzel, II, and Perkins, N.D. (2011). p53-dependent regulation of mitochondrial energy production by the RelA subunit of NF-kappaB. Cancer Res *71*, 5588-5597.

Kaltenecker, D., Mueller, K.M., Benedikt, P., Feiler, U., Themanns, M., Schlederer, M., Kenner, L., Schweiger, M., Haemmerle, G., and Moriggl, R. (2017). Adipocyte STAT5 deficiency promotes adiposity and impairs lipid mobilisation in mice. Diabetologia *60*, 296-305.

Kamareddine, L., Robins, W.P., Berkey, C.D., Mekalanos, J.J., and Watnick, P.I. (2018). The Drosophila Immune Deficiency Pathway Modulates Enteroendocrine Function and Host Metabolism. Cell Metab.

Kang, P., Chang, K., Liu, Y., Bouska, M., Birnbaum, A., Karashchuk, G., Thakore, R., Zheng, W., Post, S., Brent, C.S., et al. (2017). Drosophila Kruppel homolog 1 represses lipolysis through interaction with dFOXO. Sci Rep *7*, 16369.

Kim, J., and Neufeld, T.P. (2015). Dietary sugar promotes systemic TOR activation in Drosophila through AKH-dependent selective secretion of Dilp3. Nat Commun *6*, 6846.

Kim, J.Y., Tillison, K., Lee, J.H., Rearick, D.A., and Smas, C.M. (2006). The adipose tissue triglyceride lipase ATGL/PNPLA2 is downregulated by insulin and TNF-alpha in 3T3-L1 adipocytes and is a target for transactivation by PPARgamma. Am J Physiol Endocrinol Metab *291*, E115-127.

Kim, S.J., Tang, T., Abbott, M., Viscarra, J.A., Wang, Y., and Sul, H.S. (2016). AMPK Phosphorylates Desnutrin/ATGL and Hormone-Sensitive Lipase To Regulate Lipolysis and Fatty Acid Oxidation within Adipose Tissue. Mol Cell Biol *36*, 1961-1976.

Kim, S.K., and Rulifson, E.J. (2004). Conserved mechanisms of glucose sensing and regulation by Drosophila corpora cardiaca cells. Nature *431*, 316-320.

Kim, T.H., Choi, S.E., Ha, E.S., Jung, J.G., Han, S.J., Kim, H.J., Kim, D.J., Kang, Y., and Lee, K.W. (2013). IL-6 induction of TLR-4 gene expression via STAT3 has an effect on insulin resistance in human skeletal muscle. Acta Diabetol *50*, 189-200.

Kleino, A., Myllymaki, H., Kallio, J., Vanha-aho, L.M., Oksanen, K., Ulvila, J., Hultmark, D., Valanne, S., and Ramet, M. (2008). Pirk is a negative regulator of the Drosophila Imd pathway. J Immunol *180*, 5413-5422.

Kleinridders, A., Schenten, D., Konner, A.C., Belgardt, B.F., Mauer, J., Okamura, T., Wunderlich, F.T., Medzhitov, R., and Bruning, J.C. (2009). MyD88 signaling in the CNS is required for development of fatty acid-induced leptin resistance and diet-induced obesity. Cell Metab *10*, 249-259.

Koltes, D.A., Spurlock, M.E., and Spurlock, D.M. (2017). Adipose triglyceride lipase protein abundance and translocation to the lipid droplet increase during leptin-induced lipolysis in bovine adipocytes. Domest Anim Endocrinol *61*, 62-76.

Kosteli, A., Sugaru, E., Haemmerle, G., Martin, J.F., Lei, J., Zechner, R., and Ferrante, A.W., Jr. (2010). Weight loss and lipolysis promote a dynamic immune response in murine adipose tissue. J Clin Invest *120*, 3466-3479.

Kraakman, M.J., Murphy, A.J., Jandeleit-Dahm, K., and Kammoun, H.L. (2014). Macrophage polarization in obesity and type 2 diabetes: weighing down our understanding of macrophage function? Front Immunol *5*, 470.

Kuhnlein, R.P. (2012). Thematic review series: Lipid droplet synthesis and metabolism: from yeast to man. Lipid droplet-based storage fat metabolism in Drosophila. J Lipid Res *53*, 1430-1436.

Kuroda, K., Nakashima, J., Kanao, K., Kikuchi, E., Miyajima, A., Horiguchi, Y., Nakagawa, K., Oya, M., Ohigashi, T., and Murai, M. (2007). Interleukin 6 is associated with cachexia in patients with prostate cancer. Urology *69*, 113-117.

Lee, J.Y., Ye, J., Gao, Z., Youn, H.S., Lee, W.H., Zhao, L., Sizemore, N., and Hwang, D.H. (2003). Reciprocal modulation of Toll-like receptor-4 signaling pathways involving MyD88 and phosphatidylinositol 3-kinase/AKT by saturated and polyunsaturated fatty acids. J Biol Chem *278*, 37041-37051.

Lee, K.A., Cho, K.C., Kim, B., Jang, I.H., Nam, K., Kwon, Y.E., Kim, M., Hyeon, D.Y., Hwang, D., Seol, J.H., et al. (2018a). Inflammation-Modulated Metabolic Reprogramming Is Required for DUOX-Dependent Gut Immunity in Drosophila. Cell Host Microbe *23*, 338-352 e335.

Lee, P.T., Lin, G., Lin, W.W., Diao, F., White, B.H., and Bellen, H.J. (2018b). A kinase-dependent feedforward loop affects CREBB stability and long term memory formation. Elife *7*.

Lemaitre, B., and Hoffmann, J. (2007). The host defense of Drosophila melanogaster. Annu Rev Immunol *25*, 697-743.

Li, S., Yu, X., and Feng, Q. (2019). Fat Body Biology in the Last Decade. Annu Rev Entomol *64*, 315-333.

Li, Z., Zhang, H., Chen, Y., Fan, L., and Fang, J. (2012). Forkhead transcription factor FOXO3a protein activates nuclear factor kappaB through B-cell lymphoma/leukemia 10 (BCL10) protein and promotes tumor cell survival in serum deprivation. J Biol Chem *287*, 17737-17745.

Lo, M.C., Chen, J.Y., Kuo, Y.T., Chen, W.L., Lee, H.M., and Wang, S.G. (2019). Camptothecin activates SIRT1 to promote lipid catabolism through AMPK/FoxO1/ATGL pathway in C2C12 myogenic cells. Arch Pharm Res.

Loftus, R.M., and Finlay, D.K. (2016). Immunometabolism: Cellular Metabolism Turns Immune Regulator. J Biol Chem *291*, 1-10.

Lukic, L., Lalic, N.M., Rajkovic, N., Jotic, A., Lalic, K., Milicic, T., Seferovic, J.P., Macesic, M., and Gajovic, J.S. (2014). Hypertension in obese type 2 diabetes patients is associated with increases in insulin resistance and IL-6 cytokine levels: potential targets for an efficient preventive intervention. Int J Environ Res Public Health *11*, 3586-3598.

Lumeng, C.N., Bodzin, J.L., and Saltiel, A.R. (2007). Obesity induces a phenotypic switch in adipose tissue macrophage polarization. J Clin Invest *117*, 175-184.

Makki, R., Cinnamon, E., and Gould, A.P. (2014). The development and functions of oenocytes. Annu Rev Entomol *59*, 405-425.

Mann, M., Mehta, A., Zhao, J.L., Lee, K., Marinov, G.K., Garcia-Flores, Y., Lu, L.F., Rudensky, A.Y., and Baltimore, D. (2017). An NF-kappaB-microRNA regulatory network tunes macrophage inflammatory responses. Nat Commun *8*, 851.

Markopoulos, G.S., Roupakia, E., Tokamani, M., Alabasi, G., Sandaltzopoulos, R., Marcu, K.B., and Kolettas, E. (2018). Roles of NF-kappaB Signaling in the Regulation of miRNAs Impacting on Inflammation in Cancer. Biomedicines *6*.

Mauro, C., Leow, S.C., Anso, E., Rocha, S., Thotakura, A.K., Tornatore, L., Moretti, M., De Smaele, E., Beg, A.A., Tergaonkar, V., et al. (2011). NF-kappaB controls energy homeostasis and metabolic adaptation by upregulating mitochondrial respiration. Nat Cell Biol *13*, 1272-1279.

McNelis, J.C., and Olefsky, J.M. (2014). Macrophages, immunity, and metabolic disease. Immunity *41*, 36-48.

Meng, X., Khanuja, B.S., and Ip, Y.T. (1999). Toll receptor-mediated Drosophila immune response requires Dif, an NF-kappaB factor. Genes Dev *13*, 792-797.

Mihajlovic, Z., Tanasic, D., Bajgar, A., Perez-Gomez, R., Steffal, P., and Krejci, A. (2019). Lime is a new protein linking immunity and metabolism in Drosophila. Dev Biol *452*, 83-94.

Mihaylova, M.M., Vasquez, D.S., Ravnskjaer, K., Denechaud, P.D., Yu, R.T., Alvarez, J.G., Downes, M., Evans, R.M., Montminy, M., and Shaw, R.J. (2011). Class IIa histone deacetylases are hormone-activated regulators of FOXO and mammalian glucose homeostasis. Cell *145*, 607-621.

Miyoshi, H., Perfield, J.W., 2nd, Souza, S.C., Shen, W.J., Zhang, H.H., Stancheva, Z.S., Kraemer, F.B., Obin, M.S., and Greenberg, A.S. (2007). Control of adipose triglyceride lipase action by serine 517 of perilipin A globally regulates protein kinase A-stimulated lipolysis in adipocytes. J Biol Chem *282*, 996-1002.

Morris, O., Liu, X., Domingues, C., Runchel, C., Chai, A., Basith, S., Tenev, T., Chen, H., Choi, S., Pennetta, G., et al. (2016). Signal Integration by the IkappaB Protein Pickle Shapes Drosophila Innate Host Defense. Cell Host Microbe *20*, 283-295.

Murray, P.J., Rathmell, J., and Pearce, E. (2015). SnapShot: Immunometabolism. Cell Metab *22*, 190-190 e191.

Musselman, L.P., Fink, J.L., Grant, A.R., Gatto, J.A., Tuthill, B.F., 2nd, and Baranski, T.J. (2017). The relationship between immunity and metabolism in Drosophila diet-induced insulin resistance. Mol Cell Biol.

Musselman, L.P., Fink, J.L., Grant, A.R., Gatto, J.A., Tuthill, B.F., 2nd, and Baranski, T.J. (2018). A Complex Relationship between Immunity and Metabolism in Drosophila Diet-Induced Insulin Resistance. Mol Cell Biol *38*.

Musselman, L.P., Fink, J.L., Ramachandran, P.V., Patterson, B.W., Okunade, A.L., Maier, E., Brent, M.R., Turk, J., and Baranski, T.J. (2013). Role of fat body lipogenesis in protection against the effects of caloric overload in Drosophila. J Biol Chem *288*, 8028-8042.

Musselman, L.P., and Kuhnlein, R.P. (2018). Drosophila as a model to study obesity and metabolic disease. J Exp Biol *221*.

Myllymaki, H., Valanne, S., and Ramet, M. (2014). The Drosophila imd signaling pathway. J Immunol *192*, 3455-3462.

Nakajima, E., Shimaji, K., Umegawachi, T., Tomida, S., Yoshida, H., Yoshimoto, N., Izawa, S., Kimura, H., and Yamaguchi, M. (2016). The Histone Deacetylase Gene Rpd3 Is Required for Starvation Stress Resistance. PLoS One *11*, e0167554.

Nguyen, K.D., Qiu, Y., Cui, X., Goh, Y.P., Mwangi, J., David, T., Mukundan, L., Brombacher, F., Locksley, R.M., and Chawla, A. (2011). Alternatively activated macrophages produce catecholamines to sustain adaptive thermogenesis. Nature *480*, 104-108.

Norata, G.D., Caligiuri, G., Chavakis, T., Matarese, G., Netea, M.G., Nicoletti, A., O'Neill, L.A., and Marelli-Berg, F.M. (2015). The Cellular and Molecular Basis of Translational Immunometabolism. Immunity *43*, 421-434.

Notari, L., Baladron, V., Aroca-Aguilar, J.D., Balko, N., Heredia, R., Meyer, C., Notario, P.M., Saravanamuthu, S., Nueda, M.L., Sanchez-Sanchez, F., et al. (2006). Identification of a lipase-linked cell membrane receptor for pigment epithelium-derived factor. J Biol Chem *281*, 38022-38037.

Nunn, A.V., Bell, J., and Barter, P. (2007). The integration of lipid-sensing and anti-inflammatory effects: how the PPARs play a role in metabolic balance. Nucl Recept *5*, 1.

Odegaard, J.I., and Chawla, A. (2013). The immune system as a sensor of the metabolic state. Immunity *38*, 644-654.

Oeckinghaus, A., Hayden, M.S., and Ghosh, S. (2011). Crosstalk in NF-kappaB signaling pathways. Nat Immunol *12*, 695-708.

Osborn, O., and Olefsky, J.M. (2012). The cellular and signaling networks linking the immune system and metabolism in disease. Nat Med *18*, 363-374.

Pagnon, J., Matzaris, M., Stark, R., Meex, R.C., Macaulay, S.L., Brown, W., O'Brien, P.E., Tiganis, T., and Watt, M.J. (2012). Identification and functional characterization of protein kinase A phosphorylation sites in the major lipolytic protein, adipose triglyceride lipase. Endocrinology *153*, 4278-4289.

Pahl, H.L. (1999). Activators and target genes of Rel/NF-kappaB transcription factors. Oncogene *18*, 6853-6866.

Palm, W., Sampaio, J.L., Brankatschk, M., Carvalho, M., Mahmoud, A., Shevchenko, A., and Eaton, S. (2012). Lipoproteins in Drosophila melanogaster--assembly, function, and influence on tissue lipid composition. PLoS Genet *8*, e1002828.

Paradkar, P.N., Trinidad, L., Voysey, R., Duchemin, J.B., and Walker, P.J. (2012). Secreted Vago restricts West Nile virus infection in Culex mosquito cells by activating the Jak-STAT pathway. Proc Natl Acad Sci U S A *109*, 18915-18920.

Park, S., Bustamante, E.L., Antonova, J., McLean, G.W., and Kim, S.K. (2011). Specification of Drosophila corpora cardiaca neuroendocrine cells from mesoderm is regulated by Notch signaling. PLoS Genet *7*, e1002241.

Patel, R.T., Soulages, J.L., Hariharasundaram, B., and Arrese, E.L. (2005). Activation of the lipid droplet controls the rate of lipolysis of triglycerides in the insect fat body. J Biol Chem *280*, 22624-22631.

Puri, V., Konda, S., Ranjit, S., Aouadi, M., Chawla, A., Chouinard, M., Chakladar, A., and Czech, M.P. (2007). Fat-specific protein 27, a novel lipid droplet protein that enhances triglyceride storage. J Biol Chem *282*, 34213-34218.

Rajan, A., Housden, B.E., Wirtz-Peitz, F., Holderbaum, L., and Perrimon, N. (2017). A Mechanism Coupling Systemic Energy Sensing to Adipokine Secretion. Dev Cell *43*, 83-98 e86.

Rao, R.R., Long, J.Z., White, J.P., Svensson, K.J., Lou, J., Lokurkar, I., Jedrychowski, M.P., Ruas, J.L., Wrann, C.D., Lo, J.C., et al. (2014). Meteorin-like is a hormone that regulates immune-adipose interactions to increase beige fat thermogenesis. Cell *157*, 1279-1291.

Rosen, E.D., and Spiegelman, B.M. (2014). What we talk about when we talk about fat. Cell *156*, 20-44.

Roy, D., Farabaugh, K.T., Wu, J., Charrier, A., Smas, C., Hatzoglou, M., Thirumurugan, K., and Buchner, D.A. (2017). Coordinated transcriptional control of adipocyte triglyceride lipase (Atgl) by transcription factors Sp1 and peroxisome proliferator-activated receptor gamma (PPARgamma) during adipocyte differentiation. J Biol Chem *292*, 14827-14835.

Royet, J. (2004). Drosophila melanogaster innate immunity: an emerging role for peptidoglycan recognition proteins in bacteria detection. Cell Mol Life Sci *61*, 537-546.

Rui, L., Aguirre, V., Kim, J.K., Shulman, G.I., Lee, A., Corbould, A., Dunaif, A., and White, M.F. (2001). Insulin/IGF-1 and TNF-alpha stimulate phosphorylation of IRS-1 at inhibitory Ser307 via distinct pathways. J Clin Invest *107*, 181-189.

Rynes, J., Donohoe, C.D., Frommolt, P., Brodesser, S., Jindra, M., and Uhlirova, M. (2012). Activating transcription factor 3 regulates immune and metabolic homeostasis. Mol Cell Biol *32*, 3949-3962.

Ryu, J.H., Kim, S.H., Lee, H.Y., Bai, J.Y., Nam, Y.D., Bae, J.W., Lee, D.G., Shin, S.C., Ha, E.M., and Lee, W.J. (2008). Innate immune homeostasis by the homeobox gene caudal and commensal-gut mutualism in Drosophila. Science *319*, 777-782.

Sajwan, S., Sidorov, R., Staskova, T., Zaloudikova, A., Takasu, Y., Kodrik, D., and Zurovec, M. (2015). Targeted mutagenesis and functional analysis of adipokinetic hormone-encoding gene in Drosophila. Insect Biochem Mol Biol *61*, 79-86.

Schoenborn, V., Heid, I.M., Vollmert, C., Lingenhel, A., Adams, T.D., Hopkins, P.N., Illig, T., Zimmermann, R., Zechner, R., Hunt, S.C., et al. (2006). The ATGL gene is associated with free fatty acids, triglycerides, and type 2 diabetes. Diabetes *55*, 1270-1275.

Schreiber, R., Xie, H., and Schweiger, M. (2019). Of mice and men: The physiological role of adipose triglyceride lipase (ATGL). Biochim Biophys Acta Mol Cell Biol Lipids *1864*, 880-899.

Schweiger, M., Schreiber, R., Haemmerle, G., Lass, A., Fledelius, C., Jacobsen, P., Tornqvist, H., Zechner, R., and Zimmermann, R. (2006). Adipose triglyceride lipase and hormone-sensitive lipase are the major enzymes in adipose tissue triacylglycerol catabolism. J Biol Chem *281*, 40236-40241.

Shakespear, M.R., Halili, M.A., Irvine, K.M., Fairlie, D.P., and Sweet, M.J. (2011). Histone deacetylases as regulators of inflammation and immunity. Trends Immunol *32*, 335-343.

Shim, J., Mukherjee, T., and Banerjee, U. (2012). Direct sensing of systemic and nutritional signals by haematopoietic progenitors in Drosophila. Nat Cell Biol *14*, 394-400.

Silverman, N., and Maniatis, T. (2001). NF-kappaB signaling pathways in mammalian and insect innate immunity. Genes Dev *15*, 2321-2342.

Sohrabi, Y., Godfrey, R., and Findeisen, H.M. (2018). Altered Cellular Metabolism Drives Trained Immunity. Trends Endocrinol Metab *29*, 602-605.

Stoven, S., Ando, I., Kadalayil, L., Engstrom, Y., and Hultmark, D. (2000). Activation of the Drosophila NF-kappaB factor Relish by rapid endoproteolytic cleavage. EMBO Rep *1*, 347-352.

Sykiotis, G.P., and Bohmann, D. (2008). Keap1/Nrf2 signaling regulates oxidative stress tolerance and lifespan in Drosophila. Dev Cell *14*, 76-85.

Taniguchi, K., and Karin, M. (2018). NF-kappaB, inflammation, immunity and cancer: coming of age. Nat Rev Immunol *18*, 309-324.

Tarantino, G., and Caputi, A. (2011). JNKs, insulin resistance and inflammation: A possible link between NAFLD and coronary artery disease. World J Gastroenterol *17*, 3785-3794.

Taschler, U., Schreiber, R., Chitraju, C., Grabner, G.F., Romauch, M., Wolinski, H., Haemmerle, G., Breinbauer, R., Zechner, R., Lass, A., et al. (2015). Adipose triglyceride lipase is involved in the mobilization of triglyceride and retinoid stores of hepatic stellate cells. Biochim Biophys Acta *1851*, 937-945.

Tieri, P., Termanini, A., Bellavista, E., Salvioli, S., Capri, M., and Franceschi, C. (2012). Charting the NF-kappaB pathway interactome map. PLoS One *7*, e32678.

Tornatore, L., Thotakura, A.K., Bennett, J., Moretti, M., and Franzoso, G. (2012). The nuclear factor kappa B signaling pathway: integrating metabolism with inflammation. Trends Cell Biol *22*, 557-566.

Toubal, A., Treuter, E., Clement, K., and Venteclef, N. (2013). Genomic and epigenomic regulation of adipose tissue inflammation in obesity. Trends Endocrinol Metab *24*, 625-634.

Valanne, S., Wang, J.H., and Ramet, M. (2011). The Drosophila Toll signaling pathway. J Immunol *186*, 649-656.

van Dijk, D., Sharon, E., Lotan-Pompan, M., Weinberger, A., Segal, E., and Carey, L.B. (2017). Large-scale mapping of gene regulatory logic reveals context-dependent repression by transcriptional activators. Genome Res *27*, 87-94.

Varma, D., Bulow, M.H., Pesch, Y.Y., Loch, G., and Hoch, M. (2014). Forkhead, a new cross regulator of metabolism and innate immunity downstream of TOR in Drosophila. J Insect Physiol *69*, 80-88.

Vihervaara, T., and Puig, O. (2008). dFOXO regulates transcription of a Drosophila acid lipase. J Mol Biol *376*, 1215-1223.

Wang, A., Luan, H.H., and Medzhitov, R. (2019). An evolutionary perspective on immunometabolism. Science *363*.

Wang, B., Moya, N., Niessen, S., Hoover, H., Mihaylova, M.M., Shaw, R.J., Yates, J.R., 3rd, Fischer, W.H., Thomas, J.B., and Montminy, M. (2011). A hormone-dependent module regulating energy balance. Cell *145*, 596-606.

Wang, Y., Zhou, Y., and Graves, D.T. (2014). FOXO transcription factors: their clinical significance and regulation. Biomed Res Int *2014*, 925350.

Weber, K., Johnson, N., Champlin, D., and Patty, A. (2005). Many P-element insertions affect wing shape in Drosophila melanogaster. Genetics *169*, 1461-1475.

Welte, M.A. (2015). Expanding roles for lipid droplets. Curr Biol *25*, R470-481.

Woodcock, K.J., Kierdorf, K., Pouchelon, C.A., Vivancos, V., Dionne, M.S., and Geissmann, F. (2015). Macrophage-derived upd3 cytokine causes impaired glucose homeostasis and reduced lifespan in Drosophila fed a lipid-rich diet. Immunity *42*, 133-144.

Xing, Y.Q., Li, A., Yang, Y., Li, X.X., Zhang, L.N., and Guo, H.C. (2018). The regulation of FOXO1 and its role in disease progression. Life Sci *193*, 124-131.

Yang, H., and Hultmark, D. (2017). Drosophila muscles regulate the immune response against wasp infection via carbohydrate metabolism. Sci Rep *7*, 15713.

Yin, J., Peng, Y., Wu, J., Wang, Y., and Yao, L. (2014). Toll-like receptor 2/4 links to free fatty acid-induced inflammation and beta-cell dysfunction. J Leukoc Biol *95*, 47-52.

Zechner, R., Madeo, F., and Kratky, D. (2017). Cytosolic lipolysis and lipophagy: two sides of the same coin. Nat Rev Mol Cell Biol *18*, 671-684.

Zhang, Q., Zhao, K., Shen, Q., Han, Y., Gu, Y., Li, X., Zhao, D., Liu, Y., Wang, C., Zhang, X., et al. (2015). Tet2 is required to resolve inflammation by recruiting Hdac2 to specifically repress IL-6. Nature *525*, 389-393.

Zhang, W., Bu, S.Y., Mashek, M.T., I, O.S., Sibai, Z., Khan, S.A., Ilkayeva, O., Newgard, C.B., Mashek, D.G., and Unterman, T.G. (2016). Integrated Regulation of Hepatic Lipid and Glucose Metabolism by Adipose Triacylglycerol Lipase and FoxO Proteins. Cell Rep *15*, 349-359.

Zhang, X., Zhang, C.C., Yang, H., Soni, K.G., Wang, S.P., Mitchell, G.A., and Wu, J.W. (2019). An Epistatic Interaction between Pnpla2 and Lipe Reveals New Pathways of Adipose Tissue Lipolysis. Cells *8*.

Zhao, X., and Karpac, J. (2017). Muscle Directs Diurnal Energy Homeostasis through a Myokine-Dependent Hormone Module in Drosophila. Curr Biol *27*, 1941-1955 e1946.

Zhong, B., Tien, P., and Shu, H.B. (2006). Innate immune responses: crosstalk of signaling and regulation of gene transcription. Virology *352*, 14-21.

Zhou, R., Gong, A.Y., Chen, D., Miller, R.E., Eischeid, A.N., and Chen, X.M. (2013). Histone deacetylases and NF-kB signaling coordinate expression of CX3CL1 in epithelial cells in response to microbial challenge by suppressing miR-424 and miR-503. PLoS One *8*, e65153.

Zhou, W., Jiang, Z.W., Tian, J., Jiang, J., Li, N., and Li, J.S. (2003). Role of NF-kappaB and cytokine in experimental cancer cachexia. World J Gastroenterol *9*, 1567-1570.